https://press.jandoo.ac/journals/ijcmp

INTERNATIONAL JOURNAL OF CLINICAL MEDICINE & PHARMACOLOGY

ISSN 2759-8756

press

Volume 1
Number 2
February
2025

International Journal of Clinical Medicine & Pharmacology

Journal Statement

1. The opinions expressed in articles published in the *International Journal of Clinical Medicine & Pharmacology* (IJCMP) are solely those of the authors and do not necessarily reflect the views of the editorial board or the editorial office.
2. The journal reserves the right to edit and revise submitted manuscripts as necessary. Authors with specific requirements should state them upon submission.
3. *IJCMP* supports an Open Access policy, making all articles freely accessible to the public. Users are permitted to read and use the content provided the original authors and source are properly credited, and the content is not used for commercial purposes.
4. The journal holds the exclusive right to publish all accepted articles online. Authors are required to ensure that their submissions are original and not under consideration elsewhere. Any objections to online publication must be stated at the time of submission.
5. *IJCMP* is indexed in CrossRef and Google Scholar. All published articles are assigned a unique DOI to facilitate citation and academic dissemination. Authors who do not wish their articles to be indexed should notify the editorial office upon submission.
6. All articles published in the journal require prior authorization from the authors. Reproduction, translation, or compilation of any published content must obtain written permission from both the editorial office and the authors.
7. The journal accepts submissions exclusively through its official website: https://press.jandoo.ac/journal/ijcmp. Due to resource constraints, submitted manuscripts will not be returned. If no decision is communicated within three months, authors are free to submit their work elsewhere.
8. *IJCMP* promotes academic integrity. Authors are responsible for ensuring the originality and accuracy of their work. Any detected plagiarism or academic misconduct will result in retraction and potential legal consequences.

Volume 1, Number 2 (February 2025)

Contents

Effects of Perioperative Implanting Intra-Aortic Balloon Pumps on the Prognostic Indicators of Coronary Artery Bypass Grafting Surgery Patients: A Retrospective Study 1

Chunlou Wei, Jingxiao Li, Weijun Li, Shenhua Qin, Ting Zhou

The Feasibility of Dissolving Phlegm with Oil Method and the Theory of Traditional Chinese Medicine 11

Yue Wang, Liping Yin

Clinical Significance and Potential Signal Pathway of Upregulated Pituitary Tumor-transforming Gene 1 in Metastatic Prostate Cancer Based on Bioinformatic Methods 17

Jingxiao Li, Kunlin He, Gushing Li, Huafu Zhou, Jun Liu

Delayed Foam Rolling Outperforms Immediate Application/ Mechanistic Synergy with Post-Exercise Repair Phases Reduces DOMS and Restores Muscle Function 28

Chunlou Wei, Jingxiao Li, Weijun Li, Shenhua Qin, Ting Zhou

Associations Between Urinary and Blood Heavy Metal Exposure and Heart Failure Risk in Elderly Adults/ Insights From an Interpretable Machine Learning Model Based on NHANES (2003-2020) 36

Yuting Yang, Shan Deng

Identification and Management Strategies for Low Cardiac Output Syndrome After Cardiac Surgery 49

Jingxiao Li, Chunlou Wei, Jianlin Wen, Ting Zhou

Integrated Traditional Chinese and Western Medicine in the Treatment of Heart Failure with Reduced Ejection Fraction Combined with Variant Angina: A Case Report 56

Siqi Li, Xiaowan Han, Lanjun Kou, Diying Zhang, Guozhong Pan

NADPH Oxidase 4 in Prostate Cancer: Expression and Potential Role in Ferroptosis 67

Kunlin He, Jingxiao Li, Gusheng Li, Guanqiang Yan, Xiang Gao, Huafu Zhou, Jun Liu

Call for Papers 80

International Journal of Clinical Medicine & Pharmacology

https://doi.org/10.70731/sxp64528

Effects of Perioperative Implanting Intra-Aortic Balloon Pumps on the Prognostic Indicators of Coronary Artery Bypass Grafting Surgery Patients: A Retrospective Study

Chunlou Wei [a], Jingxiao Li [a], Weijun Li [a], Shenhua Qin [a], Ting Zhou [a,*]

[a] *The First Affiliated Hospital of Guangxi Medical University Cardiothoracic Surgery Intensive Care Unit, Nanning, Guangxi, China*

KEYWORDS

Coronary Atherosclerotic Heart Disease,
Coronary Artery Bypass Grafting,
Intra-Aortic Balloon Pump

ABSTRACT

This study evaluated the effect of intra-aortic balloon pump (IABP) usage on clinical outcomes in patients undergoing coronary artery bypass grafting (CABG). A total of 258 patients were divided into two groups based on perioperative IABP implementation. The analysis included serum biomarkers, echocardiographic parameters, and hospitalization details before and within 72 hours post-surgery, using t-tests and $\chi 2$ tests as appropriate. The IABP group had higher rates of left main artery stenosis, greater use of bridging vessels, and higher preoperative New York Heart Association (NYHA) grades compared to the control group, while showing lower extracorporeal circulation usage ($p < 0.05$). Postoperatively, the IABP group demonstrated increased levels of myoglobin and pro-brain natriuretic peptide, longer ventilator support duration, extended intensive care unit (ICU) stays, larger left ventricular end-systolic and end-diastolic diameters, reduced left ventricular ejection fraction, and higher hospital mortality and ICU readmission rates ($p < 0.05$). These findings suggest that while IABP may improve certain preoperative parameters, its perioperative use is associated with significant changes in postoperative prognostic indicators.

1. Introduction

Recent research has highlighted coronary atherosclerotic heart disease (CAHD) as one of the most common cardiovascular diseases, contributing to high all-cause mortality rates in developed and developing countries [1]. Coronary artery bypass grafting (CABG) is considered as an effective treatment method for improving cardiac blood supply in CAHD patients, significantly extending their lifespan and enhancing their quality of life [2]. However, patients undergoing CABG often suffer from hypotension, cardiogenic shock, and postoperative low cardiac output syndrome during the perioperative period. In cases where patients face a poor prognosis, intra-aortic balloon pumps (IABP) are often inserted into their descending aorta to improve peripheral organ perfusion and coronary blood supply [3].

* Corresponding author. E-mail address: 921132@sr.gxmu.edu.cn

Received 20 January 2025; Received in revised form 7 February 2025; Accepted 24 February 2025; Available online 28 February 2025.

Being the earliest and most widely used mechanical circulation support device, the IABP, with its ease of insertion, offers rapid availability and relative affordability [4]. Nevertheless, despite its historical application in improving cardiac blood supply in various heart diseases, IABP is no longer the primary choice in the majority of cases due to the increasing use of emergency percutaneous coronary intervention and other new mechanical circulation support technologies, challenging its status in treating cardiogenic shock caused by CAHD[5]. Consequently, opinions on its active use remain divided. Apart from its recognized benefits in reducing the use of inotropic agents and the risk of renal replacement therapy, the IABP may also potentially induce or exacerbate adverse cardiovascular and cerebrovascular events [6-9].). Numerous current studies have treated patients who underwent CABG with and without IABP during the perioperative period as a homogeneous group, without considering the unique characteristics and clinical situations of each subgroup during this period. As a result of this approach, significant differences were observed in certain postoperative indicators between the two groups. Therefore, to objectively evaluate the role and significance of IABP in patients undergoing CABG surgery, a comprehensive study encompassing hemodynamics, cardiac ultrasound, and prognostic indicators before, during the perioperative period is needed.

This study collected and analyzed data on hemodynamic, cardiac ultrasound, and prognostic indicators from 258 patients during the perioperative period of CABG to ascertain the impact of IABP usage on these indicators and the patient's prognosis.

2. Methods

2.1. Ethical Statement

The present study had been approved by Ethics Review Committee of the First Affiliated Hospital of Guangxi Medical University (approval number: 2023-E188-01). All patients are aware of the purpose and method of this study and have signed an informed consent form for sample use.

2.2. Sample Source

The current study received approval from the Ethics Review Committee of the First Affiliated Hospital of Guangxi Medical University (approval number: 2023-E188-01). Samples were acquired from the Department of Cardiothoracic Surgery, the First Affiliated Hospital of Guangxi Medical University. Inclusion criteria comprised the following: ① Visits between January 1, 2018, and December 31, 2022; ② Patients diagnosed with CAHD who underwent CABG surgery; ③ Completion of all or part of the required examinations; ④ Admission for treatment based on CAHD as the primary diagnosis, excluding any other secondary diagnoses; ⑤ Age range of patients between 18 and 80 years. Exclusion criteria were as follows: ① Simultaneous performance of CABG surgery with other cardiac surgeries; ② Patients receiving invasive treatments (including mechanical assisted circulation, other cardiac surgeries, etc.) prior to this CABG surgery. All patients were informed about the purpose and method of the study and provided signed informed consent for sample use. According to Chinese guidelines, patient evaluations included dopamine dosage, cardiac output, mean arterial pressure, left atrial pressure, central venous pressure, urine output, and peripheral circulation [10]. IABP-assisted circulation was immediately administered when patients met the indications for using IABP. Senior surgeons discussed treatment options for all cases (including whether to use extracorporeal circulation during surgery, timing of IABP usage, etc.) to ensure maximal benefit for patients during the treatment process. The study collected data encompassing age, height, weight, sex, smoking history, hypertension history, diabetes history, hyperthyroidism history, cerebrovascular accident history, myocardial infarct history, cardiac pathology, New York Heart Association (NYHA) classification, myocardial enzyme index, electrocardiogram results (including arrhythmia and ST-T segment changes), cardiac ultrasound results, CABG operation history, IABP usage, and postoperative hospitalization. CAHD patients were categorized into IABP and control groups based on whether they had an IABP during the perioperative period of CABG.

2.3. Data Analysis

The collected data were organized, and any outliers (such as samples with significant missing values or misclassified data) were excluded. Various methods were used to analyze the included indicators based on whether they represented categorical or quantitative data. Quantitative data encompassed the patient's age, height, weight, percentage of left main

Table 1 | Comparison of preoperative and intraoperative quantitative data between the IABP group and the control group

Variable	Control group			IABP group			t	p-value
	N	M	SD	N	M	SD		
Age	150	60.000	9.991	108	60.917	8.955	-0.759	0.449
BMI	145	24.845	3.482	105	24.064	3.413	1.766	0.079
BSA	145	1.699	0.172	105	1.665	0.187	1.470	0.143
Stenosis degree of left main artery	110	31.773	36.451	78	51.256	39.564	-3.485	0.001
CK before CABG	146	106.178	73.393	106	88.745	71.363	1.883	0.061
CK-MB before CABG	146	15.062	8.981	106	14.446	10.869	0.491	0.624
Number of bypass vessels	149	2.698	0.852	108	2.917	0.799	-2.107	0.036
Left ventricular end systolic diameter	76	35.829	7.915	58	38.328	11.112	-1.454	0.149
Left ventricular end diastolic diameter	76	53.026	6.827	58	54.276	8.577	-0.911	0.364
Interventricular septum thickness	76	11.368	1.495	58	11.224	1.464	0.559	0.577
EF	76	59.658	11.004	58	56.362	15.236	1.393	0.167
CO	75	5.580	1.455	58	5.610	1.645	-0.113	0.910

IABP, intra-aortic balloon pump; N, number; M, mean; SD, standard deviation; BMI, body mass index; BSA, body surface area; CK, creatine kinase; CABG, coronary artery bypass grafting; CK-MB, CK myocardial band; EF, left ventricular ejection fraction; CO, cardiac output.

artery stenosis (obtained from digital subtraction angiography and independently evaluated by two senior radiologists), myocardial enzyme indicators, number of bypass vessels, postoperative hospitalization, and cardiac ultrasound results (including left ventricular ejection fraction and cardiac output). To compare differences in these indicators between the IABP and control groups, independent sample t-tests were used. The patient's gender, smoking history, hypertension history, diabetes history, hyperthyroidism history, cerebrovascular accident history, myocardial infarction history, three-vessel lesions, extracorporeal circulation, and electrocardiogram results constituted categorical data, for which $\chi 2$ tests were employed to compare these indicators between the groups.

Additionally, to investigate the impact of IABP on patients' myocardial enzyme indicators and cardiac ultrasound results, eight metrics were used for follow-up analysis: creatine kinase (CK), CK myocardial band (CK-MB), serum troponin I, left ventricular end-diastolic diameter, left ventricular end-systolic diameter, interventricular septum thickness, ejection fraction, and cardiac output. These indicators were collected pre-operation and after 72 hours. Paired sample t-tests were conducted to examine changes in various indicators before and after surgery within each group of samples. Subsequently, a two-sample mean t-test was used to assess differences in the indicator changes between the two groups. Data analysis was performed using IBM SPSS 23.0, and a significance level of $p < 0.05$ was considered statistically significant.

3. Results

A total of 258 patients underwent CABG surgery from January 1, 2018, to December 31, 2022. Among them, 108 patients used IABP during the perioperative period, while the remaining 150 did not. Analysis of preoperative and intraoperative indicators revealed significantly higher stenosis in the left main artery ($p = 0.001$), increased use of bridging vessels during surgery ($p = 0.007$), and elevated preoperative NYHA classification ($p = 0.006$) in the IABP group compared to the control group. Conversely, the frequency of extracorporeal circulation during surgery was notably lower among IABP patients than in the control group ($p = 0.002$). The remaining preoperative and intraoperative indicators did not display differences between the two groups (Tables 1 and 2).

Table 2 | Comparison of preoperative and intraoperative categorical data between the IABP group and the control group

Term		IABP group	Control group	p-value
NYHA	I	12	23	0.026
	II	46	65	
	III	32	45	
	IV	10	2	
Sex	male	87	21	0.891
	female	119	30	
Smoking	Yes	58	81	0.917
	No	50	68	
Hypertension	Yes	61	95	0.238
	No	47	54	
Diabetic	Yes	34	46	0.917
	No	74	103	
Hyperthyroidism	Yes	1	3	0.487
	No	107	146	
Cerebrovascular accident	Yes	11	18	0.635
	No	97	131	
AMI	Yes	20	27	0.935
	No	88	122	
Triple vessel lesion	Yes	92	115	0.116
	No	15	32	
Unstable angina pectoris	Yes	54	83	0.335
	No	54	65	
Arrhythmias	Yes	14	23	0.622
	No	40	54	
Extracorporeal Circulation	Yes	25	59	0.006
	No	83	90	

IABP, intra-aortic balloon pump; NYHA, New York Heart Association; AMI, acute myocardial infarction

Examination of postoperative indicators indicated that the IABP group exhibited markedly higher myoglobin levels ($p = 0.045$), pro-brain natriuretic peptide (pro-BNP) levels ($p = 0.015$), and longer ventilation duration ($p = 0.006$) and intensive care unit (ICU) stay ($p < 0.001$) compared to the control group. Moreover, the left ventricular end-systolic diameter ($p = 0.039$), left ventricular end-diastolic diameter ($p = 0.023$), hospital mortality rate ($p = 0.027$), and frequency of ICU readmissions ($p = 0.019$) were significantly higher in the IABP group. Conversely, the postoperative left ventricular ejection fraction was notably lower in the IABP group than in the control group ($p = 0.034$). The remaining postoperative indicators did not demonstrate differences between the two groups (Tables 3 and 4).

In addition, independent sample t-tests were conducted to analyze changes in myocardial enzymes and cardiac ultrasound indicators. The improvement rate of left ventricular end-diastolic diameter was found to be significant ($p = 0.041$). However, no differences were observed between the IABP and control groups for CK, CK-MB, serum troponin I, left ventricular end-systolic diameter, interventricular septum thickness, ejection fraction, and cardiac output ($p > 0.05$) (Table 5).

4. Discussion

The current study initially compared the prevalence of preoperative cardiovascular disease between patients in the IABP group and the control group, investigating the potential impact of these differences on surgical outcomes. The results revealed that the average degree of stenosis in the left main artery and the NYHA cardiac function classification of patients in the IABP group were significantly higher compared to those in the control group. This sug-

Table 3 | Comparison of postoperative quantitative data between the IABP group and the control group

Variable	Control group			IABP group			t	p-value
	N	M	SD	N	M	SD		
CK	138	655.935	484.626	105	782.038	778.033	-1.459	0.146
CK-MB	138	26.732	24.450	105	26.152	17.454	0.206	0.837
CK-MB/CK	138	0.046	0.053	105	0.044	0.025	0.319	0.750
Serum troponin I	40	3.290	7.365	39	3.195	12.465	0.041	0.967
Hypersensitive troponin	124	244.712	850.639	97	136.231	313.263	1.194	0.234
Myoglobin	84	332.433	366.263	63	517.372	647.069	-2.037	0.045
Pro-BNP	141	1167.958	1762.393	105	1930.139	2865.560	-2.407	0.017
Duration of ventilator	149	32.106	38.891	108	62.258	93.557	-3.157	0.002
Duration of ICU	150	64.344	58.943	107	111.296	90.777	-4.691	0.000
Left ventricular end systolic diameter	77	33.779	6.882	56	37.304	9.417	-2.377	0.019
Left ventricular end diastolic diameter	77	49.117	6.356	56	52.286	8.051	-2.443	0.016
Interventricular septum thickness	77	11.416	1.321	56	11.250	1.297	0.719	0.473
EF	77	59.533	8.405	56	55.232	13.062	2.160	0.034
CO	75	5.705	1.359	55	5.986	1.622	-1.069	0.287

IABP, intra-aortic balloon pump; N, number; M, mean; SD, standard deviation; CK, creatine kinase; CK-MB, CK myocardial band; Pro-BNP, brain natriuretic peptide precursor; ICU, intensive care unit; EF, left ventricular ejection fraction; CO, cardiac output.

Table 4 | Comparison of postoperative categorical data between the IABP group and the control group

Term		IABP group	Control group	p-value
Death in hospital	Yes	8	2	0.031
	No	100	147	
ST-T segment changes on the ECG	Yes	24	50	0.207
	No	23	30	
Retracheal intubation	Yes	7	2	0.065
	No	101	145	
Re-entering the ICU	Yes	9	3	0.019
	No	99	144	

IABP, intra-aortic balloon pump; ECG, electrocardiogram; ICU, intensive care unit.

gests that patients in the IABP group had diminished exercise tolerance due to reduced cardiac blood supply. To enhance postoperative quality of life, an increased utilization of bypass vessels is recommended for CABG surgery. Thus, it can be inferred that observed patients undergoing IABP application during the perioperative period presented with a relatively suboptimal baseline status characterized by insufficient cardiac perfusion and reduced exercise endurance. According to *2021: The American Association for Thoracic Surgery Expert Consensus Document*, for heart failure and ventricular remodeling patients, IABP use is recommended [11]. Among our included patients, those in the IABP group exhibited lower preoperative cardiac blood supply compared to the control group, reflecting poorer baseline conditions. However, IABP was found to effectively improve postoperative cardiac blood supply in patients with poor baseline conditions. Conversely, our findings suggest that preoperative and intraoperative IABP use can notably reduce the need for extracorporeal circulation among patients. As such, we recommend comprehensive preoperative evaluation and early IABP application in high-risk CAHD patients. Furthermore, our analysis indicates that, compared to the control group, patients receiving IABP therapy

Table 5 | Changes in myocardial enzyme indicators and cardiac ultrasound indicators between IABP group and control group.

Variable	Paired sample t-test Paired t-test										Two sample mean t-test	
	IABP group					Control group						
	N	M	SD	t	p-value	N	M	SD	t	p-value	t	p-value
CK	103	701.107	787.081	9.04	<0.001	136	540.669	483.124	13.051	<0.001	1.943	0.053
CK-MB	100	11.834	21.125	5.685	<0.001	128	10.952	25.349	4.964	<0.001	0.28	0.78
Serum troponin I	39	2.93	12.58	1.455	0.154	39	3.181	7.516	2.643	0.012	-0.107	0.915
Left ventricular end-systolic diameter	51	-1.054	5.125	-1.538	0.13	70	-2.066	5.522	-3.262	0.002	1.038	0.302
Left ventricular end-diastolic diameter	52	-2.018	4.65	-3.248	0.002	73	-3.921	5.611	-6.092	<0.001	1.903	0.041
Interventricular septum thickness	56	0.018	1.228	0.109	0.914	76	0.026	1.222	0.188	0.852	-0.037	0.97
EF	56	-1.304	10.429	-0.935	0.354	76	-0.118	8.806	-0.117	0.907	-0.689	0.492
CO	55	0.336	2.372	0.152	0.298	73	0.129	1.831	0.601	0.55	0.557	0.578

IABP, intra-aortic balloon pump; N, number; M, mean; SD, standard deviation; CK, creatine kinase; CK-MB, CK myocardial band; EF, left ventricular ejection fraction; CO, cardiac output

during the perioperative period had a significantly lower incidence of requiring extracorporeal circulation during CABG surgery. Extracorporeal circulation involves systemic heparinization, potentially leading to severe inflammatory reactions. Additionally, there is a risk of vascular reperfusion injury after cardiac arrest, while intraoperative heart movement may increase the likelihood of ventricular fibrillation [12]. The use of IABP helps prevent cardiac arrest and reduces the need for extracorporeal circulation, thereby minimizing the risk of postoperative complications, including acute respiratory distress syndrome, kidney injury, arrhythmia, and low cardiac output syndrome [14]. This is especially crucial for improving the postoperative survival rate of patients undergoing CABG surgery [14]. Future multi-center research is necessary to determine whether IABP can reduce the use of extracorporeal circulation without worsening patient prognosis after surgery.

Although not statistically significant, we observed a potential trend indicating that CK levels in patients may be higher than those in the control group after receiving IABP treatment. Intriguingly, the changes in CK-MB between the two groups did not exhibit this pattern, suggesting that alterations in CK and CK-MB were not synchronous. As commonly known, CK is a blood marker used to assess muscle tissue damage, originating from myocardial tissue as well as other organ tissues and skeletal muscles. The primary insertion of IABP through femoral artery puncture could potentially reduce blood supply to immobilized lower limbs. Diminished circulation in these muscles can release CK into the bloodstream, causing asynchronous CK and CK-MB levels [15].

Elevated postoperative CK levels may signify a systemic stress response and tissue damage during surgery, while CK-MB is more specific to myocardial tissue damage. Therefore, substantial trauma to the body's tissues during surgery may keep CK-MB levels relatively constant, with CK levels showing a significant increase [16,17].

Moreover, myoglobin serves as a frequently used indicator for myocardial damage, with increased concentrations signifying significant heart muscle injury [18]. However, there is a lack of research on the impact of IABP on postoperative myoglobin levels in patients. Upon analysis, we found that patients' postoperative myoglobin levels were notably higher than those in the control group following IABP application during the perioperative period. This suggests that inevitable cardiac injury during surgery is the primary factor contributing to elevated serum myoglobin. Yet, despite experiencing similar surgical trauma, cardiac injury alone does not seem to fully explain the significant differences in myoglobin levels between the two groups. Upon further investigation, we discovered that the average CK-MB/CK levels were below 5% for both patient groups. According to the 2014 AHA/ACC

guideline for managing patients with non-ST-elevation acute coronary syndromes, when CK-MB/CK levels are less than 5%, the increased serum markers of myocardial injury are attributed to skeletal muscle lesions [19]. Consequently, we propose a daring conjecture: the IABP implantation through the femoral artery not only enhances myocardial perfusion but also reduces blood flow to the lower extremities. Ischemic damaged striated muscles release significant amounts of myoglobin and CK, leading to differences in myoglobin levels and CK growth rates between the two groups. Hence, to assess the extent of perioperative myocardial infarction and bridging vascular patency, clinical practitioners should integrate electrocardiograms and other auxiliary examinations with the analysis of myocardial injury indicators. In cases involving IABP use, close attention should focus on blood supply, skin temperature, and limb color to mitigate the risk of lower limb ischemic necrosis.

Our analysis reveals that postoperative pro-BNP levels among patients in the IABP group are significantly higher than those observed in the control group. Pro-BNP serves as a readily accessible blood marker for timely detection of heart failure [20]. However, in this study, a higher level of pro-BNP does not necessarily indicate that patients in the IABP group have a greater risk of heart failure. While the implantation of IABP led to a significant improvement in the patient's cardiac blood supply, it also increased the burden on the heart. In cases where CABG surgery had already caused substantial damage to the myocardium, the additional strain on the heart due to the high load could exacerbate the heart damage, leading to the release of large amounts of pro BNP [21]. Additionally, a substantial amount of myoglobin released by damaged striated muscles can potentially obstruct renal tubules, resulting in reduced renal function and an increase in pro-BNP [22]. Another crucial factor that should not be overlooked is the potential impact of postoperative diuretics or angiotensin-converting enzyme inhibitors on the measurement of pro-BNP levels [23]. Unfortunately, due to the challenge in obtaining medication usage data, this study cannot currently rule out the impact of medication to further explore the mechanisms of IABP's impact on pro-BNP. As a result, caution must be exercised in determining whether patients implanted with IABP are at a higher risk of heart failure based solely on the level of pro-BNP.

Recent research suggests that the prognosis for patients who have undergone cardiac surgery and received IABP treatment is unfavorable. Thiele et al. conducted a randomized controlled study revealing higher mortality rates among patients in the IABP group [24]. Similarly, Ali et al.'s study demonstrated that patients using IABP before cardiac surgery had elevated mortality rates, increased red blood cell input, and longer periods of invasive ventilation compared to the control group [25]. Sayed et al.'s single-center study also reported extended postoperative ICU time, invasive ventilation duration, and higher mortality rates in the IABP group compared to the control group, possibly related to the preoperative ejection fraction of patients [26]. In our study, the IABP-receiving group had significantly prolonged ventilator usage, extended ICU stay, and higher hospital mortality rates, consistent with previous research findings. These results can be attributed to the fact that patients requiring IABP support often present more severe coronary artery disease and poorer health conditions before surgery, leading to a heightened perioperative mortality risk. Our findings indicate that among high-risk patients implanted with IABP during the perioperative period, although they experienced longer mechanical ventilation and extended ICU stays, only 8 out of 110 patients died in the hospital after receiving active treatment. This suggests that IABP was effective in reducing the risk of mortality for most patients during the intraoperative and postoperative periods. Nonetheless, our results solely describe the mortality rate of CABG patients using IABP, necessitating further randomized controlled studies to determine whether IABP can improve the prognosis of such patients. It's important to note that despite IABP support, some patients with severe lesions may still succumb to death. Therefore, it is crucial to utilize various scoring scales such as European system for cardiac operative risk evaluation (EuroSCORE II) and European Society of Thoracic Surgeons Risk Scores (ESTS scores) for early and accurate preoperative evaluations, closely monitor patients during the perioperative period, and make decisive decisions regarding the need for stronger mechanical circulatory devices such as extracorporeal membrane oxygenation [27,28]. Physicians should carefully assess the patient's condition, determine whether to use IABP early or opt for stronger mechanical circulatory support, and provide suitable postoperative monitoring and rehabilitation plans to reduce complications and risks,

ultimately ensuring that patients receive optimal treatment outcomes [29].

Our study indicates that patients treated with IABP had a larger post-surgery left ventricular diameter compared to the control group. However, no significant difference in left ventricular diameter was observed between the two groups before surgery. These findings suggest that despite the use of IABP during the perioperative period, left ventricular compliance decreases, and the heart remains in a decompensated state due to factors such as low preoperative cardiac blood supply, poor energy metabolism, and less effective myocardial work in high-risk CAHD patients. These observations are consistent with previous studies. Libera et al. found that IABP utilization can decrease the efferent activity of the sympathetic nerve, leading to a slower heart rate and lower myocardial contractility. Additionally, IABP prolongs the diastole period of the heart, consequently enhancing the degree of heart filling [30]. In high-risk patients with CAHD who underwent IABP therapy during the perioperative period, ongoing left ventricular remodeling increases the risk of heart failure. Therefore, it is recommended to implement more rigorous heart failure treatment plans to improve ventricular remodeling and enhance the patients' quality of life.

In summary, the perioperative implementation of IABP during CABG surgery may moderately improve prognostic outcomes among patients with CAHD. Nevertheless, in cases of severe lesions, caution is crucial when selecting the IABP treatment process. It's important to note that this study is limited as a single-center study, potentially impacting the reliability and generalizability of the results. Moreover, since most patients only receive postoperative follow-up examinations at local hospitals, long-term postoperative information for both patient groups was unattainable. Clinical use of an IABP as a cardiovascular support measure remains effective but requires evaluation and decision-making under medical professional guidance. Furthermore, it's worth noting that certain confounding factors may have influenced the study results, necessitating systematic randomized controlled studies to eliminate these confounding factors.

The present study analyzed 258 samples that underwent CABG surgery, revealing that the use of IABP can enhance heart blood supply, improve energy metabolism, and contribute to ventricular remodeling to some extent. However, for those with severe cardiovascular disease, early implementation of IABP or selection of more effective extracorporeal circulation regimens may offer greater benefits.

Declarations

Abbreviations

IABP: Intra-aortic balloon pump

CABG: Coronary artery bypass grafting

NYHA: New York Heart Association

ICU: Intensive care unit

CAHD: Coronary atherosclerotic heart disease

CK: Creatine kinase

CK-MB: Creatine kinase myocardial band

Ethics approval and consent to participate

The present study had been approved by Ethics Review Committee of the First Affiliated Hospital of Guangxi Medical University (approval number: 2023-E188-01). All patients are aware of the purpose and method of this study and have signed an informed consent form for sample use.

Consent to Publish declaration

Written informed consent was obtained from the participant for publication of identifying information/images in an online open-access publication.

Availability of Data and Materials

The datasets used and/or analysed during the current study available from the corresponding author on reasonable request.

Clinical trial number

Not applicable.

Competing interests

The authors declare no competing interests.

Funding

The present article was supported by the National Key Clinical Specialty Construction Project, Guangxi Medical And Health Key Discipline Construction Project, Guangxi Key Clinical Specialty Construction Project and the Research project funded by the Health Commission of Guangxi Zhuang Autonomous Region (ID: Z20211014).

Acknowledgements

Not Applicable.

Reference

1. Global, regional, and national age-sex specific all-cause and cause-specific mortality for 240 causes of death, 1990-2013: a systematic analysis for the Global Burden of Disease Study 2013. Lancet (London, England). 2015;385(9963):117-71. doi:10.1016/s0140-6736(14)61682-2
2. Velioglu Y, Isik M. Early-Term Outcomes of Off-Pump versus On-Pump Beating-Heart Coronary Artery Bypass Surgery. The Thoracic and cardiovascular surgeon. 2019;67(7):546-553. doi:10.1055/s-0039-1679923
3. Webb C, Weyker P, Flynn BJSic, anesthesia v. Management of intra-aortic balloon pumps. 2015;19(2):106-21. doi:10.1177/1089253214555026
4. Gajanan G, Brilakis E, Siller-Matula J, Zolty R, Velagapudi PJJoveJ. The Intra-Aortic Balloon Pump. 2021; (168)doi:10.3791/62132
5. Ozaki Y, Hara H, Onuma Y, et al. CVIT expert consensus document on primary percutaneous coronary intervention (PCI) for acute myocardial infarction (AMI) update 2022. 2022;37(1):1-34. doi:10.1007/s12928-021-00829-9
6. Nakahira J, Sawai T, Minami TJAo. Elective use of intra-aortic balloon pump during aortic valve replacement in elderly patients to reduce postoperative cardiac complications. 2014;38(6):503-7. doi:10.1111/aor.12207
7. Miller P, Bromfield S, Ma Q, et al. Clinical Outcomes and Cost Associated With an Intravascular Microaxial Left Ventricular Assist Device vs Intra-aortic Balloon Pump in Patients Presenting With Acute Myocardial Infarction Complicated by Cardiogenic Shock. 2022;182(9):926-933. doi:10.1001/jamainternmed.2022.2735
8. Nan Tie E, Dinh D, Chan W, et al. Trends in Intra-Aortic Balloon Pump Use in Cardiogenic Shock After the SHOCK-II Trial. 2023;191:125-132. doi:10.1016/j.amjcard.2022.12.019
9. Li H, Li LJFicm. Successful treatment of fulminant myocarditis with intra-aortic balloon pump counterpulsation combined with immunoglobulin and glucocorticoid in a young male adult. 2022;9:905189. doi:10.3389/fcvm.2022.905189
10. Consensus of Experts on the Perioperative Application of Intra-Aortic Balloon Counterpulsation in Cardiac Surgery. 2017; 97(28): 2168-2175. (in Chinese).
11. Bakaeen F, Gaudino M, Whitman G, et al. 2021: The American Association for Thoracic Surgery Expert Consensus Document: Coronary artery bypass grafting in patients with ischemic cardiomyopathy and heart failure. 2021;162(3):829-850.e1. doi:10.1016/j.jtcvs.2021.04.052
12. Pasechnik I, Dvoryanchikova V, Tsepenshchikov VJK. [Extracorporeal circulation in cardiac surgery: state of the problem]. 2017;(6):72-78. doi:10.17116/hirurgia2017672-78
13. Kawahito S, Soga T, Yagi S, et al. Pathophysiology and Complications during Extracorporeal Circulation. 2020;67(3.4):229-235. doi:10.2152/jmi.67.229
14. Ouweneel D, Schotborgh J, Limpens J, et al. Extracorporeal life support during cardiac arrest and cardiogenic shock: a systematic review and meta-analysis. 2016;42(12):1922-1934. doi:10.1007/s00134-016-4536-8
15. Minamidate N, Takashima N, Suzuki TJJocs. The impact of CK-MB elevation in patients with acute type A aortic dissection with coronary artery involvement. 2022;17(1):169. doi:10.1186/s13019-022-01924-5
16. Fan J, Ma J, Xia N, Sun L, Li B, Liu HJCl. Clinical Value of Combined Detection of CK-MB, MYO, cTnI and Plasma NT-proBNP in Diagnosis of Acute Myocardial Infarction. 2017;63(3):427-433. doi:10.7754/Clin.Lab.2016.160533
17. Pöyhönen P, Kylmälä M, Vesterinen P, et al. Peak CK-MB has a strong association with chronic scar size and wall motion abnormalities after revascularized non-transmural myocardial infarction - a prospective CMR study. 2018;18(1):27. doi:10.1186/s12872-018-0767-7
18. Servonnet A, Dubost C, Martin G, et al. [Myoglobin: still a useful biomarker in 2017?]. 2018;76(2):137-141. doi:10.1684/abc.2018.1326
19. Amsterdam E, Wenger N, Brindis R, et al. 2014 AHA/ACC guideline for the management of patients with non-ST-elevation acute coronary syndromes: a report of the American College of Cardiology/American Heart Association Task Force on Practice Guidelines. 2014;130(25):e344-426. doi:10.1161/cir.0000000000000134
20. Doust J, Lehman R, Glasziou PJAfp. The role of BNP testing in heart failure. 2006;74(11):1893-8.
21. Nishikimi T, Nakagawa YJJoc. Potential pitfalls when interpreting plasma BNP levels in heart failure practice. 2021;78(4):269-274. doi:10.1016/j.jjcc.2021.05.003
22. Okamoto R, Ali Y, Hashizume R, Suzuki N, Ito MJIjoms. BNP as a Major Player in the Heart-Kidney Connection. 2019;20(14)doi:10.3390/ijms20143581
23. Myhre P, Vaduganathan M, Claggett B, et al. B-Type Natriuretic Peptide During Treatment With Sacubitril/Valsartan: The PARADIGM-HF Trial. 2019;73(11):1264-1272. doi:10.1016/j.jacc.2019.01.018
24. Thiele H, Zeymer U, Neumann F, et al. Intra-aortic balloon counterpulsation in acute myocardial infarction complicated by cardiogenic shock (IABP-SHOCK II): final 12 month results of a randomised, open-label trial. 2013;382(9905):1638-45. doi:10.1016/s0140-6736(13)61783-3
25. Ali U, Lan N, Gilfillan M, et al. Preoperative Intra-Aortic Balloon Pumps in Cardiac Surgery: A Propensity Score Analysis. 2021;30(5):758-764. doi:10.1016/j.hlc.2020.09.924
26. Shah S, Awan N, Jan A, Rehman MJPjoms. Characteristics, morbidity and mortality factors associated with Intra-Aortic Balloon Pump in Coronary Artery Bypass Graft Surgery patients. 2020;36(6):1318-1324. doi:10.12669/pjms.36.6.2649

27.Nashef S, Roques F, Sharples L, et al. EuroSCORE II. 2012;41(4):734-44; discussion 744-5. doi:10.1093/ejcts/ezs043

28.Brunelli AJTsc. European Society of Thoracic Surgeons Risk Scores. 2017;27(3):297-302. doi:10.1016/j.thorsurg.2017.03.009

29.Ihdayhid A, Chopra S, Rankin JJCoic. Intra-aortic balloon pump: indications, efficacy, guidelines and future directions. 2014;29(4):285-92. doi:10.1097/hco.0000000000000075

30.Fresiello L, Khir A, Di Molfetta A, Kozarski M, Ferrari GJTIjoao. IABP timing and ventricular performance--comparison between a compliant and a stiffer aorta: a hybrid model study including baroreflex. 2013;36(11):749-57. doi:10.5301/ijao.500024

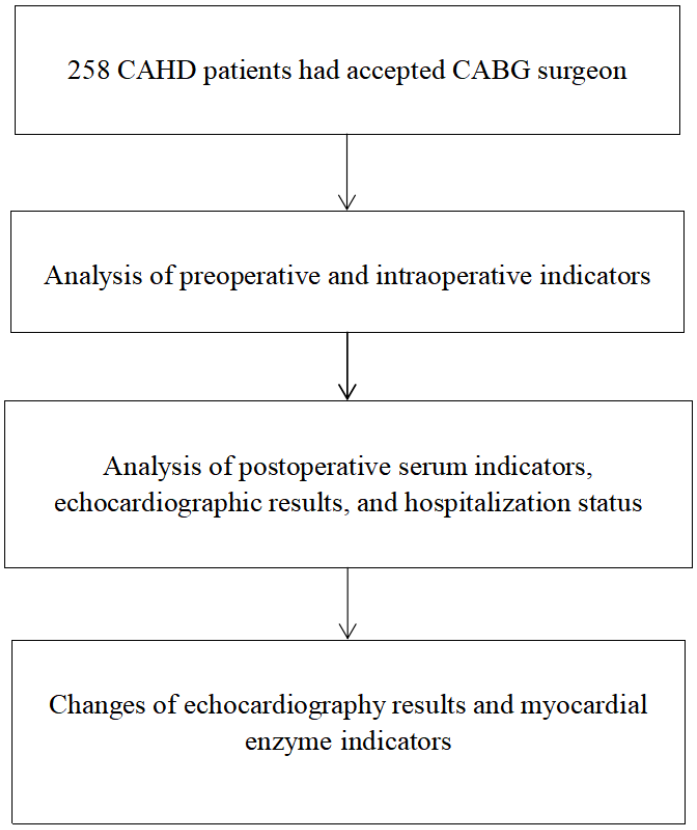

Figure 1 | The flow charts of this study

CAHD, coronary atherosclerotic heart disease;CABG, coronary artery bypass grafting

International Journal of Clinical Medicine & Pharmacology

https://doi.org/10.70731/8g8saf85

The Feasibility of Dissolving Phlegm With Oil Method and the Theory of Traditional Chinese Medicine

Yue Wang [a], Liping Yin [a,*]

[a] *Affiliated Hospital of Chengdu University of Traditional Chinese Medicine, Chengdu, China*

KEYWORDS

Dissolving Phlegm With Oil,
Expectorant,
Phlegm-Damp Syndrome

ABSTRACT

Sputum is the product of water metabolism disorder. It is characterized by a thick texture and poor fluidity. According to the traditional Chinese medicine of the same energy attracts each other and drawing analogies by comparing images, the application of medications with a consistency similar to sputum, rich in oils or volatile oils, serves to achieve the objective of "oil-dissolving sputum". This not only facilitates the expulsion of sputum but also addresses the depletion of body fluids caused by the production of phlegm and fluid retention. This approach is particularly suitable for treating phlegm-related syndromes and holds significant clinical promotion value.

1. Introduction

The historical roots of the "dissolving phlegm with oil" method are deeply intertwined with traditional Chinese medicine principles. This practice stems from ancient techniques involving the topical application and ingestion of oils to moisturize and expel phlegm. The *Huangdi's Canon of Meidcine* discusses how "phlegm" formation is linked to internal dampness and pathogenic factors, suggesting that oils can help dredge meridians, hydrate the lungs, and assist in resolving phlegm and dampness. Throughout history, oils have also played a role in the preparation of medicinal formulations and dietary therapies, serving to lubricate and penetrate tissues. During the Ming and Qing Dynasties[1], there were actual cases of using oil to dissolving phlegm in medical books, emphasizing the positive effects of oil on lung health. *Compendium of Materia Medica* mentioned that a variety of fats (such as sesame oil, peanut oil) has a good phlegm-reducing effect. [2]. Contemporary medical research has demonstrated that the unsaturated fatty acids present in certain vegetable oils exhibit significant anti-inflammatory properties, which can enhance lung tissue function and facilitate sputum expectoration[3]. Simultaneously, the lubricating properties of the oil assist in reducing irritation to the airway mucosa and mitigating cough responses[4]. These findings offer contemporary biomedical validation for traditional Chinese medicine theory, demonstrating the scientific rigor and practical efficacy of the "dissolving phlegm with oil" method.

2. The Concept of "Phlegm" in Medical Theory

Phlegm is the pathological product of thick turbidness caused by the disturbance of water and liquid

* Corresponding author. E-mail address: 1808004907@qq.com

Received 19 Ferbruary 2025; Received in revised form 24 Ferbruary 2025; Accepted 26 Ferbruary 2025; Available online 28 Ferbruary 2025.

metabolism[5]. "Sputum" and "Fluid retention" are both pathological products of water and liquid metabolism disorders, but in nature, the texture of "sputum" is thick, thick and turidity, while "Fluid retention" is relatively clear. In addition to the general "sputum", there are "visible sputum" and "invisible sputum", tangible sputum refers to the visible, audible and tactile sputum of tangible quality, intangible sputum is also caused by water and liquid metabolism disorders, but compared with tangible sputum, invisible sputum intangible quality is visible, although not visible, but there are signs, often clinical symptoms and signs. Such as body aches, head heavy such as wrapping, tongue coating greasy and so on to judge the existence of invisible phlegm[6]. In summary, sputum results from disorders in water and fluid metabolism, characterized by poor mobility and a thick consistency. According to traditional Chinese medicine (TCM) theory, phlegm-dampness is categorized into exogenous and endogenous types. Endogenous phlegm-dampness is primarily associated with spleen deficiency, improper dietary habits, emotional disturbances, and other contributing factors[7].

3. Feasibility of "Dissolving Phlegm With Oil" Method

On the basis of the pathology of "phlegm", the method of "dissolving phlegm with oil" utilizes the good dissolving characteristics of oil used externally or orally to gradually decomposition the stubborn phlegm components into forms that are easy to be eliminated, so as to achieve the effect of expectorating phlegm. The article Synopsis of Golden Chamber · Phlegm and Drink Cough Pulse Syndrome and Treatment twelfth points out, when a patient is sick with phlegm-rheum, harmonize with warm medicines" as the treatment principle[8]. Disease cause pulse treatment emphasizes the importance of "treating fire" in the treatment of "phlegm"[9]. This paper expounds the important role of "treating phlegm and fire" in the treatment of TCM from the aspects of lung, spleen and kidney. Lung phlegm syndrome and autumn dryness syndrome are the same, both belong to "fire" accumulation. To restrain Yin and reduce fire as the rule of treatment. Kidney phlegm syndrome takes nourishing Yin and clearing heat as the treatment principle, spleen phlegm syndrome takes invigorating spleen and relieving cough as the treatment principle[10]. Most of the drugs used for phlegm syndrome are Phellodendri, Zhimu, cooked ground, orange peel, fritillaria, Trichosanthes and so on. The rhizome and Phellodendron chinensis have anti-inflammatory and antioxidant effects[11]. Ripe ground is rich in mannotriose, which can antagonize the damage of hippocampal nerve cells by corticosterone and prevent the decline of learning and memory, which is the embodiment of the role of "reinforcing lean marrow" in traditional Chinese medicine[12]. The effect of dried tangerine or orange peel has expectorant, whets the appetite, cough, and play a major role is dried tangerine or orange peel naphtha composition[13]. Fritillaria and trichosanthis are also seed kernel expectorant drugs, and the expectorant effect mainly comes from their oil components[14-15].

Compendium of Materia Medica points out that "to treat dampness phlegm with ginger juice and alum soup, to treat wind phlegm with ginger juice and soapying boiled juice, to treat fire phlegm with ginger juice, bamboo drain or jing drain, to treat cold phlegm with ginger juice, alum soup and white mustard seed[16]. Phlegm toxicity can be divided into three types: "fire", "cold" and "wet", among which "fire phlegm" is the main type of phlegm syndrome. In the treatment of heat phlegm syndrome, it is emphasized that different prescriptions should be selected according to the urgency of the disease, the severity of the disease and the combination of the disease and syndrome.For mild phlegm-heat conditions, medications such as Fructus Trichosanthis, Loquat Leaves, Pinellia, and Fritillaria are commonly used to clear phlegm-heat. Among these, Fructus Trichosanthis is classified as a seed-kernel expectorant due to its properties. In contrast, Loquat Leaves and Pinellia do not fall under the category of seed-kernel expectorants. Notably, the active component in Pinellia is pinellian, which is fat-soluble[17].Loquat leaves are rich in triterpenoid acids, volatile oils and flavonoids, and also have the characteristics of fat solubility[18]. For patients with severe phlegm-heat syndrome, the combination of heat-clearing powder and dampness-resolving, phlegm-expelling medication is employed to enhance the efficacy of treating heat syndromes. For instance, in the treatment of phlegm-heat cough characterized by symptoms such as flushed face, dry mouth, rapid pulse, and other manifestations, the use of Pinellia ternata, processed Aconitum carmichaelii, and Scutellaria baicalensis can be considered[19-21]. The active constituents of these three medications are polysaccharides and flavonoids, which exhibit lipophilic properties.

"Chinese Materia Medica" divided phlegm-reducing drugs into warming cold phlegm drugs, clearing hot phlegm drugs, cough and antiasthmatic drugs, a total of 36 kinds[22]. Among them, mustard seed, Gleditsia sinensis, Thunbergii Fritillaria, Fritillary Fritillaria, bitter almond, Perilla seed, nemorosa seed, ginkgo and so on are seed kernel drugs in plant medicine, although some plant drugs are not seed kernel medicine, such as aster, Baibu, etc., but clinical studies have confirmed that aster contains volatile oil, polysaccharides, flavonoids and other substances[23]. These substances are fat-soluble and have the characteristics of oils. Clinical medium temperature cold phlegm drugs used pinellia, white mustard seeds, white front, Qinghua hot phlegm drugs used Sichuan Fritillaria, Zhejiang Fritillaria, Fructus trichosanthis, platycodon, front Hu. In addition to platycodon platycodon, rhizome, white rhizome and pinellia pinellia are non-seed kernel drugs, other drugs are seed kernel or contain seed kernel[24]. Clinical studies on the pharmacology of San Zi Yang Qin Tang[25] pointed out that the three medicines in San Zi Yang Qin Tang contain fatty acids in varying degrees, especially Lapis lazuli, which contains 45% fatty oils, which is closely related to the mucolytic effect of the formula.

There are also some special non-kernel expectorant drugs, such as Pinellia, pinellia is tuber medicine, and Pinellia is toxic, so Zhang Zhongjing uses the word "washing" when Pinellia, because there is a layer of mucus on the surface of the pinellia, this mucus will cause irritation to the human respiratory tract, may cause laryngeal edema, suffocate the patient[26]. The author posits that the viscous mucus secreted by Pinellia is a substance akin to "sputum" with low fluidity. This mucus can encapsulate and integrate with the sputum in the human body following medicinal administration, thereby facilitating the combination of pharmacological agents and pathological products for more effective elimination from the body.Modern pharmacological studies have shown that pinellia contains volatile oil components [27], and the mucus covered on the surface of raw pinellia is the external manifestation of volatile oil components. Therefore, although pinellia is not a seed drug, it also has the characteristic of "disresolving phlegm with oil" in the cognition of traditional Chinese medicine

Seed kernel expectorant contains rich plant volatile oil, good at moistening dryness, so it is more suitable for dryness sputum. However, the author believes that where phlegm exists, body fluid must be lost. There are two reasons: First, because the phlegm itself is difficult to flow and thick characteristics, it shows that the phlegm itself is lack of body fluid. Second, there is limited space for normal body fluid. If pathological phlegm and fluid increase, occupying the space of physiological body fluid, normal body fluid cannot be transferred, and human body fluid can also be deficient. Therefore, seed seeds and expectorant drugs are not only suitable for dryness phlegm syndrome, but also suitable for other phlegm syndrome, because where there is sputum generation, normal body fluid will inevitably decrease in the body.

4. Exploration of TCM Theory by Oil-Soluble Sputum Method

4.1. Same Energy Attracts Each Othe

According to the principle of TCM, expectorant drugs that are more similar to phlegm should be used, and expectorant drugs containing oil are obviously more appropriate[28]. Phlegm is the predecessor of the drink, sputum is characterized by poor fluidity, thick texture, indicating that the sputum itself is "lack of water", if the use of oil-rich seed drugs, have the effect of moistening dryness, can moisten the sputum, make the sputum easy to flow, and then easy to spit or discharge. Such drugs contain less water, oil into the body relative to body fluid and other poor mobility, similar to the nature of sputum, easy to dissolve into a body, and oil expectorant drugs along the normal qi and blood operation of the human body, the expectorant will be discharged from the body, to complete the expectorant process. At the same time, in addition to moistening and smoothing phlegm, the oil-rich seed kernel can also moisten and smooth the joints, meridians and zangfu organs of the whole body, further regulate the channel of Qi, restore the balance of qi, blood and Yin and Yang of the body, and naturally contribute to the elimination of phlegm.

4.2. Drawing Analogies by Comparing Images

The core of TCM thinking is "comparing image with class" [29]. The conventional approach to treating phlegm disorders involves the use of warming medications. According to Zhang Zhongjing's Synopsis of the Golden Chamber, it is stated that "phlegm and fluid retention should be treated with warming medicines." This principle is based on the fact that phlegm and fluid retention are pathological products resulting from disordered water metabolism, which retains the

characteristic of being "damp." Therefore, it is logical to employ warming medicines to eliminate dampness and resolve phlegm and fluid retention. As a pathological product, phlegm can complicate the disease process in various ways: it may affect mental functions, lead to subcutaneous nodules or tumors, and obstruct qi movement, causing stagnation and fever. Ultimately, phlegm results from impaired fluid metabolism, forming a viscous mass with poor mobility. Over time, the fluid content decreases further, eventually leading to blood stasis and even solid masses. If fluid metabolism remains abnormal, initial dampness transforms into fluid accumulation, and warming medicines can help dry dampness and purify fluids. However, when phlegm has already formed a viscous mass with poor mobility, it indicates a deficiency in body fluids, making it difficult for the phlegm to flow. In this case, using warming medicines may exacerbate the deficiency of body fluids and worsen the mobility of phlegm. Instead, employing "warm-moist" expectorants, such as those derived from seeds or containing volatile oils, can not only replenish body fluids but also enhance the mobility of phlegm, thereby achieving better therapeutic effects.

4.3. Theory of Meridian Tropism

Supported by the theory of sex and taste normalization, oil-soluble drugs can exert significant effects on specific pathological conditions. For instance, oily and warm drugs can facilitate the expulsion of phlegm by lubricating the respiratory tract, thereby aiding in its dissolution. In practical applications, traditional Chinese medicines such as Fructus Trichosanthes, Fritillaria Thunbergii, and Perilla seed, which possess soluble and lubricating properties, can be effectively combined with the theory of drug sex and taste to promote sputum discharge.

4.4. Western Medicine Theory Support

Seed kernel expectorants are abundant in triterpenoids, flavonoids, polysaccharides, and antioxidant compounds, which collectively enhance the body's capacity to eliminate pathological products. The clinical application of the "oil-dissolving sputum" method is closely associated with the physiological characteristics of the airway. When seed kernel phlegm-reducing drugs form an oily film within the airway, they effectively protect airway epithelial cells, mitigate external stimuli on the respiratory system, improve local blood circulation, and promote better drug penetration and absorption, thereby enhancing mucus clearance[30]. Simultaneously, the lubricating properties of the oil can alleviate airway obstruction caused by viscous sputum and fulfill respiratory physiological requirements. The extraction and utilization of bioactive compounds are also a focal point in modern medicine. Research has demonstrated that certain bioactive substances found in kernel oils, such as glycosides, polyphenols, organic acids, saponins, tannins, and vitamin B1[31], possess antioxidant and anti-inflammatory properties, thereby enhancing the efficacy of expectorant treatments. Modern pharmaceutical formulations are increasingly emphasizing the emulsifying characteristics of oils to improve drug bioavailability and achieve superior clinical outcomes.

5. Case Analysis of Kernel Expectorants

Pu Fuzhou once treated a case of sputum asthma in children [32], identified the pathogenesis as phlegm block, lung loss, depression and heat, and treated lung to reduce phlegm, with fried draba seed, fried Perilla seed, fried white mustard seed, gualou kernel shell, fried raphanus seed, white front, aster, bamboo leaves, reed root, scallion white and other 10 flavors of medicine, half of which are seed kernel expectorant drugs. Because of the delicate organs of children, for the young Yin and Yang body, the disease is more pure, affected by other system diseases may be less, so the treatment of children's phlegm syndrome, the drug has a high guiding value.

6. Conclusion

The theory of phlegm disease in traditional Chinese medicine (TCM) is rooted in a profound understanding of "phlegm," which is not only recognized as a pathological product but also serves as an indicator of internal dysfunction. TCM classifies phlegm into two categories: "tangible phlegm" and "intangible phlegm." Tangible phlegm results from the accumulation of dampness and turbidity within the body, while intangible phlegm arises from Qi deficiency and Yin deficiency. The formation of phlegm is closely associated with the functions of the spleen, lung, and kidney. Specifically, the spleen governs transportation and transformation, the lung oversees dispersion and 肃降 (sedation), and the kidney accumulates essence; these three organs interact and influence each other.

Clinically, common phlegm syndromes include damp-phlegm, cold-phlegm, hot-phlegm, and dry-phlegm. Each type has distinct manifestations and etiologies. Damp-phlegm primarily results from insufficient spleen and stomach function, leading to endogenous dampness and turbidity, with clinical symptoms such as chest tightness, coughing, and excessive phlegm. Cold-phlegm is caused by cold pathogenic factors or spleen-stomach yang deficiency, often accompanied by thin white phlegm and cold extremities. Hot-phlegm is due to internal heat or improper diet, manifesting as yellow thick phlegm, thirst, and constipation. Dry-phlegm mainly stems from Yin deficiency or invasion by dryness, characterized by dry cough with scant sputum.

In terms of differential diagnosis and treatment, TCM emphasizes the integration of "treating the root cause" (治本) and "addressing the symptoms" (治标). For phlegm syndromes, various methods such as resolving phlegm (化痰), warming transformation (温化), and clearing heat (清热) are commonly employed for comprehensive regulation. Through in-depth study of TCM's phlegm disease theory, it becomes evident that many modern therapeutic approaches share similarities with TCM principles. Oil-dissolving phlegm can effectively improve damp-phlegm conditions. Emulsification using plant extracts or combining traditional Chinese medicine with oil aids in diluting and expelling phlegm.

The theory of phlegm disease in TCM underscores the importance of adopting different regulatory and therapeutic methods based on individual constitution and causative factors. This not only provides a theoretical foundation for the "oil-dissolving phlegm" method but also holds significant guiding value and clinical significance in practical applications. A comprehensive treatment approach grounded in TCM's phlegm disease theory can facilitate effective integrated Chinese-Western medicine interventions and enhance overall therapeutic outcomes. In conclusion, expectorant drugs, particularly those rich in volatile oils or derived from seeds and kernels, align well with the characteristics of "oil-dissolved phlegm" and are more effective in treating phlegm and fluid disorders. Further clinical pharmacological research is needed to substantiate these findings.

References

1. Feng Nannan, Duan Mingming. Analysis on the application and characteristics of therapeutic therapy in sputum Fire and Snow [J]. Hunan Journal of Traditional Chinese Medicine, 2024,40 (06): 103-106.
2. Li Yiwen. Study on the health preservation literature of edible dried fruit [D]. Nanjing University of Traditional Chinese Medicine, 2022.
3. Yu Junlin, Che Xiquan, Chang Jiqing. The chemical composition and efficacy of the pine kernel [J]. Ginseng Research, 2001, (01): 25-27.
4. Yin Nan, Zhang Yonggang, Song Wenting. Optimizing the β -Preparation process of cyclodextrin inclusion compound by Box-Behnken response surface method [J]. Chinese TCM Science and Technology, 2023,30 (02): 247-251 + 412
5. Jian Wang. Basic theory of Traditional Chinese Medicine [M]. Beijing: China Traditional Chinese Medicine Press, 2016:88-89.
6. Zhang Zhang, Qiu Yi, Wang Hebao, et al. Analysis of the shape and meaning of "phlegm" in Traditional Chinese medicine [J]. Journal of Traditional Chinese Medicine, 2019,60 (10): 811-814.
7. Li Xiao, Li Lin, Jin Xinyao, et al. Theory on the origin and evolution of sputum syndrome [J]. Journal of Traditional Chinese Medicine, 2020,61 (15): 1303-1306.
8. Yu Tao, Ding Ming, Yu Qiangqiang, Xue Hanrong. "sick phlegm drinkers should be treated with warm medicine" [J]. Chinese Journal of Basic Medicine of Traditional Chinese Medicine, 2022,28 (02): 177-179.
9. Yuan Xing and, Zhang Zhuxi, Jiang Tingzhen, et al. "Because of pulse treatment" from fire and phlegm to treat cough hook xuan [J]. Jiangsu Traditional Chinese Medicine, 2024,56 (05): 65-67.
10. Shen Liguo, Ma Zuoying, Meng Jingyan, et al. Analysis of the theory of spleen main transport in the Treatment of Pulse [J]. Journal of Tianjin University of Traditional Chinese Medicine, 2015,34 (02): 73-76.
11. Yang Jingyi, Wang Jiayi, Zhang Yue, Nie Jiaxuan, Liu Huimin, Song Lili, Yang Zhen. Research progress of "mother-cypress chinensis" [J]. Chinese Journal of Traditional Chinese Medicine, 1-9.
12. Zhang Lina, Jin Guoqin. Effect of mannonose, the cooked active component, on SGK \ BDNF \ GCR expression in hippocampal neural cells with high concentrations of corticosterone damage [J]. Pharmacology and Clinical Practice of Traditional Chinese Medicine, 2011,27 (05): 16-20
13. Wang Ruifang, Liu Bing, Sun Jie, et al. Volatile aroma analysis of tangerine peel [J]. Fine Chemical, 2022,39 (02): 321-329.
14. Baco, Li Ying, He Wenkai, et al. Experimental study on cough, expectorant and anti-inflammatory effects of different preparations [J]. Journal of Southwest University for Nationalities: Natural Science Edition, 2018,44 (1): 52-55.

15. Li Yuan, Wang Yu'e, Bai Guan Ya, et al. Based on the comparison of principal components and cough and phlegm [J]. Traditional Chinese Medicine Guide, 2018,24 (13): 46-49,56.
16. Li Chenquan, Guo Zhaohui, Jin Wanjun, Zhang Shihua, Liu Jing, Song Pingshun, Ni Lin. Research on the changes of many nucleosides' components before and after pinellia Pinellia [J]. Traditional Chinese medicine, 2023,46 (07): 1664-1668.
17. Du Lunjing, Song Ning Ning, Li Xiaojiao, et al. Progress on factors influencing the active ingredients of white anago [J]. Southern Agriculture, 2022,16 (19): 148-152.
18. Sun Yanli, Hu Qiaoyun, Xie Lusheng. Progress on chemical composition and pharmacological effects of loquat leaves [J]. Straits Pharmacy, 2019,31 (08): 57-59.
19. Yuan Yijing, Wang Qiuhong. Progress in processing technology, chemical composition and pharmacological action of Teneracin [J]. Journal of Liaoning University of Traditional Chinese Medicine, 2024,26 (06): 135-139.
20. Wang Wanyi, Zhu Zhijun, Li Hangfei, Xu Shumei. Progress in chemical composition and pharmacological effects of pinellia pinellia and predictive analysis of quality markers [J]. Journal of Liaoning University of Traditional Chinese Medicine, 2024,26 (03): 203-215.
21. Hou Xiaojie, Zhang Jianfeng, Hou Changzhou, et al. Progress in the pharmacological activity and mechanism of action of Baicalin [J]. Drug Evaluation Study, 2024,47 (11): 2688-2696.
22. Zhong Gansheng. science of Chinese materia medica [M]. Beijing: China Traditional Chinese Medicine Press, 2016.
23. Yang Bin, Xiao Yongqing, Liang Ruixin, et al. Study on active chemical components in aster volatile oil [J]. Chinese Journal of Traditional Chinese Medicine, 2008,33 (3): 281-283.
24. Wang Fei. Law of sputum drugs for pulmonary diseases [D]. Shandong University of Traditional Chinese Medicine, 2012:1-41.
25. Man Gwan Wong. Pharmacological study on the suppression of cough, expectorant and asthma [J]. Bright Traditional Chinese Medicine, 2021,36 (20): 3525-3526.
26. Leon. A clinical safety evaluation study of representative expectorant containing Pinellia pinellia based on Mete analysis [D]. Beijing University of Traditional Chinese Medicine, 2019:1-164.
27. Wang Wanyi, Zhu Zhijun, Li Hangfei, Xu Shumei. Progress in chemical composition and pharmacological effects of pinellia pinellia and predictive analysis of quality markers [J]. Journal of Liaoning University of Traditional Chinese Medicine, 2024,26 (03): 203-215.
28. Xue Jinxu, MAO Huifang, Li Dongling, Ge Development, Liang Yonglin. "Huangdi Neijing" "the same qi" view [J]. Journal of Gansu University of Traditional Chinese Medicine, 2024,41 (03): 20-23.
29. Chen Xiping. Image comparison: clever traditional Chinese medicine treatment [J]. Traditional Chinese medicine health regimen, 2022,8 (07): 66-68.
30. Liu Yuying, Wan Shaofen. Progress of the pharmacological mechanism of phlegm-resolving traditional Chinese medicine in the prevention and treatment of lung cancer [J]. Sichuan Traditional Chinese Medicine, 2020,38 (05): 218-220.
31. Yin Xiuyin. Pharmacological analysis and efficacy of phlegm and cough granules in children [J]. The Electronic Journal of Cardiovascular Diseases of Integrated Traditional Chinese and Western Medicine, 2016,4 (06): 86-87.
32. Pu Fu Zhou. Pu Fu Zhou Medical [M]. Beijing: People's Health Press, 2005:141.

International Journal of Clinical Medicine & Pharmacology

https://doi.org/10.70731/5q7pm525

Clinical Significance and Potential Signal Pathway of Upregulated Pituitary Tumor-Transforming Gene 1 in Metastatic Prostate Cancer Based on Bioinformatic Methods

Jingxiao Li [a], Kunlin He [b], Gushing Li [b], Huafu Zhou [a], Jun Liu [a,*]

[a] *Department of Thoracic Surgery, The First Affiliated Hospital of Guangxi Medical University, Nanning, 530021, Guangxi Zhuang Autonomous Region, China*

KEYWORDS

PTTG1,
Prostate Cancer (PCa),
Metastatic Prostate Cancer (MPCa),
Differentially Co-Expressed Genes (DCEGs),
Biomarker Discrimination

ABSTRACT

This study examined the expression and clinical significance of pituitary tumor-transforming gene 1 (PTTG1) in prostate cancer (PCa) and metastatic prostate cancer (MPCa). Analysis of 19 PCa and 10 MPCa public datasets showed that PTTG1 expression was significantly upregulated in PCa (SMD=0.55, 95% CI: 0.29, 0.83) and MPCa (SMD=2.28, 95% CI: 1.38, 3.19). PTTG1 also demonstrated moderate discriminatory ability for PCa (AUC=0.75, 95% CI: 0.71, 0.79) and high discriminatory potential for MPCa from localized PCa (AUC=0.97, 95% CI: 0.95, 0.98). Differential co-expressed gene (DCEG) analysis identified 314 PTTG1-related genes, with CCNA2, CCNB1, and CDK1 emerging as key hub genes positively correlated with PTTG1. While most clinical parameters showed no correlation with PTTG1 expression, data from The Cancer Genome Atlas (TCGA) revealed an association between PTTG1 and both M-stage and recurrence. Enrichment analyses indicated that PTTG1 DCEGs were involved in cell division, nucleoplasm, protein binding, and the cell cycle pathway. These findings suggest that PTTG1 may serve as a marker for distinguishing MPCa from localized PCa and provide insights into its potential role in prostate cancer progression.

1. Introduction

Prostate cancer (PCa) brings a serious threat to health of patients in males, which is one of the most prevalent malignant tumor among males. In terms of incidence rate, PCa was identified as the most common cancer in males, and ranks the second most common mortality among cancers in males [1]. According to prediction of *Cancer Statistics, 2024*, about 34130 patients in United States will die caused by PCa [2]. To date, surgery and radiotherapy were considered as the main treatments for PCa in early stage, the 5-year-survival rate of patients after surgery or radiotherapy is able to reach 99% [3, 4]. Though localized PCa has a considerable prognosis, with the development of disease, the 5-year-survival

* Corresponding author. E-mail address: lj_gxmuyfy_c_t_s@163.com

Received 15 January 2025; Received in revised form 18 February 2025; Accepted 26 February 2025; Available online 28 February 2025.

rate of patients is less than 30% once tumor cells metastasize [5]. Previous studies had shown that the metastasis rate of PCa is increasing each year [6]. Unfortunately, early prediction for metastatic prostate cancer (MPCa) is immature, the molecular mechanisms of MPCa also had never been clarified yet. Therefore, it is vital to discover a molecular markers and explore the molecular mechanisms in MPCa.

Pituitary tumor-transforming gene 1 (PTTG1, also known as securin), located on 5q33.3, which is one of the major regulatory factors in separation of sister chromatids, transcription of mRNA and development of organs. Generally accepted function of PTTG1 is ensuring the stability of chromosome structure in mitotic stage [7, 8]. Recently, limited studies indicated that the expressed level of PTTG1 was upregulated in PCa, and might promote the development of PCa by regulating apoptosis of LNCaP cells [9]. Lin and colleagues reported that overexpressed PTTG1 could promote the occurrence of prostate cancer by activing MMP13 [10]. In vitro experiments, Huang et al. reported that the expression of PTTG1 was upregulated in PCa, and promote prostate cancer cell proliferation by regulating SMAD3 [11]. However, though PTTG1 expressed higher in PCa was also observed, Castilla et al. thought the downregulation of PTTG1 was able to promote the multiplication of prostate cancer cells through in vitro experiments [12]. Existed studies about the expression level of PTTG1 in PCa was consistent, but the functions of PTTG1 in PCa remains controversial. In addition, more stress was put on investigating the expression level of PTTG1 in localized PCa in previous studies, the expression level and molecular mechanism of PTTG1 in MPCa was still unclear.

Therefore, the present study is aiming to prove the expression level and effect of PTTG1 in PCa, meanwhile to investigate the expression and molecular mechanism of PTTG1 in MPCa, and the clinical value of PTTG1 differential expression in MPCa was identified. In addition, the co-expressed genes (CEGs) of PTTG1 were used to investigate the potential molecular mechanism in MPCa. PPI network analysis was conducted to determine the potential target genes of PTTG1 in MPCa. The molecular pathway of metastasis of PCa regulated by differential expressed PTTG1 was assessed through enrichment analysis.

2. Materials and Methods

2.1. Obtaining of the Expression Data of PTTG1 in PCa and MPCa

The microarray and RNA-seq data of PCa and MPCa were obtained from Gene Expression Omnibus (GEO), Sequence Read Archive (SRA), ArrayExpress, Oncomine and The Cancer Genome Atlas (TCGA) database. The following words were applied to retrieval datasets we need: (parastata OR prostatic gland OR prostate gland OR prostat*) AND (cancer OR carcinoma OR tumor OR neoplas* OR malignan* OR adenocarcinoma) AND (miR OR miRNA OR microRNA). The process of data screening was performed on Supplementary material 1 The microarray and RNA-seq data including PCa and non-PCa was showed on Figure 1, the microarray and RNA-seq data including MPCa and LPCa was showed on Figure 2. We downloaded the mRNA expression matrix data of mentioned series, and extracted mRNA expression data of PTTG1. Then, transferring PTTG1 expression data according to log2(x+1) conversion, the groups with cancer, normal, MPCa and LPCa patients were divided. RNA-seq data and clinical parameters of the TCGA and GTEx database were downloaded from UCSC Xena. The included datasets were showed in Table 1.

2.2. The Screening of PTTG1 Potential Target Genes in MPCa

2.2.1. The Screening of PTTG1 CEGs in MPCa

To gain the CEGs of PTTG1 in MPCa, we estimated Pearson's r-values of chips, and chose the gene for next step if p values < 0.05 and $r > 0.3$. The gene would be identified as CEG of PTTG1 when it appeared more than 5 times in 10 series.

2.2.2. The Screening of PTTG1 Differential Upregulated Genes in MPCa

We analyzed mRNA-seq series with limma-voom package and analyzed chip-seq with limma package, then we got DEGs in resepective series (p values $<$ 0.05, |log2FC| $>$ 1). The differential upregulated genes of PTTG1 in MPCa would be identified when it appeared more than 5 times in 10 series. Genes meeting from CEGs and differential upregulated genes were interacted and considered as PTTG1 potential target genes.

2.3. Functional Enrichment Analysis of Potential PTTG1 Targets

The potential target genes of PTTG1 were entered into the Database for Annotation, Visualization, and

Table 1 | The included databases with PTTG1 expression in PCa and non-PCa.

ID	Country	Platform	year	Number of samples	
				PCa	Non-PCa
GSE26910	Italy	GPL570	2011	6	6
GSE32448	USA	GPL570	2011	40	40
GSE32982	Finland	GPL570	2011	6	3
GSE38043	USA	GPL570	2012	3	3
GSE46602	Denmark	GPL570	2013	34	14
GSE69223	Germany	GPL570	2015	15	15
GSE104749	China	GPL570	2017	4	4
GSE27616	USA	GPL4133	2011	9	4
GSE12378	UK	GPL5175	2008	36	3
GSE72220	USA	GPL5175	2015	57	90
GSE94767	UK	GPL5175	2017	185	33
GSE28204	China	GPL6480	2011	4	4
GSE35988	USA	GPL6480	2012	76	12
GSE32571	Germany	GPL6947	2011	59	39
GSE134073	Germany	GPL11154	2020	56	8
GSE60329	Italy	GPL14550	2014	108	28
GSE73397	China	GPL20952	2015	3	3
GSE88808	USA	GPL22571	2016	49	49
GSE134051	Germany	GPL26898	2020	216	39
TCGA+GTEx	NA	NA	NA	499	152

NOX4, NADPH oxidase 4; PCa: prostate cancer; TCGA: The Cancer Genome Atlas; GTEx: The Genotype-Tissue Expression.

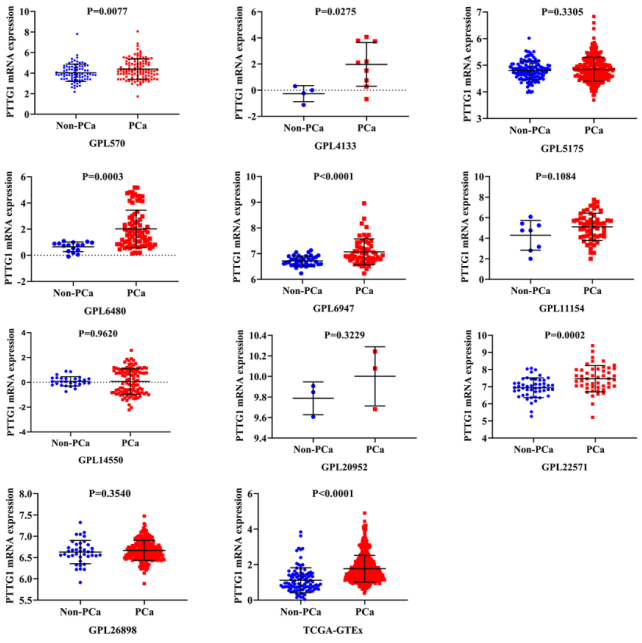

Figure 1 | The expression levels of PTTG1 in Non-PCa and PCa.

PTTG1, Pituitary tumor-transforming gene 1; PCa, prostate cancer.

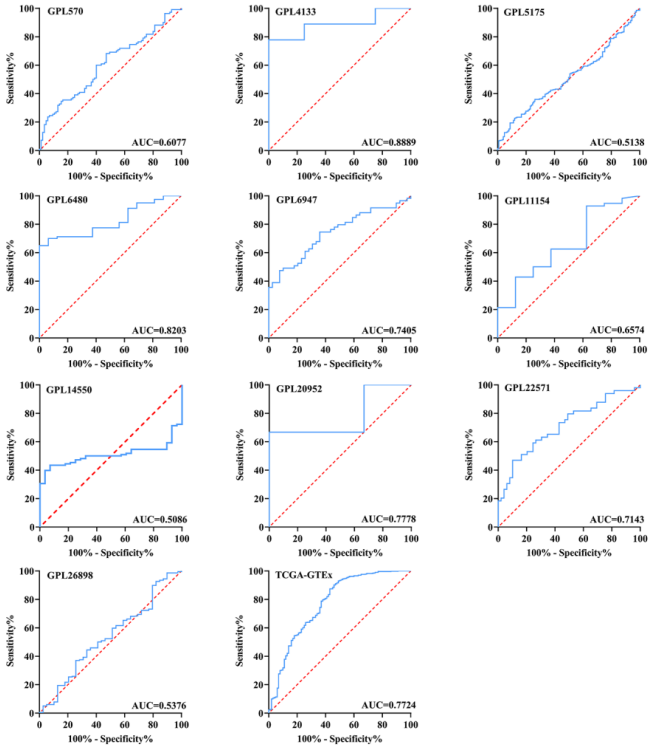

Figure 2 | ROC curves of PTTG1 in PCa.

PTTG1, Pituitary tumor-transforming gene 1; ROC, receiver operating characteristic; AUC, area under the curve;PCa, prostate cancer.

Table 2 | The means and standard deviations of PTTG1 expression values for PCa and non-PCa based on 11 studies.

Study	Sample type	PCa			Non-PCa		
		N	M	SD	N	M	SD
GPL570	Tissue	110	4.393	0.987	85	4.034	0.838
GPL4133	Tissue	9	1.971	1.676	4	-0.265	0.613
GPL5175	Tissue	278	4.847	0.455	126	4.802	0.345
GPL6480	Tissue	80	2.017	1.436	16	0.647	0.370
GPL6947	Tissue	59	7.068	0.504	39	6.717	0.192
GPL11154	Tissue	56	5.105	1.325	8	4.281	1.443
GPL14550	Tissue	108	0.072	1.029	28	0.081	0.379
GPL20952	Tissue	3	10.001	0.288	3	9.787	0.159
GPL22571	Tissue	49	7.466	0.767	49	6.939	0.575
GPL26898	Tissue	216	6.667	0.234	39	6.628	0.274
TCGA+GTEx	Tissue	499	1.767	0.754	152	1.120	0.708

NOX4, NADPH oxidase 4; PCa: prostate cancer; N: number; M: mean; SD: standard deviation; TCGA: The Cancer Genome Atlas; GTEx: The Genotype-Tissue Expression.

Integrated Discovery (DAVID) 6.8. for Gene Ontology (GO) and Kyoto Encyclopedia of Genes and Genomes (KEGG) analysis to predict potential signal pathways. The terms with p values < 0.05 were screened out. The PPI network was constructed by Search Tool for the Retrieval of Interacting Genes (STRING) and Cytoscape software 3.8.2. CCNA2, CCNB1 and CDK1 had the highest degree of connectivity in the PPI network and were further discussed.

2.4. Correlation Analysis Between PTTG1 and CCNA2, CCNB1 and CDK1

The expression data and clinical parameters of PTTG1 and CCNA2, CCNB1 and CDK1 in MPCa was obtained from public database. And then the correlation between miRNA-221-3p and CELSR3 was analyzed.

2.5. Immune-Related Analysis

The correlation modules supported by Tumor Immune Estimation Resource (TIMER) 2.0 and Gene Expression Profiling Interactive Analysis (GEPIA) were used to assess the abundance of immune infiltrates in PCa tumor and paired paracancerous tissue. We verified significantly correlated immune genes of PTTG1 through GEPIA database.

2.6. Statists Analysis

All statistical analysis were computed using SPSS 23.0. Student's t-tests were used to assess differences between different groups, mean ± standard deviation was represent values. In addition, receiver operating characteristic (ROC) curves analysis was conducted to evaluate sensitivity and specificity of above datasets. We also used Stata 14.0 to estimate standard mean difference (SMD) and summary ROCs (sROCs). Study was considered to be heterogeneous when $P < 0.05$ or $I^2 > 50\%$, and a random-effects model would be adopted, or else a fixed-effects model was applied. To probe the source of heterogeneity, subgroup and sensitivity analysis was applied. Begg's test and Egger's test were applied to uncover publication bias. Supplementary material 2 depicts our study workflow.

3. Result

3.1. Expression and Discrimination Potential of PTTG1 in PCa

First, a total of 19 qualified GEO chips and some TCGA+GTEx sequencing data were collected, including 1,467 prostate cancer samples and 549 normal samples, from which we extract the expression data of PTTG1. The expression of PTTG1 in each mRNA chip or section of TCGA+GTEx sequencing data was clarified through independent t-tests. According to collected data, PTTG1's mRNA was found to be upregulated in prostate cancer tissues compared to normal tissues (Table.2 and Fig.1), the ROC curves of all data was drawn (Fig. 2). The meta-analysis results indicated that PTTG1 was significantly upregu-

Table 3 | The means and standard deviations of PTTG1 expression values in LPCa and MPCa based on 10 studies

Study	Country	Year	Sample type	MPCa			LPCa		
				N	M	SD	N	M	SD
GSE3325	USA	2005	tissue	4	11.805	1.797	5	8.945	0.177
GSE32269	USA	2011	tissue	29	6.613	1.247	22	4.879	1.257
GSE77930	USA	2016	tissue	149	3.446	0.848	22	0.791	1.079
GSE6919	USA	2007	tissue	25	8.010	0.557	66	6.511	0.548
GSE116918	UK	2018	tissue	22	0.172	0.306	225	0.148	0.121
GSE68882	USA	2015	tissue	9	7.848	0.263	23	7.579	0.265
GSE55935	Norway	2014	tissue	8	9.371	1.339	38	6.281	0.902
GSE27616	USA	2011	tissue	4	13.937	1.367	5	-3.681	0.543
GSE35988	USA	2012	tissue	32	14.108	1.411	59	13.309	1.353
TCGA	NA	NA	tissue	21	2.506	0.890	478	1.733	0.722

CELSR3: cadherin EGF LAG seven-pass G-type receptor 3; LPCa: localized prostate cancer; MPCa: metastatic prostate cancer; N: number; M: mean; SD: standard deviation; TCGA: The Cancer Genome Atlas.

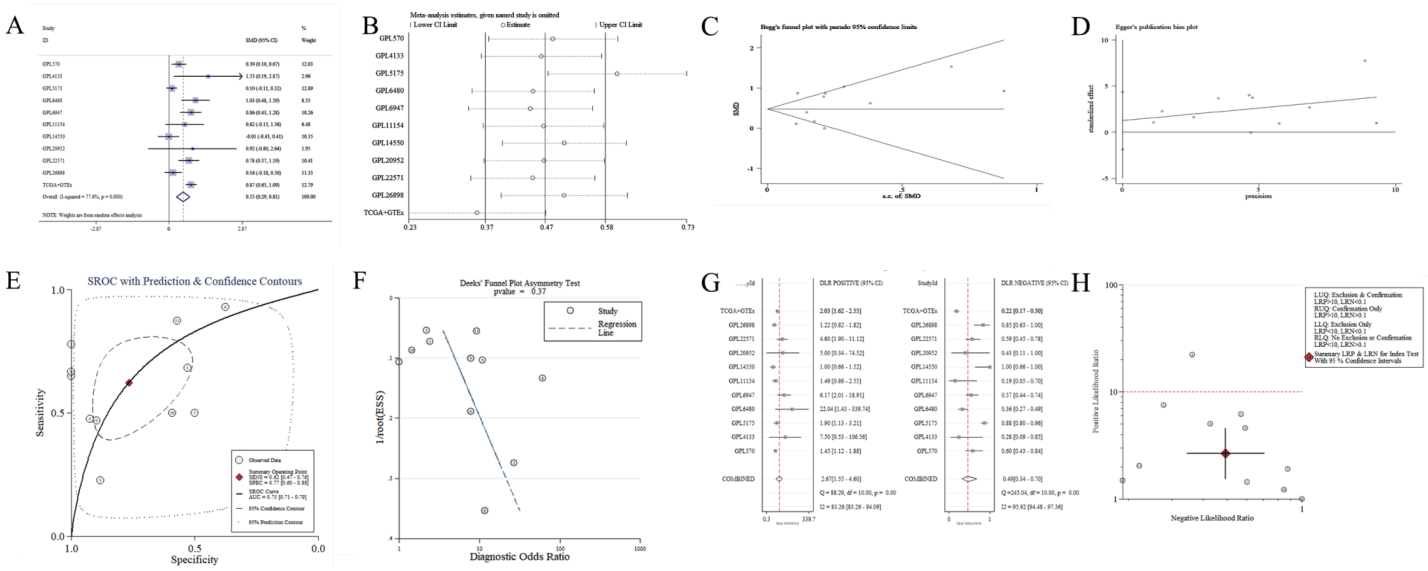

Figure 3 | The expression level and discrimination potential of PTTG1 in PCa.

(A) Forest plot showing the combined SMD of 0.55 (0.29 to 0.81), indicating that the expression of PTTG1 in PCa is higher compared to that of non-PCa. (B) Sensitivity analysis showing the combined SMD is stable. (C) Begg's test showing no publication bias ($p > 0.05$). (D) Egger's test showing no publication bias ($p > 0.05$). (E) sROC curve assessing the discrimination potential of PTTG1 in PCa. (F) Funnel chart showed no publication bias ($p = 0.37$). (G)The expression of PTTG1 is able to distinguish PCa and non-PCa. (H) Likelyhood ratio of PTTG1 in PCa. PTTG1, Pituitary tumor-transforming gene 1; SMD, standard mean deviation; CI, confidence interval; sROC, summary receiver operating characteristic; AUC, area under the curve; PCa, prostate cancer.

lated in PCa tissues with the SMD of the random-effect model being 0.55 (95CI%: 0.29, 0.83), and there was no publication bias (Fig. 3). We also did not find significant data heterogeneity (Fig.3). In addition, the AUC of sROC was 0.75 (95%CI: 0.71, 0.79), with pooled sensitivity and specificity being 0.62 and 0.77 which showed PTTG1 has a medium discrimination potential to discriminate PCa from normal cells (Fig. 3).

3.2. Expression and Discrimination Potential of PTTG1 in MPCa Based on Chips, TCGA Data

Subsequently, 303 metastatic prostate cancer (MPCa) samples and 943 localized prostate

cancer(LPCa) samples were performed to the follow-up research (Fig.4 and Fig.5). We found the expression of PTTG1 was clearly high expressed in MPCa tissues with the SMD of the random-effect model being 2.28 (95CI%: 1.38, 3.19) (Table 3 and Fig.6), the result was no publication bias (Fig.6). Similarly, we did not find the source of heterogeneity (Fig.6). After producing the ROC curves and constructing the sROC curve, we thought PTTG1 has an extremely high potential to be identified as a target to discriminate MPCa from LPCa cells, for the AUC of sROC was 0.97 (95%CI: 0.95, 0.98) (Fig.5 and Fig.6).

3.3. Identification of PTTG1 DCEGs in MPCa

After interacting 1054 CEGs with 742 DEGs, 314 genes were identified as PTTG1 DCEGs in MPCa totally.

3.4. Enrichment Analysis of PTTG1 DCEGs

Through GO analysis, PTTG1 DCEGs were significantly enriched in cellular response to cell division, nucleoplasm and protein. Moreover, KEGG analysis demonstrated PTTG1 DCEGs was significantly enriched in cell cycle (Fig.7). The Fig.8 presents PPI network of PTTG1 DCEGs. CCNA2, CCNB1 and CDK1 were identified as PTTG1 hubgenes in MPCa (Fig.9).

3.5. Association of PTTG1 Expression With Hubgenes and Clinical Parameters

As mentioned, CCNA2, CCNB1 and CDK1 were identified as hubgenes of PTTG1 in MPCa, the correlation between PTTG1 and hubgenes was showed on Fig.10. Interestingly, there were significant differences in the expression of M-stage and recurrence in the larger TCGA samples (Fig.11). As for other factors such as T, N stages of PCa or ages, there is no significant relevance to be found.

4. Discussion

Herein we extracted the mRNA microarray and RNA-Seq data with 325 MPCa samples and 724 LPCa samples from GEO and TCGA databases, and determined the PTTG1 expression level by estimating SMD and sROCS. Our analysis was observed that the PTTG1 expression level in MPCa was higher than that in LPCa. In addition, PTTG1 is also highly expressed in PCa. Moreover, enrichment analysis were also used to explore the potential molecular mecha-

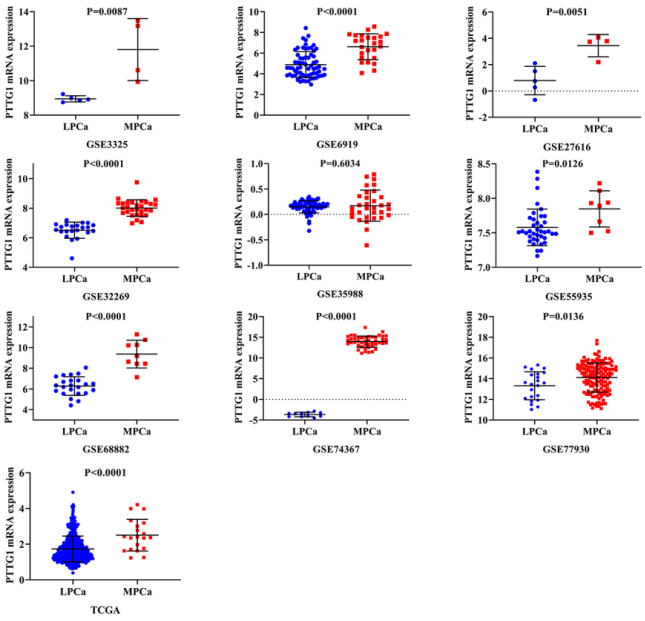

Figure 4 | The expression levels of PTTG1 in LPCa and MPCa

PTTG1, Pituitary tumor-transforming gene 1; MPCa, metastatic prostate cancer; LPCa, localized prostate cancer.

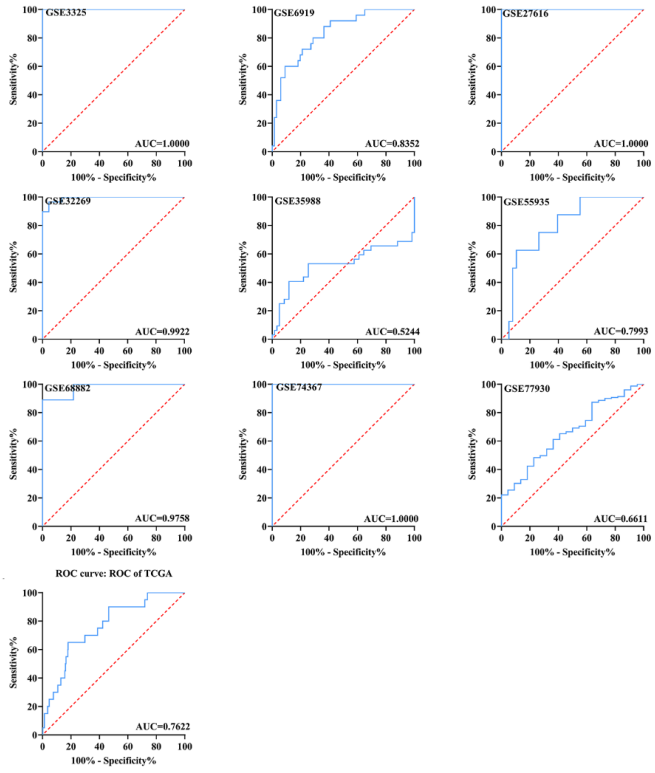

Figure 5 | ROC curves of PTTG1 in MPCa.

PTTG1, Pituitary tumor-transforming gene 1; ROC, receiver operating characteristic; AUC, area under the curve; MPCa, metastatic prostate cancer.

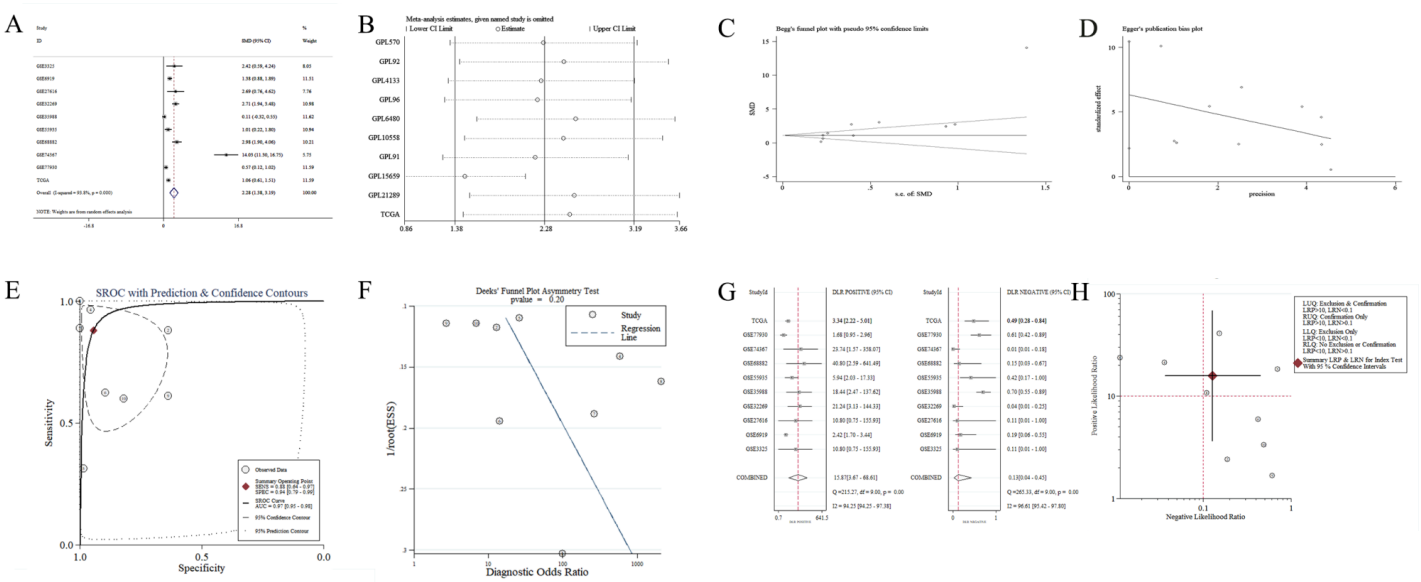

Figure 6 | The expression level and discrimination potential of PTTG1 in MPCa

(A) Forest plot showing the combined SMD of 2.28 (1.38 to 3.19), indicating that the expression of PTTG1 in MPCa is higher compared to that of LPCa. (B) Sensitivity analysis showing the combined SMD is stable. (C) Begg's test showing no publication bias ($p > 0.05$). (D) Egger's test showing no publication bias ($p > 0.05$). (E) sROC curve assessing the discrimination potential of PTTG1 in PCa. (F) Funnel chart showed no publication bias ($p = 0.20$). (G)The expression of PTTG1 is able to distinguish MPCa and LPCa. (H) Likelyhood ratio of PTTG1 in MPCa. PTTG1, Pituitary tumor-transforming gene 1; SMD, standard mean deviation; CI, confidence interval; sROC, summary receiver operating characteristic; AUC, area under the curve; PCa, prostate cancer.

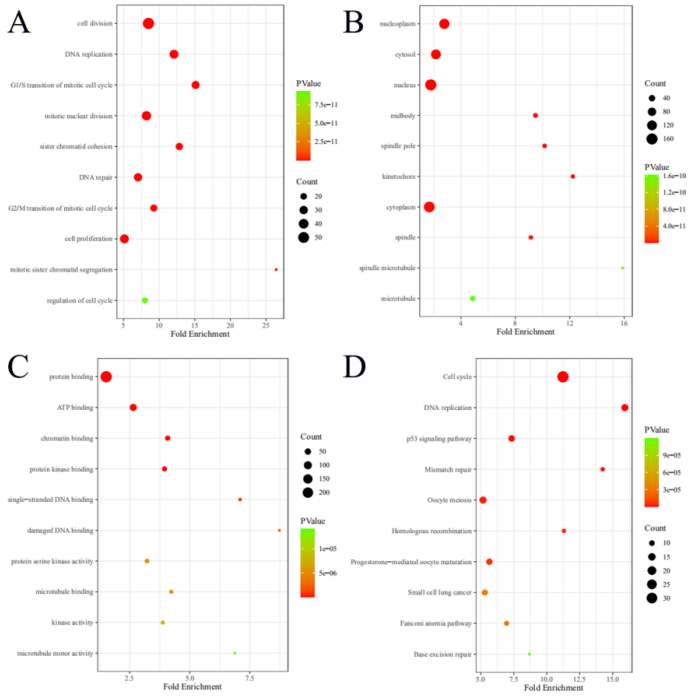

Figure 7 | GO and KEGG analysis based on PTTG1 related differentially expressed and co-expressed genes

(A) Biological process; (B) Cellular component; (C) Molecular function; (D) KEGG pathway. GO, Gene Ontology; KEGG, Kyoto Encyclopedia of Genes and Genomes; PTTG1, Pituitary tumor-transforming gene 1.

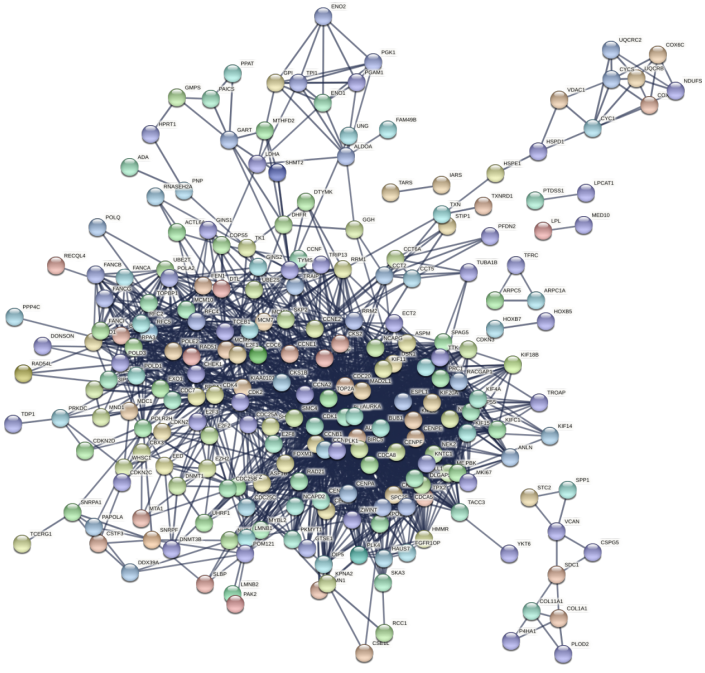

Figure 8 | PPI network analysis of PTTG1 target genes in MPCa

PPI, Protein-protein interaction; PTTG1, Pituitary tumor-transforming gene 1; MPCa, metastatic prostate cancer.

nisms and signal pathways of differential expressed PTTG1 in regulating of PCa metastasis.

As a multifunctional protein, PTTG1 plays an important role in cell transformation, repairing of DNA, and transcriptional regulation. Previous study have shown that overexpression of PTTG1 plays important roles in accelerating the division and differentiation of tumor cells and the formation of tumor cells [13]. Currently, many studies have shown that upregulated PTTG1 was associated with poor prognosis in many malignant tumors, including liver cancer, lung cancer, breast cancer and esophageal squamous cell carcinoma [14-18]. Through changing the transcriptional profile of siRNA-mediated LNCap-AI cells, Cao et al. found that downregulated PTTG1 could inhibit the invasions of PCa cells and promote their apoptosis [19]. After treating LNCap cells with paclitaxel, Castilla et al. believed that the overexpression of PTTG1 in PCa was a protective factor in tumor apoptosis [12]. Moreover, PTTG1 has also been shown to be associated with MPCa. Dai et al. predicted that PTTG1 was differential expressed in MPCa by bioinformatics method, which had been verified in small samples [20]. However, to our knowledge, no studies have proved the differences of PTTG1 expression levels between MPCa and LPCa. Fraune et al. concluded that the differential expression of PTTG1 in MPCa but the result was not statistically significant [21]. It is noteworthy that, for the first time, we reported the upregulation of PTTG1 expression is significantly associated with metastasis of PCa and have a high potential to discriminate MPCa from LPCa cells.

At present, the molecular mechanism of PTTG1 in MPCa transfer had never been reported. Lin et al. suggested that upregulated PTTG1 might upregulate the expression of MMP3 through the PI3K/Akt pathway, and then promoted PCa metastasis. A research managed by Zhang reported that androgen response elements on the PTTG1 promoter increased the affinity of androgen and the receptor, which promoted PCa metastasis [22]. Nevertheless, existed researches were not able to clarify the potential signal pathways that how PTTG1 influences the metastasis of PCa. Our enrichment results showed that the DCEGs of PTTG1 were significantly enriched in the cell cycle pathway. After searching the literature, we found some meaningful views. It has been reported that high PTTG1 expression probably promoted the proliferation of PCa cells by inhibiting TGFβ signaling mediated through activating the cell cycle inhibitor SMAD3, which was similar to our results [11]. Al-

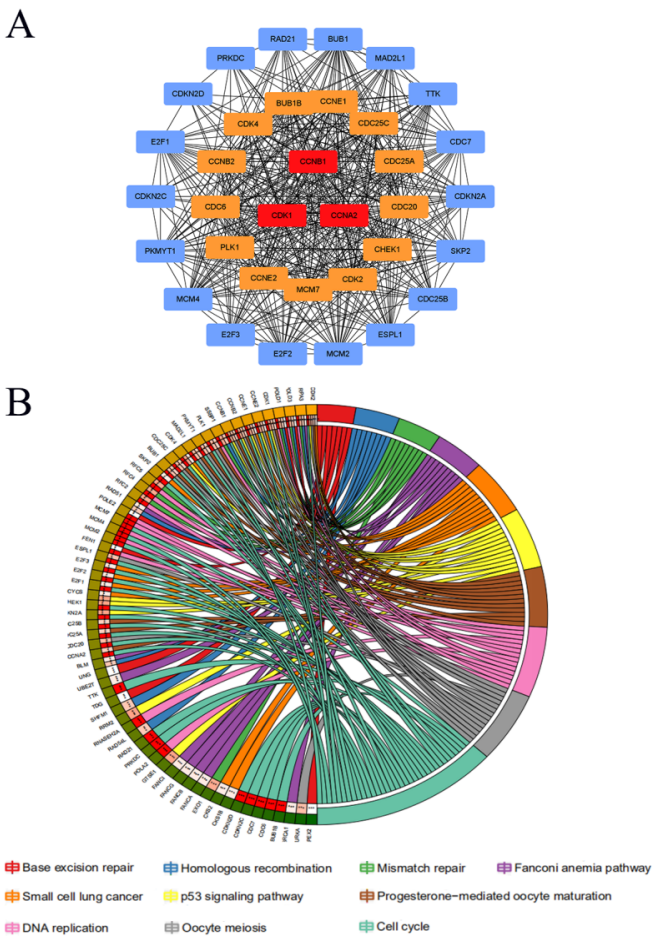

Figure 9 | PTTG1 related differentially expressed and co-expressed genes were significantly enriched in Cell cycle pathway; CCNA2, CCNB1 and CDK1 were identified as hubgenes in Cell cycle

(A) Ten signaling pathways were analyzed based on KEGG enrichment; (B) The 34 genes enriched in Cell cycle pathway of KEGG were further explored. PTTG1, Pituitary tumor-transforming gene 1;KEGG, Kyoto Encyclopedia of Genes and Genomes.

though there is no direct evidence that overexpressed PTTG1 promotes PCa metastasis by participating in the cell cycle pathway, many studies have reported that the occurrence and development of MPCa was correlated with the cell cycle pathway. Huang et al. found that Ganoderma tsugae ethanol extract was able to inhibit the cell cycle by inhibiting the expression of cyclin, and blocking the PI3K/Akt and MAPK/ERK signaling pathways, and then inhibiting the proliferation and metastasis of PCa cells [23]. Marques et al. indicated that Radium-223 had the ability to activate cell cycle checkpoints, which causing MPCa cell cycle arrest and promoting cell death [24]. Besides, existed studies also suggested that the cell cycle pathway was involved in the metastasis of a vari-

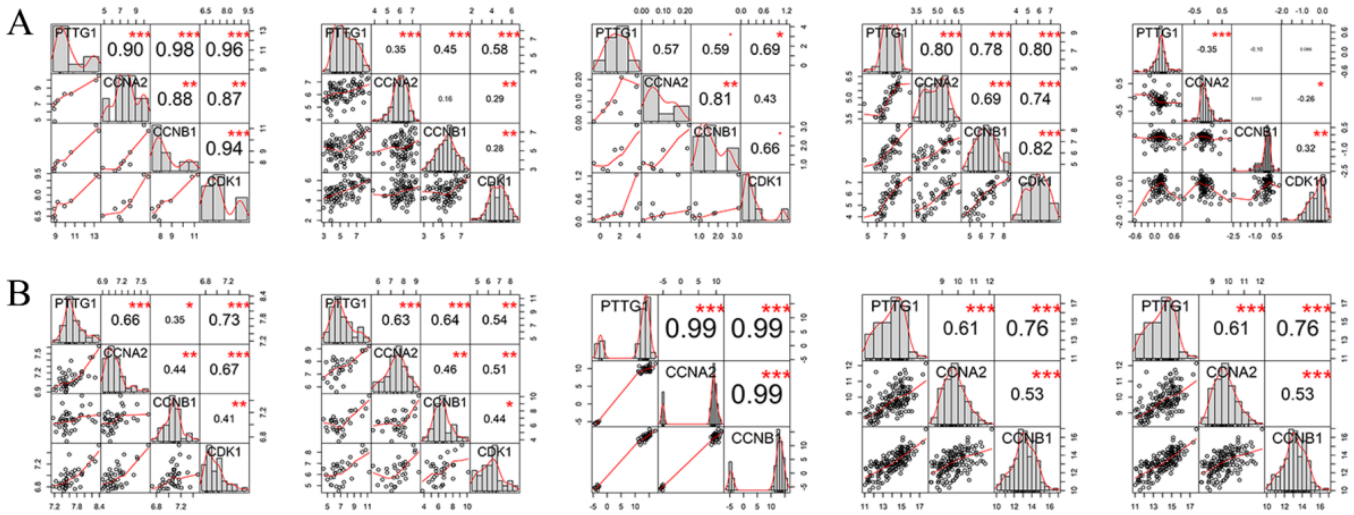

Figure 10 | The expression of PTTG1 is positively correlated with the expression of CCNA2, CCNB1 and CDK1

The number in bold represents Pearson correlation coefficient, and one or more " * " represent significant difference. A: GSE3325, GSE6919, GSE27616, GSE32269, GSE35988; B: GSE55935, GSE68882, GSE74367, GSE77930, TCGA.

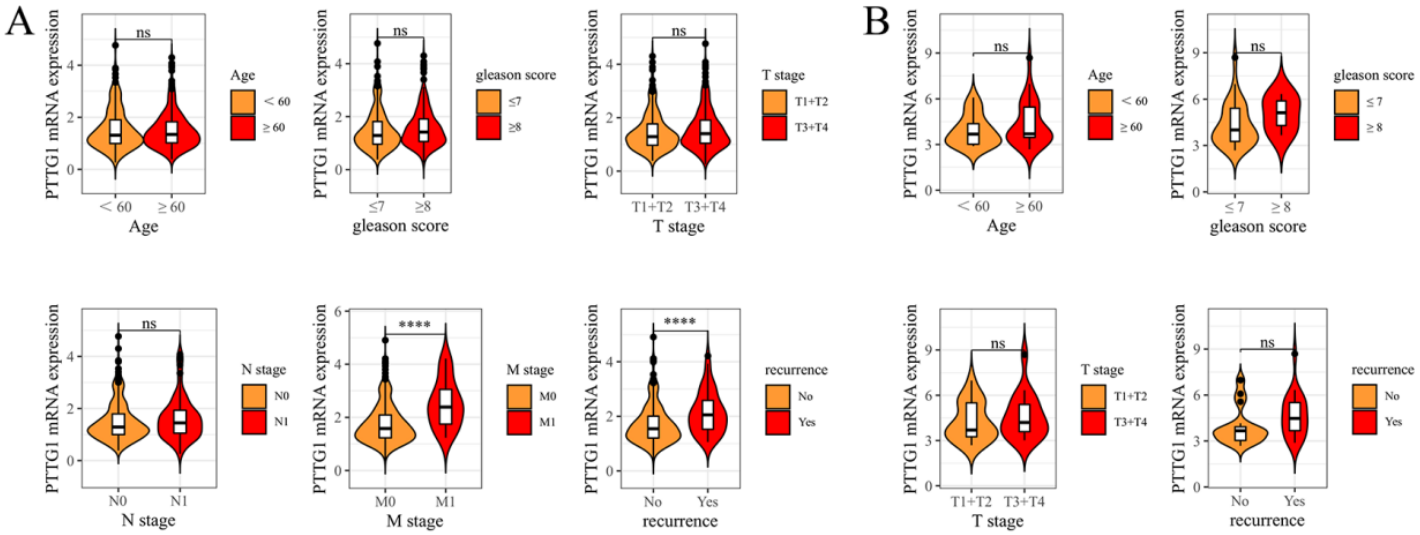

Figure 11 | Correlation analysis of clinical parameters

One or more " * " represent significant difference. (A) TCGA data set; (B) GSE46602 data set.

ety of cancers, such as hepatocellular carcinoma and breast cancer [25, 26]. However, whether the upregulated PTTG1 promotes the occurrence and development of MPCa through the cell cycle pathway still requires further in vitro and in vivo experiments.

By analyzing PTTG1 expression levels in PCa patients with different clinical parameters, the authors found that PTTG1 expression levels did not differ among patients with different ages, stages, relapses, and Gleason scores in datasets with a small sample. However, in larger sample sizes (data from TCGA), we found that PTTG1 is upregulated in patients with tumor metastatic and recurrence, which is very interesting. In the processes of literature retrieval, we did not find any studies that reported the relationship between the expression level of PTTG1 and patients with different clinical parameters. Our results provides a new research idea and need to be verified with more samples in the future.

This study also has some limitations: (1) a significant heterogeneity was observed in this study. Due to insufficient sample size and sample information, we

were unable to find the source of heterogeneity, a random-effects model was applied. Further validation of our findings is required in a larger clinical cohort. (2) all the samples of MPCa herein were collected from tissues, thus the expression of PTTG1 in the body fluids of MPCa should be estimated to verify their diagnostic value. (3) the functions of PTTG1 and three identified hubgenes in MPCa need to be further validated in vivo and in vitro.

In conclusion, by analyzing samples from public databases, we proposed for the first time that PTTG1 is upregulated in MPCa and plays an important role in the occurrence and development of MPCa.

Reference

1. Sung, H., et al., Global Cancer Statistics 2020: GLOBOCAN Estimates of Incidence and Mortality Worldwide for 36 Cancers in 185 Countries. CA Cancer J Clin, 2021. **71**(3): p. 209-249.
2. Siegel, R.L., A.N. Giaquinto, and A. Jemal, *Cancer statistics, 2024.* CA Cancer J Clin, 2024. **74**(1): p. 12-49.
3. Hamdy, F.C., et al., 10-Year Outcomes after Monitoring, Surgery, or Radiotherapy for Localized Prostate Cancer. N Engl J Med, 2016. **375**(15): p. 1415-1424.
4. Wu, X., et al., Increased EZH2 expression in prostate cancer is associated with metastatic recurrence following external beam radiotherapy. Prostate, 2019. **79**(10): p. 1079-1089.
5. Kelly, S.P., et al., Past, Current, and Future Incidence Rates and Burden of Metastatic Prostate Cancer in the United States. Eur Urol Focus, 2018. **4**(1): p. 121-127.
6. Russler-Germain, D.A. and B.S. Kahl, Recent Advances in Antibody Drug Conjugates for Lymphoma. Oncology (Williston Park), 2020. **34**(12): p. 522-534.
7. Tong, Y. and T. Eigler, Transcriptional targets for pituitary tumor-transforming gene-1. J Mol Endocrinol, 2009. **43**(5): p. 179-85.
8. Hsieh, Y.Y., T.P. Liu, and P.M. Yang, In silico repurposing the Rac1 inhibitor NSC23766 for treating PTTG1-high expressing clear cell renal carcinoma. Pathol Res Pract, 2019. **215**(6): p. 152373.
9. Wei, Y.Y., et al., [Down-regulated PTTG1 expression promotes the senescence of human prostate cancer LNCaP-AI]. Zhonghua Nan Ke Xue, 2019. **25**(3): p. 216-222.
10. Lin, Y.H., et al., Pituitary tumor-transforming gene 1 regulates invasion of prostate cancer cells through MMP13. Tumour Biol, 2015.
11. Huang, S., et al., PTTG1 inhibits SMAD3 in prostate cancer cells to promote their proliferation. Tumour Biol, 2014. **35**(7): p. 6265-70.
12. Castilla, C., et al., Prostate cancer cell response to paclitaxel is affected by abnormally expressed securin PTTG1. Mol Cancer Ther, 2014. **13**(10): p. 2372-83.
13. Ma, K., et al., Expression of Serum PTTG1 in Laryngeal Carcinoma and Its Correlation to Prognosis. Clin Exp Otorhinolaryngol, 2020. **13**(1): p. 64-68.
14. Tao, H., et al., [Pituitary tumor transforming gene 1 (PTTG1) is highly expressed and associated with poor prognosis in patients with hepatocellular carcinoma]. Xi Bao Yu Fen Zi Mian Yi Xue Za Zhi, 2020. **36**(4): p. 337-343.
15. Qiu, M., et al., aarF domain containing kinase 5 gene promotes invasion and migration of lung cancer cells through ADCK5-SOX9-PTTG1 pathway. Exp Cell Res, 2020. **392**(1): p. 112002.
16. Yin, L., et al., Simvastatin Suppresses Human Breast Cancer Cell Invasion by Decreasing the Expression of Pituitary Tumor-Transforming Gene 1. Front Pharmacol, 2020. **11**: p. 574068.
17. Pan, X.W., et al., Identification of a novel cancer stem cell subpopulation that promotes progression of human fatal renal cell carcinoma by single-cell RNA-seq analysis. Int J Biol Sci, 2020. **16**(16): p. 3149-3162.
18. Chen, S.W., et al., The Clinical Significance and Potential Molecular Mechanism of PTTG1 in Esophageal Squamous Cell Carcinoma. Front Genet, 2020. **11**: p. 583085.
19. Cao, X.L., et al., [Downregulation of PTTG1 expression inhibits the proliferation and invasiveness and promotes the apoptosis of human prostate cancer LNCaP-AI cells]. Zhonghua Nan Ke Xue, 2017. **23**(7): p. 589-597.
20. Dai, L., et al., CDC20 and PTTG1 are Important Biomarkers and Potential Therapeutic Targets for Metastatic Prostate Cancer. Adv Ther, 2021. **38**(6): p. 2973-2989.
21. Fraune, C., et al., Upregulation of PTTG1 is associated with poor prognosis in prostate cancer. Pathol Int, 2020. **70**(7): p. 441-451.
22. Zhang, Z., et al., PTTG1, A novel androgen responsive gene is required for androgen-induced prostate cancer cell growth and invasion. Exp Cell Res, 2017. **350**(1): p. 1-8.
23. Huang, W.C., et al., Chinese Herbal Medicine Ganoderma tsugae Displays Potential Anti-Cancer Efficacy on Metastatic Prostate Cancer Cells. Int J Mol Sci, 2019. **20**(18).
24. Marques, I.A., et al., Kinetics of radium-223 and its effects on survival, proliferation and DNA damage in lymph-node and bone metastatic prostate cancer cell lines. Int J Radiat Biol, 2021. **97**(5): p. 714-726.
25. Huang, J.L., et al., The long non-coding RNA PTTG3P promotes cell growth and metastasis via up-regulating PTTG1 and activating PI3K/AKT signaling in hepatocellular carcinoma. Mol Cancer, 2018. **17**(1): p. 93.
26. Meng, C., et al., Estrogen-regulated PTTG1 promotes breast cancer progression by regulating cyclin kinase expression. Mol Med, 2020. **26**(1): p. 33

Supplementary material 1 | The process of data screening

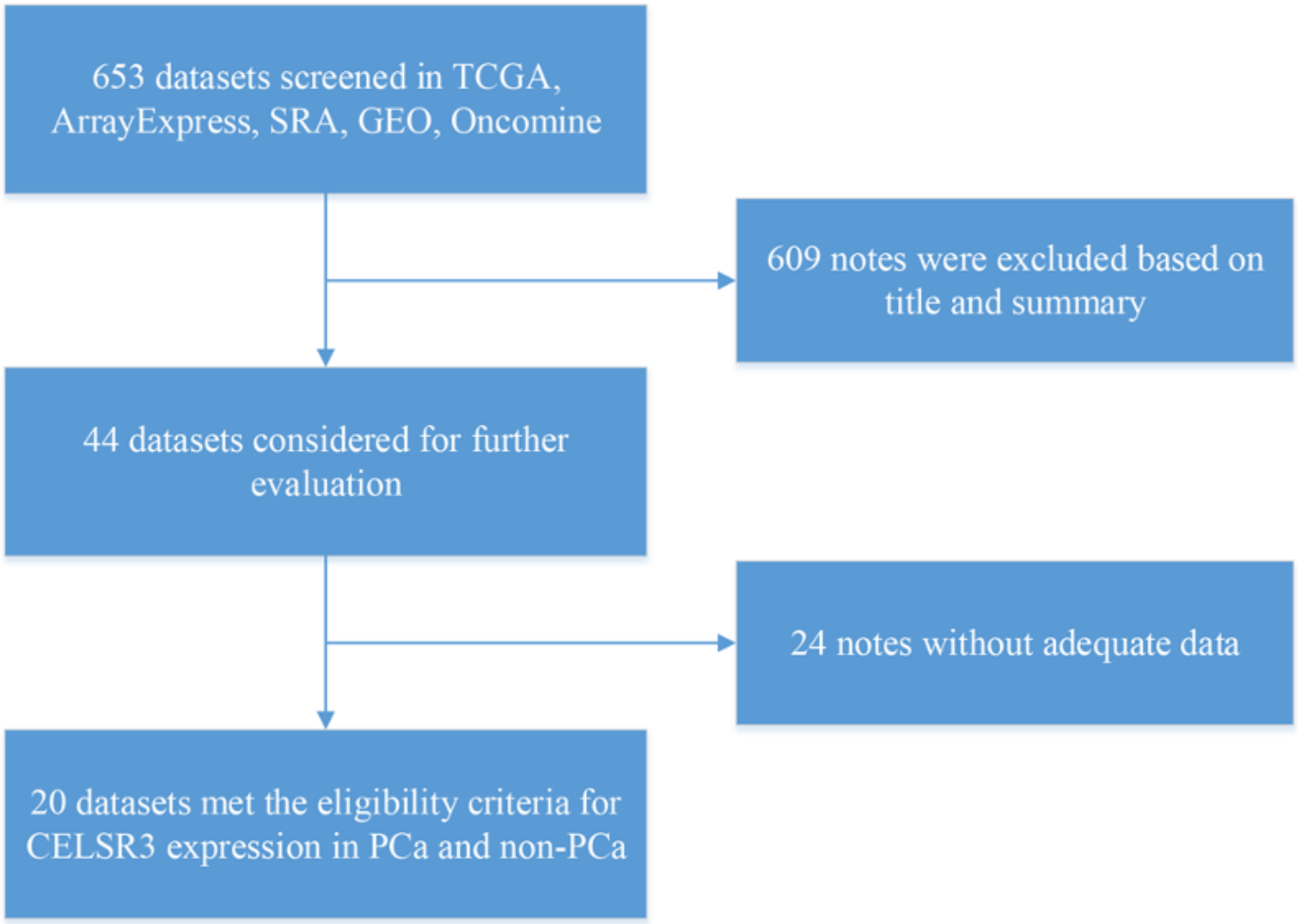

Supplementary material 2 | The study workflow

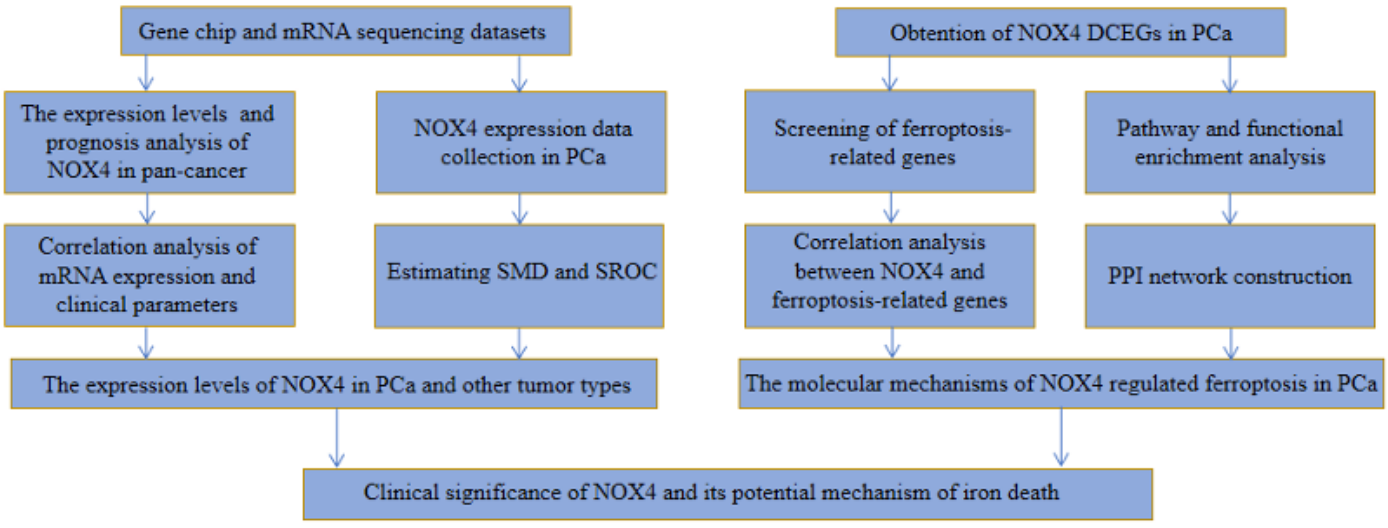

International Journal of Clinical Medicine & Pharmacology

https://doi.org/10.70731/t1kn1t14

Delayed Foam Rolling Outperforms Immediate Application: Mechanistic Synergy With Post-Exercise Repair Phases Reduces DOMS and Restores Muscle Function

Qiuyu Ruan [a], Wei Ni [a,*]

[a] *School of Physical Education, Shanghai Normal University, Shanghai 201418, China*

KEYWORDS

Foam Rolling,
Delayed-Onset Muscle Soreness,
Muscle Recovery,
Mechanical Stress,
Neuromuscular Function.

ABSTRACT

A randomized controlled trial was conducted with 66 male track and field jumpers to evaluate the effects of immediate and delayed foam rolling (FR) on muscle recovery. Participants performed a standardized exercise protocol and were divided into three groups: immediate FR post-exercise, delayed FR 15 hours post-exercise, and a no-intervention control group. Recovery was measured through vertical jump power and pressure pain threshold (PPT) to assess delayed-onset muscle soreness (DOMS). While both FR protocols significantly reduced DOMS compared to the control, only the delayed FR group showed meaningful improvements in jump power recovery. Delayed FR appears more effective due to its timing, allowing initial inflammation and repair processes to occur before intervention, which enhances tissue remodeling and waste clearance. These results suggest that delayed FR (≥15 hours post-exercise) is a more effective recovery strategy for athletes.

1. Introduction

Foam rolling (FR) training, a form of self-myofascial release (SMR) technique, is currently one of the most popular SMR methods due to its large rolling area and standardized operational procedures. (Michalak et al. 2024) Although existing studies have demonstrated that FR may enhance flexibility, facilitate muscle recovery, improve athletic performance, and reduce delayed onset muscle soreness (DOMS), the results remain inconclusive due to heterogeneity in research methods.(Cheatham et al. 2015) Emerging evidence suggests that the immediate post-exercise period (0–12 hours) coincides with a pro-inflammatory peak phase, during which mechanical loading may exacerbate exercise-induced microtrauma. In contrast, the subsequent repair phase (12–24 hours post-exercise) is characterized by heightened fibroblast activity, where controlled interventions such as foam rolling (FR) can leverage shear forces to facilitate organized collagen realignment and tissue remodeling.(Friden and Lieber 1992, Hendricks et al. 2020, Aune et al. 2019) Concurrently, emerging evidence supports the efficacy of immediate post-exercise FR. Acute FR application reduces arterial stiff-

* Corresponding author. E-mail address: nw1979@shnu.edu.cn

Received 7 February 2025; Received in revised form 18 February 2025; Accepted 24 February 2025; Available online 28 February 2025.

Table 1 | Participant Characteristics

Group	Age (years)	Height (cm)	Weight (kg)
Experimental Group 1(E1)	22.5 ± 1.5	180 ± 5	75 ± 5
Experimental Group 2(E2)	23 ± 1.8	178 ± 4.5	73 ± 4.8
Control Group(C)	22.8 ± 1.6	179 ± 4.7	74 ± 4.9

ness and elevates nitric oxide bioavailability, transiently enhancing range of motion (ROM).(Pearcey et al. 2015) Mechanistically, mechanical pressure activates mechanotransduction pathways that drive transcriptional upregulation of COX7B and ND1, accelerating muscle repair,(Crane et al. 2012) while concurrently enhancing lymphatic clearance of metabolic byproducts (e.g., lactate, myoglobin) to mitigate inflammation.(Baechle and Earle 2008) Notably, acute FR intervention correlates with diminished expression of stress markers (e.g., heat shock proteins) and pro-inflammatory cytokines,(Crane et al. 2012) alongside elevated neutrophil mobilization and attenuated plasma creatine kinase levels,(Smith et al. 1994) collectively suggesting optimized tissue recovery with reduced secondary damage.

In this study, we conducted experiments to investigate: (i) the effects of immediate versus delayed (15 hours post-exercise) FR on athletic performance recovery; and (ii) the impact of immediate versus delayed FR on the occurrence of DOMS. We hypothesized that: (i) there would be no significant differences between the two FR timing protocols regarding athletic performance recovery; and (ii) all participants would experience DOMS post-exercise, but the decline in PPT would be less pronounced in the FR groups.

2. Methods

2.1. Sample Size Justification

A priori power analysis was performed using G*Power 3.1 (Heinrich-Heine-Universität Düsseldorf, Germany) to determine the minimum sample size required for detecting medium-effect differences among groups. Based on a one-way ANOVA design (three groups: immediate FR, delayed FR, control) with an assumed effect size of (f = 0.25) (Cohen's convention for medium effects), α = 0.05 (two-tailed), and power = 0.80, the analysis yielded a total sample size of 66 participants (22 per group). To account for potential attrition (estimated at 10%), the target enrollment was adjusted to 73 participants. This calculation aligns with prior studies investigating foam rolling interventions and DOMS recovery, ensuring robust detection of clinically meaningful differences in neuromuscular function and pain thresholds.Shanghai Normal University Academic Ethics and Ethics Committee approved the study.

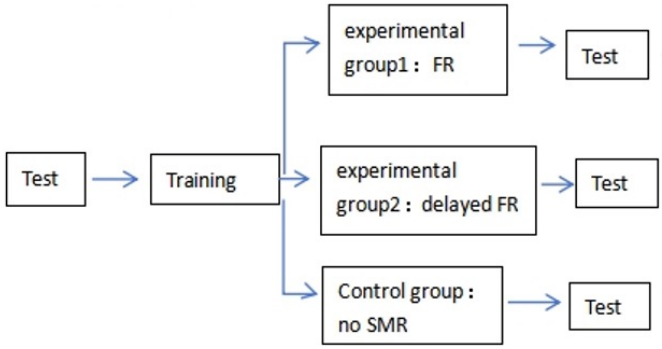

Figure 1 | Flowchart

2.2. Participants

Sixty-six male track and field athletes specializing in jumping events, with over two years of training experience, participated in the study（Table 1）. Participants were randomly assigned to Experimental Group 1 (immediate FR), Experimental Group 2 (delayed FR), or the control group (no FR), with eight participants in each group. All participants volunteered for the study, had no acute joint or muscle injuries in the past six months, and had at least two years of resistance training experience.

2.3. Design

The study included two experimental groups and a control group. All participants were familiarized with the experimental procedures prior to the study (Figure 1). Experimental Group 1 performed FR immediately after the exercise protocol, Experimental Group 2 performed FR 15 hours post-exercise (at 8:00 AM the next day), and the control group did not perform

Figure 2 | Exercise Protocol (from top to bottom: half squat, high pull from knee level, pogo jump;From left to right, the start and end poses)

any form of SMR. Testing was conducted at 2:00 PM the day after the exercise protocol.

2.4. Exercise Protocol

Participants received instruction on the exercise protocol one week in advance and were required to execute it accurately. The training included traditional resistance exercises to simulate the daily training of track and field athletes (Figure 2):

Barbell half squats (70%–80% 1RM; repetitions: 8, 6, 5),High pulls from knee level (70%–80% 1RM; repetitions: 8, 6, 5).

Functional strength exercises:4 sets of 12 consecutive pogo jumps,4 sets of 20 seconds of high-knee running in place.

One-repetition maximum (1RM) was defined as the maximum weight lifted with proper form in a squat to parallel position, with incremental load increases. Participants' 1RM values were tested in advance to calculate individual training loads with precision.

2.5. Foam Rolling Protocol

Both experimental groups followed the same FR protocol(Peacock et al. 2014, Behara and Jacobson 2017, Aune et al. 2019) using a conventional high-density foam roller (length 30 cm, diameter 15 cm; BLACKROLL, Bottighofen, Switzerland).

The FR protocol was performed as shown in Figure 3, following the sequence from A to E: This includes 2 minutes per side for the gluteus maximus

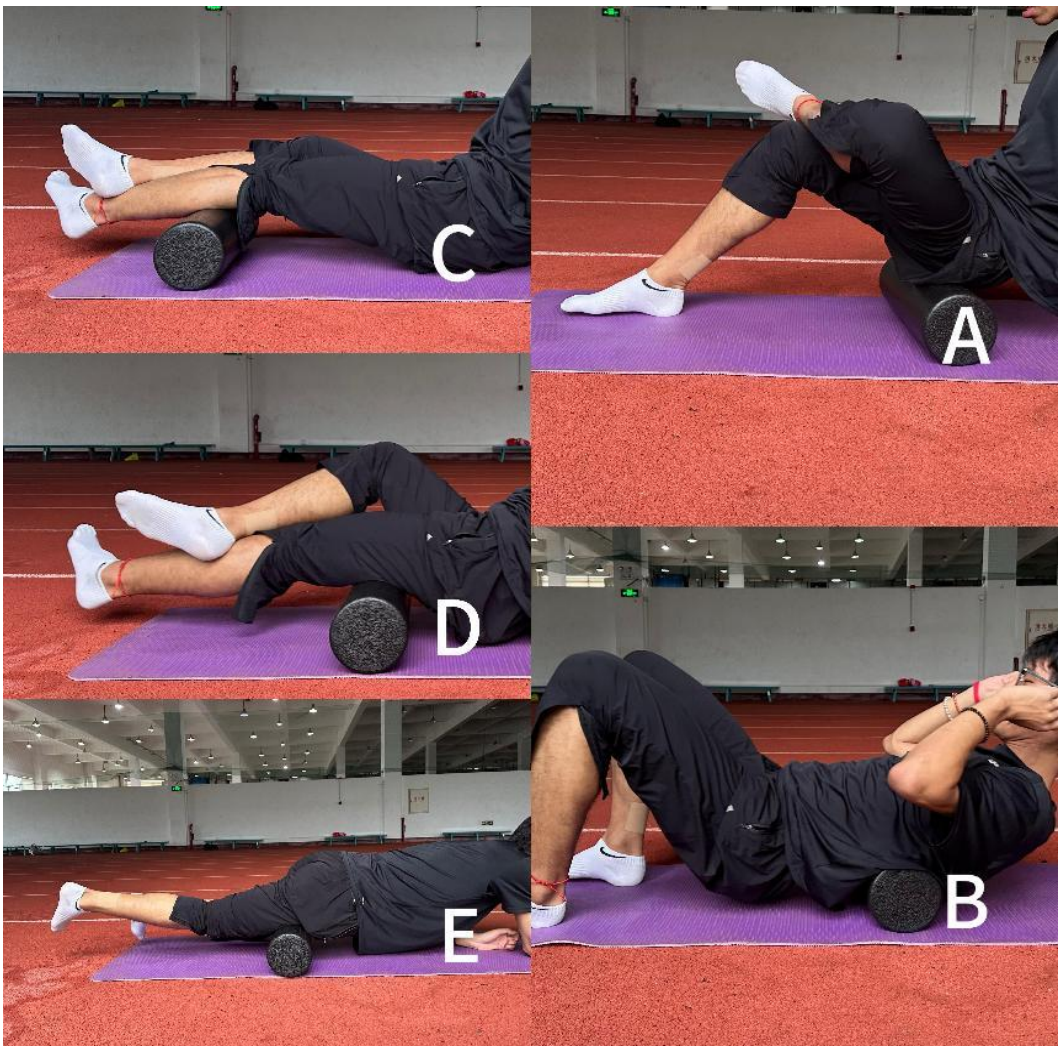

Figure 3 | Foam Rolling Protocol Diagram

and gluteus medius in the hip region, 1.5 minutes for the latissimus dorsi and lower back, 2 minutes per leg for the gastrocnemius and soleus in the calf, 2 minutes per leg for the semitendinosus, semimembranosus, and biceps femoris in the posterior thigh, and 2 minutes per leg for the rectus femoris, vastus medialis, vastus lateralis, and vastus intermedius in the anterior thigh.

3. Equipment and Variables

3.1. Testing Overview

Each testing session comprises the following assessments to comprehensively evaluate the subjects' muscular function and pain perception.

3.2. Muscle Strength

Lower limb muscle power was estimated using the formula proposed by Sayers et al. (Sayers et al. 1999):

Power(W)=[Vertical Jump Height(cm)60.7]+[Body Mass(kg)×45.3]–2055；

Participants were weighed using the same electronic scale (Delixi, Zhejiang, China), and jump height was measured using the My Jump 2 application, which has been validated for high reliability and validity.(Bogataj et al. 2020, Chow, Kong, and Pun 2023, Haynes et al. 2019) The jump test was adapted from Vaisman et al.(Vaisman et al. 2017) Participants began from a half-squat position with knees flexed at 90°,maintained the position for 2 seconds to minimize the influence of the stretch-shortening cycle (SSC). They then performed a maximal vertical jump. Each participant performed three non-consecutive trials, (Booher et al. 1993)with the highest jump height recorded.

Table 2 | Test Results for PPT and Power

	PPT(kPa)			POWER(W)		
	Pre	Post	Mean Comparison	Pre	Post	Mean Comparison
E1	601.88±13.34	577.50±14.72	P＜0.01	5210.66±143.24	5068.18±181.84	P=0.2156
E2	603.13±12.58	588.13±12.58	P＜0.01	5149.25±101.84	5193.29±96.08	P＜0.01
C	605.00±10.00	548.75±7.98	P＜0.01	5203.89±171.95	5024.43±172.39	P＜0.01

3.3. Pressure Pain Threshold (PPT)

The pressure pain threshold is assessed using a hand-held dolorimeter with a 1 cm rubber tip (Algometer II, Somedic SenseLab, Sweden). This device applies controlled and gradually increasing pressure to specific muscle sites. We put the device on the rectus femoris muscle at 50% of the distance between the anterior spina iliaca superior and the superior part of the patellain the rate of 30kPa/s until the participant reports the sensation of pressure turning into pain.(Baumgart et al. 2019)The data is referred to as Pressure Pain Threshold (PPT), currently defined as "the minimum necessary intensity of a pressure stimulus that is perceived as painful."(Ylinen 2007)Before testing, participants are asked to sit on a chair with their legs naturally bent and feet flat on the ground to ensure the rectus femoris is in a relaxed state.

4. Data Processing

For data analysis, Hedges' g is utilized to evaluate the effects of foam rolling (FR) interventions at different time points on performance and muscle pain between two groups. The calculation of Hedges' g is as follows:

$$g = c_p \frac{\left(M_{\text{post, foam rolling}} - M_{\text{pre, foam rolling}}\right)\left(M_{\text{post, control}} - M_{\text{pre, control}}\right)}{SD_{\text{pre}}}$$

In this context, c_p is a bias correction factor used for small sample sizes,(Morris 2008)aimed at minimizing the bias that may arise from small sample measurements. $M_{post,foamrolling} - M_{pre,foamrolling}$ represents the difference between the post-test and pre-test means for the foam rolling group, while $M_{post,control} - M_{pre,control}$ represents the difference between the post-test and pre-test means for the control group. SD_{pre} denotes the pooled standard deviation of the pre-test measurements.

5. Result

The results of the experimental tests are shown in Table 2 and Figure 4-5.Independent sample t-tests for each group (E1 vs E2; E1 vs C; E2 vs C) revealed no significant differences (t=0.409, p=0.6888; t=0.069, p=0.946; t= -0.3272, p=0.7483), followed by paired sample t-test for the difference between the two data except E1 (P <0.01). To compare the magnitude of the differences, the Hedges' g value analysis was performed, and the results are shown in Table 3.

6. Discussion

Post-exercise stretching and relaxation are essential for recovery,(Medicine 2013)and SMR is an effective method for promoting recovery in most cases . (Casanova et al. 2018) Regarding the timing of post-exercise stretching, many individuals, including athletes, are accustomed to performing it immediately

Table 3 | Hedges' g Effect Sizes for PPT and Power

	PPT	POWER
E1 vs C	2.355	0.159
E2 vs C	3.305	1.337

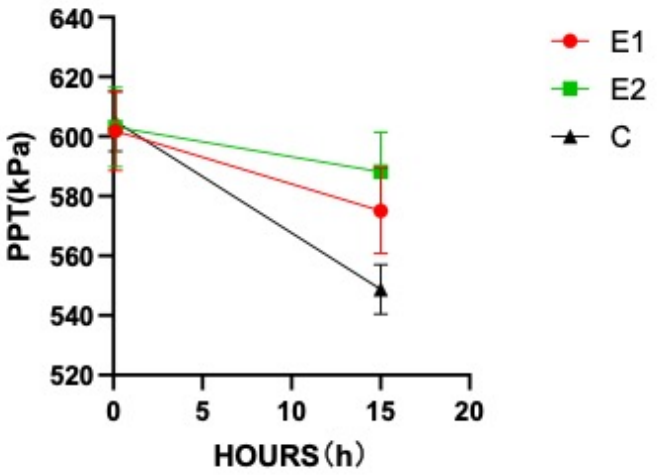

Figure 4

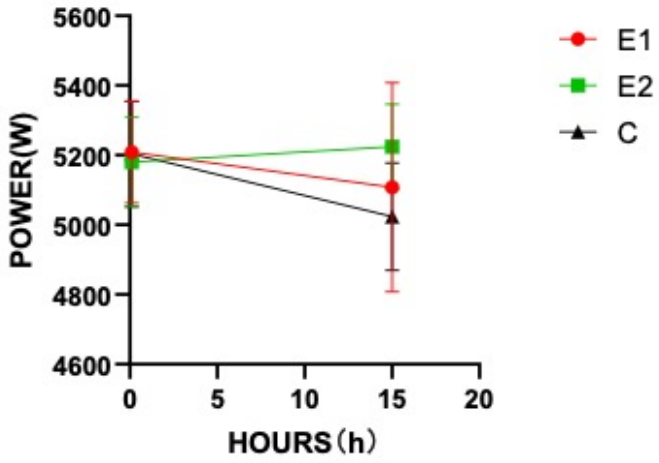

Figure 5

after exercise (immediate recovery), while others prefer to schedule muscle relaxation training for the next morning or on a separate day (delayed recovery).

6.1. Pressure Pain Threshold (PPT)

All groups exhibited a significant decrease in PPT post-exercise,indicating the presence of exercise-induced muscle soreness (Figure 4). However, the reduction in PPT was less pronounced in both the E1 and E2 groups compared to the Control group. This suggests that foam rolling effectively mitigated DOMS. Notably, the E2 group demonstrated the smallest decrease in PPT, with a Hedges' g effect size of 3.305, indicating a large effect. This finding implies that delayed foam rolling is more effective in alleviating muscle soreness than immediate foam rolling.

This finding aligns with current international research.(Pearcey et al. 2015, Cheatham et al. 2015, D'Amico and Gillis 2019, Hendricks et al. 2020, Nazarudin et al. 2021)

Furthermore, Experimental Group 2 (delayed FR) exhibited a larger effect size compared to Experimental Group 1 (immediate FR). This may be because delayed FR better facilitates muscle recovery. Post-exercise, muscles experience micro-damage and inflammatory responses.(Friden and Lieber 1992) Immediate FR might increase mechanical stress on the muscles, potentially hindering the initial repair process. Delaying FR by 15 hours allows for initial self-repair, after which FR can enhance blood circulation, reduce the accumulation of inflammatory mediators, expedite the removal of metabolic waste, and more effectively alleviate muscle pain and promote strength recovery.

6.2. Jump Power

In terms of muscle strength recovery, both Experimental Group 2 and the control group showed significant reductions in jump power. Interestingly, Experimental Group 1 did not show a significant change in jump power ($p = 0.216$). An examination of the mean values and standard deviations suggests that this may be due to outliers within the group (e.g., one participant's post-test jump power increased by approximately 395 W compared to the pre-test, while others remained stable or slightly decreased). The Hedges' g results for jump power also indicated a large effect size for delayed FR, whereas immediate FR did not show a significant effect. This contrasts with the PPT effect sizes and suggests that delayed FR may have advantages over immediate FR in terms of strength recovery.

The scatter plots in Figure 4 and Figure 5 support these results. In Figure 4, the Control group's PPT values decreased substantially post-exercise, whereas the E1 and E2 groups exhibited smaller reductions, with the E2 group's post-test PPT values remaining closer to pre-test levels. In Figure 5, the Control group's jump power decreased notably post-exercise; the E1 group showed minimal change, and the E2 group participants either maintained or improved their jump power in the post-test.

7. Conclusion

Comparative analysis indicates comparable efficacy between immediate and delayed FR interventions

in attenuating exercise-induced myalgia. However, delayed FR protocols demonstrated superior performance in restoring neuromuscular function and mitigating symptoms of DOMS. Practical implementation considerations suggest preferential application of delayed FR regimens, particularly within self-administered recovery contexts. Post-exercise fatigue states associated with high-intensity training may compromise subject adherence and technique precision in self-administered FR interventions when implemented immediately following physical exertion. Furthermore, acute mechanical loading through FR modalities on fatigued musculature may transiently amplify tissue stress biomarkers, potentially counteracting early-phase regenerative pathways.

Reference

1. Aune, Anne AG, Chris Bishop, Anthony N Turner, Kostas Papadopoulos, Sarah Budd, Mark Richardson, and Sean J Maloney. 2019. "Acute and chronic effects of foam rolling vs eccentric exercise on ROM and force output of the plantar flexors." Journal of sports sciences no. 37 (2):138-145.
2. Baechle, Thomas R, and Roger W Earle. 2008. Essentials of strength training and conditioning: Human kinetics.
3. Baumgart, Christian, Jürgen Freiwald, Matthias Kühnemann, Thilo Hotfiel, Moritz Hüttel, and Matthias Wilhelm Hoppe. 2019. "Foam rolling of the calf and anterior thigh: biomechanical loads and acute effects on vertical jump height and muscle stiffness." Sports no. 7 (1):27.
4. Behara, Brandon, and Bert H Jacobson. 2017. "Acute effects of deep tissue foam rolling and dynamic stretching on muscular strength, power, and flexibility in division I linemen." The Journal of Strength & Conditioning Research no. 31 (4):888-892.
5. Bogataj, Špela, Maja Pajek, Slobodan Andrašić, and Nebojša Trajković. 2020. "Concurrent validity and reliability of my jump 2 app for measuring vertical jump height in recreationally active adults." Applied Sciences no. 10 (11):3805.
6. Booher, Laurie D, Karla M Hench, Teddy W Worrell, and Jill Stikeleather. 1993. "Reliability of three single-leg hop tests." Journal of Sport Rehabilitation no. 2 (3):165-170.
7. Casanova, Nuno, Joana F Reis, João R Vaz, Rita Machado, Bruno Mendes, Duane C Button, Pedro Pezarat-Correia, and Sandro R Freitas. 2018. "Effects of roller massager on muscle recovery after exercise-induced muscle damage." Journal of sports sciences no. 36 (1):56-63.
8. Cheatham, Scott W, Morey J Kolber, Matt Cain, and Matt Lee. 2015. "The effects of self-myofascial release using a foam roll or roller massager on joint range of motion, muscle recovery, and performance: a systematic review." International journal of sports physical therapy no. 10 (6):827.
9. Chow, Gary Chi-Ching, Yu-Hin Kong, and Wai-Yan Pun. 2023. "The concurrent validity and test-retest reliability of possible remote assessments for measuring countermovement jump: My jump 2, HomeCourt & Takei vertical jump meter." Applied Sciences no. 13 (4):2142.
10. Crane, Justin D, Daniel I Ogborn, Colleen Cupido, Simon Melov, Alan Hubbard, Jacqueline M Bourgeois, and Mark A Tarnopolsky. 2012. "Massage therapy attenuates inflammatory signaling after exercise-induced muscle damage." Science translational medicine no. 4 (119):119ra13-119ra13.
11. D'Amico, Anthony P, and Jason Gillis. 2019. "Influence of foam rolling on recovery from exercise-induced muscle damage." The Journal of Strength & Conditioning Research no. 33 (9):2443-2452.
12. Friden, JAN, and Richard L Lieber. 1992. "Structural and mechanical basis of exercise-induced muscle injury." Medicine & Science in Sports & Exercise no. 24 (5):521-530.
13. Haynes, Tom, Chris Bishop, Mark Antrobus, and Jon Brazier. 2019. "The validity and reliability of the My Jump 2 app for measuring the reactive strength index and drop jump performance." The Jounral of Sports Medicine and Physical Fitness.
14. Hendricks, Sharief, Steve den Hollander, Wayne Lombard, and Romy Parker. 2020. "Effects of foam rolling on performance and recovery: A systematic review of the literature to guide practitioners on the use of foam rolling." Journal of bodywork and movement therapies no. 24 (2):151-174.
15. Medicine, American College of Sports. 2013. ACSM's guidelines for exercise testing and prescription: Lippincott williams & wilkins.
16. Michalak, Bartłomiej, Anna Kopiczko, Robert Gajda, and Jakub Grzegorz Adamczyk. 2024. "Recovery effect of self-myofascial release treatment using different type of a foam rollers." Scientific Reports no. 14 (1):15762.
17. Morris, Scott B. 2008. "Estimating effect sizes from pretest-posttest-control group designs." Organizational research methods no. 11 (2):364-386.
18. Nazarudin, Mohamad Nizam, Mohd Firdaus Abdullah, Mohd Radzani Abdul Razak, Abu Yazid Abu Bakar, Denise Koh Choon Lian, and Wan Ahmad Munsif Wan Pa. 2021. "Dealing with delayed onset muscle soreness (DOMS): Foam roller or mechanical manipulation of body tissue." International Journal of Human Movement and Sports Sciences no. 9 (3):383-393.
19. Peacock, Corey A, Darren D Krein, Tobin A Silver, Gabriel J Sanders, and Kyle-Patrick A Von Carlowitz. 2014. "An acute bout of self-myofascial release in the form of foam rolling improves performance testing." International journal of exercise science no. 7 (3):202.
20. Pearcey, Gregory EP, David J Bradbury-Squires, Jon-Erik Kawamoto, Eric J Drinkwater, David G Behm, and Duane C Button. 2015. "Foam rolling for delayed-onset

muscle soreness and recovery of dynamic performance measures." Journal of athletic training no. 50 (1):5-13.

21. Sayers, Stephen P, David V Harackiewicz, Everett A Harman, Peter N Frykman, and Michael T Rosenstein. 1999. "Cross-validation of three jump power equations." Medicine and science in sports and exercise no. 31 (4):572-577.
22. Smith, Lucille L, Madge N Keating, Donald Holbert, Debbie J Spratt, Michael R McCammon, Susan S Smith, and Richard G Israel. 1994. "The effects of athletic massage on delayed onset muscle soreness, creatine kinase, and neutrophil count: a preliminary report." Journal of Orthopaedic & Sports Physical Therapy no. 19 (2):93-99.
23. Vaisman, Alex, Rodrigo Guiloff, Juan Rojas, Iris Delgado, David Figueroa, and Rafael Calvo. 2017. "Lower limb symmetry: Comparison of muscular power between dominant and nondominant legs in healthy young adults associated with single-leg-dominant sports." Orthopaedic journal of sports medicine no. 5 (12):2325967117744240.
24. Ylinen, Jari. 2007. "Pressure algometry." Aust J Physiother no. 53 (3):207.

International Journal of Clinical Medicine & Pharmacology

https://doi.org/10.70731/g7k4ek15

Associations Between Urinary and Blood Heavy Metal Exposure and Heart Failure Risk in Elderly Adults: Insights From an Interpretable Machine Learning Model Based on NHANES (2003-2020)

Yuting Yang [a,b], Shan Deng [a,b,c,d,*],

[a] *Department of Cardiology, Union Hospital, Tongji Medical College, Huazhong University of Science and Technology, Wuhan, China.*
[b] *Clinic Center of Human Gene Research, Union Hospital, Tongji Medical College, Huazhong University of Science and Technology, Wuhan, 430022, China.*
[c] *Hubei Key Laboratory of Metabolic Abnormalities and Vascular Aging, Huazhong University of Science and Technology, Wuhan, China.*
[d] *Hubei clinical research center for metabolic and cardiovascular disease, Huazhong University of Science and Technology, Wuhan, China.*

KEYWORDS

Heavy Metals,
Heart Failure,
Machine Learning,
NHANES

ABSTRACT

This study examines the link between heavy metal exposure and heart failure risk in individuals aged 50 and older, utilizing machine learning models and data from the NHANES dataset. Five models were evaluated, with Gradient Boosting Decision Trees (GBDT) selected for its accuracy, interpretability, and ability to capture nonlinear relationships. The GBDT model achieved an accuracy of 0.78, sensitivity of 0.93, and an AUC of 0.92. Analysis revealed that higher levels of urinary iodine, blood cadmium, urinary cobalt, urinary tungsten, and urinary arsenic acid were significantly associated with increased heart failure risk. Synergistic effects with age and BMI further amplified these risks. Interpretability tools such as SHAP, permuted Feature Importance, ICE, and PDP were used to enhance model transparency and understanding. These findings underscore the importance of ongoing research into the mechanisms linking heavy metals and heart failure and the need for monitoring and regulatory measures to protect vulnerable populations.

1. Introduction

Individuals are unavoidably exposed to environments containing heavy metals, and these elements can infiltrate the human body via ingestion and inhalation[1]. The threat of heavy metals to human health continues to exist and has now become a global public health issue. Heavy metals typically function by displacing essential metal ions in the human body[2], leading to disruptions in critical biological pathways. Such disruptions can result in endothelial cell damage[3-5], disturbances in lipid metabolism[6], increased oxidative stress[7, 8], immune

* Corresponding author. E-mail address: dengshan1020@qq.com

Received 18 February 2025; Received in revised form 23 February 2025; Accepted 26 February 2025; Available online 28 February 2025.

homeostasis imbalance[9, 10], and epigenetic modifications[11], all of which may contribute to the development of various cardiovascular diseases. Exposure to heavy metals during pregnancy has been linked to an increased risk of congenital heart defects in offspring [12, 13]. Additionally, exposure in preschool children may lead to arrhythmias[14], while heavy metal exposure has been associated with hypertension[15]. The impact of exposure to some heavy metals on the incidence of heart failure has also been studied[16, 17].

Heart failure isn't a standalone illness but rather the end stage of various heart diseases, which continues to be a significant contributor to mortality, morbidity, and diminished quality of life globally[18]. Heart failure impacts the health of more than 60 million people worldwide[19], and the lifetime risk of heart failure has risen to 24%, roughly one in four people will develop heart failure in their lifetime[20]. Research indicates a significant correlation between cadmium exposure and the incidence of heart failure[21-24]. And the level of urinary antimony appears to be directly proportional to the risk of heart failure[25]. Besides, epidemiological research has indicated that exposure to cobalt and lead elevates the risk of heart failure[16, 26]. However, previous research has predominantly relied on conventional statistical methods, which exhibit limited flexibility in modeling complex relationships and often operate under restrictive assumptions regarding underlying data distributions[27]. Furthermore, much of the existing literature has focused on examining the effects of a single type of heavy metal in isolation. This approach may overlook potential interactions and cumulative effects of multiple heavy metals, thereby limiting the comprehensiveness of the findings. Thus, a more integrated and flexible modeling framework, machine learning, may be necessary to capture the intricacies of heavy metal exposure and its multifaceted impact on heart failure risk.

Our study conducted a comprehensive analysis of laboratory indicators for various heavy metal elements in both blood and urine, utilizing data from the National Health and Nutrition Examination Survey (NHANES) database spanning 2003 to 2020. This robust database provides high-quality, nationally representative data essential for public health research, integrating interviews, physical examinations, and laboratory assessments. Furthermore, we employed advanced machine learning algorithms for the analysis, enhancing our ability to uncover meaningful relationships within the data. Machine learning tends to prioritize predictive performance and generalization over interpretability, with a mathematical emphasis on cross-validation and iterative enhancement of algorithms[28]. This implies that machine learning algorithms frequently outshine traditional statistical prediction methods, however, less transparent compared to conventional statistical approaches. Consequently, there is a need for explanatory models in machine learning. SHAP (SHapley Additive exPlanations) is a technique for interpreting machine learning models, employing the computation of Shapley values to ascertain the contribution of each feature to a given prediction, and thus facilitates the generation of transparent explanations by leveraging these calculated Shapley values[29, 30]. In this study, we chose five machine learning algorithms for our analysis, identified the best-performing model, and utilized the SHAP model for interpreting.

2. Method

2.1. Data Source

All variable information was sourced from the NHANES (the National Health and Nutrition Examination Survey) database (https://wwwn.cdc.gov/Nchs/Nhanes). The NHANES database, carried out by the Centers for Disease Control and Prevention (CDC) in the United States, combines interviews, laboratory tests and physical examinations on a nationally representative sample of American residents every two years. We downloaded the variables data from the annual datasets of NHANES 2003-2004, NHANES 2005-2006, NHANES 2007-2008, NHANES 2009-2010, NHANES 2011-2012, NHANES 2013-2014, NHANES 2015-2016, NHANES 2017-2018, and NHANES 2019-2020, match all variables for each year by the unique sequence numbers, and ultimately merged the datasets for all the years. The features and labels encompassed in the study include gender, age (year), race, education level, poverty-to-income ratio (PIR), height, weight, body mass index (BMI, kg/m^2), urinary heavy metals (including urine mercury, urine barium, urine beryllium, urine cadmium, urine cobalt, urine cesium, urine molybdenum, urine lead, urine platinum, urine antimony, urine thallium, urine tungsten, urine uranium, urine arsenous acid, urine arsenobetaine, urine arsenocholine, urine dimethylarsonic acid, urine monomethylacrsonic acid, urine total arsenic, and

urine iodine), blood heavy metals (including blood cadmium, blood lead, blood mercury), and heart failure. The diagnosis of heart failure is ascertained through self-reported physician diagnoses acquired via standardized medical questionnaires in individual interviews. Participants were queried: "Has a doctor or other health professional ever told that you had congestive heart failure?" If a person responds 'yes', they will be regarded as having heart failure. According to the 10th revised edition of the International Classification of Diseases and Related Health Problems (ICD-10), the code for congestive heart failure is I50.0, I50.1, I50.9[31]. Heavy metal samples in blood and urine were processed, stored, and transported to the Centers for Disease Control and Prevention and the Science Department of the Environmental Health Laboratory of the National Environmental Health Center for analysis.

2.2. Study Population

The inclusion criteria were as follows: (1) participants were aged 50 or above; (2) participants underwent heavy metal laboratory testing in blood and urine samples; (3) heart failure status was 1 (ever had a heart failure) or 2 (didn't have a heart failure) based on the NHANES questionnaires. Exclusion criteria were as follows: (1) heart failure status was 7 (refused to answer this question) or 9 (means uncertain heart failure status) according to NHANES questionnaires. Finally, a total of 6879 participants were included in the present analysis.

2.3. Statistical Analysis

2.3.1. Statistical Description of Baseline Characteristics Between Heart Failure Group and no Heart Failure Group

The demographic description section was analyzed using R 4.2.3. In the baseline table, we divided the participants into the heart failure group and the no heart failure group for comparison. The baseline covariates were presented as mean (standard deviation) for continuous variables and count (percentage) for categorical variables, respectively. The t tests and $\chi 2$ tests were employed to compare the differences between the groups for continuous and categorical variables, separately. variables associated with heavy metals concentration were depicted using geometric mean and geometric standard deviation.

2.3.2. Machine Learning Processing

2.3.2.1. Data Preprocessing and Splitting

The analysis of the machine learning section is accomplished using Python 3.10.8 and Python libraries, including "sklearn", "imblearn", "numpy", and "pandas". An overview of our methodology is presented in (Figure 1). BMI, age, gender, blood heavy metals, and urinary heavy metals were selected as feature variables, and heart failure as the target variable for the machine learning model. "missForest" was used for missing value imputation, which is an iterative imputation approach based on random forest method and can concurrently interpolate different types of data[32]. The raw data was standardized using the "StandardScaler" function. The dataset was randomly split into a training set (N=5159) and a testing set (N=1720) in accordance with a specific ratio, with the training set constituting 75% of all the dataset. We calculated the Pearson correlation coefficients of all predictor variable in the training set and plotted heatmaps respectively before and after deleting highly correlated variables (Supplementary figure 1). To reduce the influence of multicollinearity on the model, features with Pearson coefficients exceeding 0.8 were removed[33]. The low variance features have been removed, which possess limited explanatory information and make a minor contribution to the model's predictive capacity.

2.3.2.2. Feature Selection and Model Training

After the initial feature filtering via the above-mentioned steps, we incorporated a pipeline consisting of "RandomUnderSample", "SelectKBest", and the model classifier for the subsequent analysis. Among the pipeline process, RUS (RandomUnderSample) is a sampling method that can create balanced classes from imbalanced ones[34, 35], and "SelectKBest" is a feature selection method that functions by scoring all features and selecting the top "k" input variables with the highest scores[36] (mutual information was selected as the scoring metric, with higher scores indicating a stronger correlation between the variables[37]). Grid search was used for hyperparameter tuning, thereby selecting the optimal hyperparameter values for each machine learning model[38] (The detailed parameter information for the model is provided in the supplementary materials). We chose five machine learning models: SVM (Support Vector Machine), RF (Random Forest), XGBoost (eXtreme Gradient Boosting), GDBT (Gradient Boosting Deci-

sion Tree), and KNN (k-nearest neighbor). Among them, the GDBT was found to be the best one.

2.3.2.3.Model Evaluation and Comparison

To conduct a thorough and systematic comparison of the machine learning models, we employed a multifaceted approach that included generating various evaluation plots alongside calculating a comprehensive set of performance metrics both in the training and testing sets. Specifically, we constructed Receiver Operating Characteristic (ROC) curves, precision-recall (PR) curves, and confusion matrices. The ROC curves provide insight into the model's diagnostic capabilities and the PR curves offer a focused analysis of the model's performance in classifying positive cases, particularly in imbalanced datasets. Confusion matrices were used to provide a detailed breakdown of the models' classification results, highlighting the number of true positives, true negatives, false positives, and false negatives. We further calculated a comprehensive suite of quantitative metrics, including accuracy, specificity, precision, sensitivity (recall), negative predictive value (NPV), positive predictive value (PPV), false positive rate (FPR), false negative rate (FNR), false discovery rate (FDR), the F1 score, and the Brier score. These metrics collectively elucidated the models' classification efficacy, with the F1 score serving to balance precision and recall and the Brier score reflecting the probabilistic accuracy of predictions. Moreover, we evaluated the area under the ROC curve (AUC) and its 95% confidence intervals as a measure of the models' overall ability to distinguish between positive and negative classes, complemented by the average precision score (AP) to quantify performance in scenarios characterized by class imbalance.

2.3.2.4.Model Explanation

In the explanation section of the optimal model, we calculated the PI (permutation importance) values of each feature in the model, constructed the SHAP (SHapley Additive exPlanations) explanation model using the "shap" package[39], and plotted ICE (Individual Conditional Expectation) plot and PDP (Partial Dependence Plot) to respectively demonstrate the impact of a single feature and two features on the target.

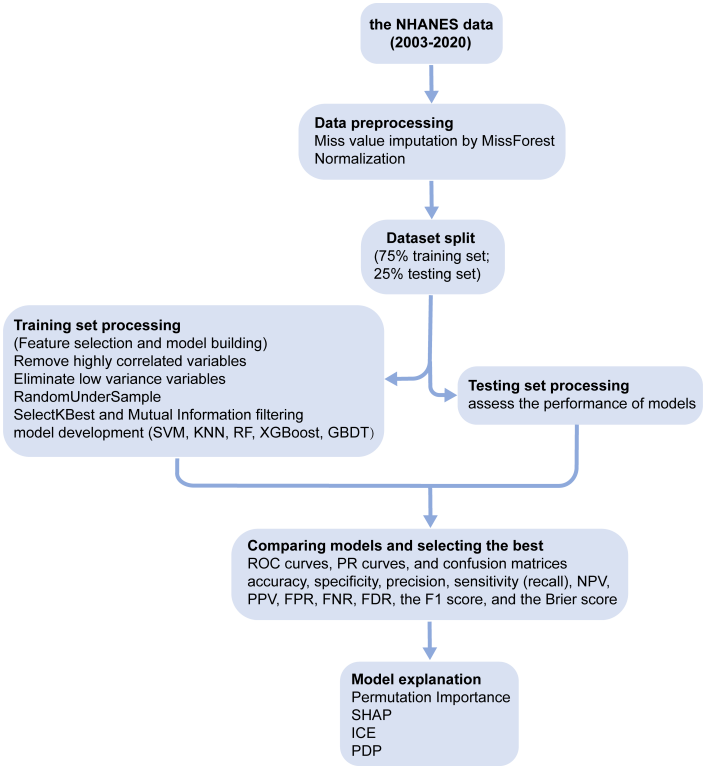

Figure 1 | Machine learning model development flowchart.

This flowchart outlines the key steps in developing a machine learning model from inception to interpretation.

3. Results

3.1. Baseline Characteristics

Among 6,879 participants, 388 were diagnosed with heart failure, while 6,491 were classified as having no heart failure. As illustrated in Table 1, a substantial proportion of the baseline characteristics exhibited significant statistical differences between the heart failure group and the group without heart failure. Compared to participants without heart failure, those in the heart failure group exhibited a higher age (69.74 $\pm$ 8.39 versus 65.33 $\pm$ 9.04; P<0.01), a greater proportion of male participants (60.1% versus 49.6%; P<0.01), and an elevated BMI (32.92 $\pm$ 16.51 versus 29.53 $\pm$ 7.22; P<0.01). Besides, significant statistical differences (P Value < 0.05) were observed in the laboratory indicators of heavy metals, including blood cadmium, blood lead, blood mercury, urinary beryllium, urinary cadmium, urinary cesium, urinary antimony, urinary thallium, urinary tungsten, urinary uranium, urinary dimethylarsonic acid, urinary total arsenic, and urinary iodine, between the two participant groups.

Table 1 | Baseline characteristics of study participants

Characteristics	Total adults (N= 6879)	Heart failure(N= 388)	No heart failure(N= 6491)	P value
Age, years, mean (SD)	65.58(9.06)	69.74(8.39)	65.33(9.04)	<0.01
Gender, n (%)				<0.01
Male	3454(50.2)	233(60.1)	3221(49.6)	
Female	3425(49.8)	155(39.9)	3270(50.4)	
BMI, kg/m^2, mean (SD)	29.72(8.07)	32.92(16.51)	29.53(7.22)	<0.01
Weight status, n (%)				
BMI <25	1727(25.1)	79(20.4)	1648(25.4)	<0.01
BMI ⩾25 & <30	2391(34.8)	108(27.8)	2283(35.2)	
BMI ⩾30	2761(40.1)	201(51.8)	2560(39.4)	
Race, n (%)				<0.01
Mexican American	812(11.8)	27(7)	785(12.1)	
Hispanic	714(10.4)	31(8)	683(10.5)	
Non-Hispanic White	2954(42.9)	196(50.5)	2758(42.5)	
Non-Hispanic Black	1613(23.4)	109(28.1)	1504(23.2)	
Other Race (Including Multi-Racial)	786(11.4)	25(6.4)	761(11.7)	
Education, n (%)				<0.01
Grades 0–12	1900(27.6)	118(30.4)	1782(27.5)	
High school graduate/GED or equivalent	3485(50.7)	223(57.5)	3262(50.3)	
College graduate or above	1494(21.7)	47(12.1)	1447(22.3)	
PIR, mean (SE)	2.61(1.56)	2.02(1.31)	2.65(1.56)	<0.01
PIR level, n (%)				<0.01
Low (<1)	1112(16.2)	83(21.4)	1029(15.9)	
Medium (⩾1 & <4)	4061(59)	257(66.2)	3804(58.6)	
High (⩾4)	1706(24.8)	48(12.4)	1658(25.5)	
Blood heavy metals, geometric mean (GSD)				
Cadmium (ug/L)	0.40(0.76)	0.48(0.79)	0.40(0.76)	<0.01
Lead (ug/dL)	1.47(0.62)	1.63(0.61)	1.46(0.62)	0.02
Mercury, total (ug/L)	0.95(1.01)	0.72(0.89)	0.96(1.02)	<0.01
Urinary heavy metals, geometric mean (GSD)				
Mercury (ug/L)	0.30(1.08)	0.25(1.05)	0.30(1.08)	0.05
Barium (ug/L)	0.96(1.03)	0.83(1.09)	0.97(1.02)	0.55
Beryllium (ug/L)	0.60(1.50)	0.55(1.41)	0.60(1.50)	<0.01
Cadmium (ug/L)	0.32(0.98)	0.37(0.98)	0.31(0.98)	<0.01
Cobalt (ug/L)	0.34(0.88)	0.43(0.91)	0.34(0.87)	0.15
Cesium (ug/L)	4.09(0.65)	3.63(0.60)	4.12(0.65)	<0.01
Molybdenum (ug/L)	34.86(0.87)	36.14(0.79)	34.79(0.70)	0.83
Lead (ug/L)	0.48(0.89)	0.49(0.94)	0.48(0.89)	0.49
Platinum (ug/L)	0.40(2.47)	0.38(2.38)	0.40(2.48)	0.08
Antimony (ug/L)	0.05(0.98)	0.07(1.22)	0.05(0.97)	<0.01
Thallium (ug/L)	0.15(0.81)	0.15(0.10)	0.15(0.80)	<0.01
Tungsten (ug/L)	0.06(1.14)	0.09(1.26)	0.06(1.13)	<0.01
Uranium (ug/L)	0.03(2.11)	0.04(2.31)	0.03(2.10)	<0.01
Arsenous acid (ug/L)	0.30(1.12)	0.30(1.16)	0.30(1.12)	0.1
Arsenic acid (ug/L)	0.64(0.24)	0.66(0.31)	0.63(0.24)	0.23
Arsenobetaine (ug/L)	2.51(1.54)	2.50(1.47)	2.51(1.54)	0.14
Arsenocholine (ug/L)	0.18(0.91)	0.20(0.99)	0.18(0.90)	0.21
Dimethylarsonic acid (ug/L)	3.63(0.81)	3.23(0.71)	3.66(0.82)	<0.01
Monomethylacrsonic acid (ug/L)	0.48(0.91)	0.50(0.89)	0.47(0.91)	0.86
Total arsenic (ug/L)	8.55(1.16)	7.80(1.06)	8.60(1.17)	0.03
Iodine (ng/mL)	146.76(0.95)	183.23(1.28)	144.83(0.92)	<0.01

All continuous demographic variables are presented as mean (standard deviation), while the categorical variables are presented as frequency (percentage). Variables related to heavy metals are represented using geometric mean (geometric standard deviation). Statistical comparisons between the heart failure and no heart failure groups were conducted using Student's t-test for continuous variables and chi-square tests for categorical variables, with a significance level set at $p < 0.05$. BMI: Body Mass Index is calculated as weight in kilograms divided by the square of height in meters; PIR: Poverty to Income Ratio is calculated based on household income relative to the federal poverty line.

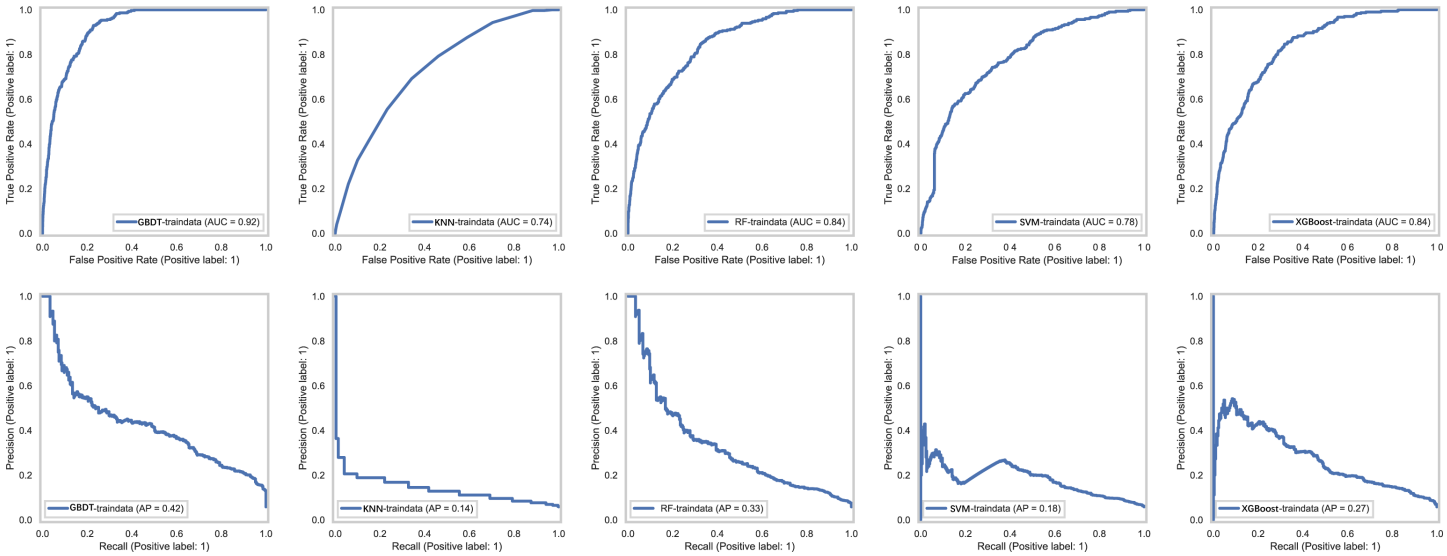

Figure 2 | ROC and PR curves of the five models in the training set

The figure depicts the ROC curves and PR curves for 5 predictive models: GBDT, KNN, RF, SVM, and XGBoost. Each model's performance is shown, demonstrating its ability to distinguish between the positive and negative classes (ROC) and the balance between precision and recall (PR).

Table 2 | Evaluation indicators for predictive models.

Model	Dataset	Accuracy	Sensitivity	Specificity	Precision	Recall	NPV	PPV	FPR	FNR	FDR	F1 score	Brier score	AUC	AUC_low	AUC_up	AP score
GBDT	Training	0.78	0.93	0.77	0.20	0.93	0.99	0.20	0.23	0.07	0.80	0.33	0.18	0.92	0.91	0.93	0.42
GBDT	Testing	0.75	0.71	0.75	0.14	0.71	0.98	0.14	0.25	0.29	0.86	0.23	0.19	0.81	0.77	0.85	0.17
KNN	Training	0.76	0.56	0.77	0.13	0.56	0.97	0.13	0.23	0.44	0.87	0.21	0.21	0.74	0.71	0.76	0.14
KNN	Testing	0.74	0.57	0.75	0.11	0.57	0.97	0.11	0.25	0.43	0.89	0.19	0.22	0.73	0.68	0.78	0.11
RF	Training	0.68	0.85	0.67	0.14	0.85	0.99	0.14	0.33	0.15	0.86	0.24	0.20	0.84	0.82	0.86	0.33
RF	Testing	0.67	0.70	0.67	0.10	0.70	0.98	0.10	0.33	0.30	0.90	0.18	0.21	0.77	0.73	0.82	0.14
SVM	Training	0.80	0.62	0.81	0.16	0.62	0.97	0.16	0.19	0.38	0.84	0.26	0.21	0.78	0.76	0.81	0.18
SVM	Testing	0.77	0.58	0.78	0.13	0.58	0.97	0.13	0.22	0.42	0.87	0.21	0.22	0.75	0.69	0.80	0.12
XGBoost	Training	0.69	0.84	0.68	0.14	0.84	0.99	0.14	0.32	0.16	0.86	0.24	0.21	0.84	0.82	0.86	0.27
XGBoost	Testing	0.68	0.65	0.68	0.10	0.65	0.97	0.10	0.32	0.35	0.90	0.17	0.21	0.75	0.70	0.80	0.15

NPV: Negative Predictive Value. FPR: False Positive Rate. FNR: False Negative Rate. FDR: False Discovery Rate. F1 score: The harmonic mean of precision and recall, calculated as 2 * (Precision * Recall) / (Precision + Recall). AUC: Area Under the Curve. AP: Average Precision.

3.2. Comparison of Machine Learning Models

Considering our dataset is imbalanced, performance metrics that account for class distribution, such as sensitivity (recall), precision, F1 score, and AUC, become more crucial in determining which model is the best, compared with other evaluating indicators. Figure 2 illustrates the ROC curves and PR curves for the five machine learning models for the training set, presented separately. The AUC for GBDT was 0.92 (95% CI: 0.91-0.93), indicating superior predictive performance in distinguishing heart failure compared to the four other models. The RF yielded an AUC of 0.84 (95% CI: 0.82-0.86), which was similar to that of XGBoost, at 0.84 (95% CI: 0.82-0.86), suggesting robust performance. In contrast, the SVM achieved an AUC of 0.78 (95% CI: 0.76-0.81), while the K-Nearest Neighbors (KNN) model had an AUC of 0.74 (95% CI: 0.71-0.76), indicating a moderate discrimination ability. Besides, GBDT stand out with the highest average precision score, demonstrating superior capability in maintaining precision and better diagnostic accuracy in heart failure compared to other models. Table 2 presents specific evaluation metrics for five machine learning models. GBDT achieves a sensitivity of 0.93, indicating excellent true positive identification. In contrast, KNN and SVM exhibit considerably lower sensitivities of 0.56 and 0.61, respectively, resulting in a greater likelihood of missing actual heart failure cases. Overall, GBDT demonstrates distinct advantages over KNN, RF, SVM, and XGBoost based on these performance metrics. Its superior sensitivity (0.93), Average Precision Score (APS) of 0.42, and accuracy of 0.78 position GBDT as an exceptional choice for predictive modeling in scenarios where both precision and recall are essential. The ROC curves and PR curves for the testing

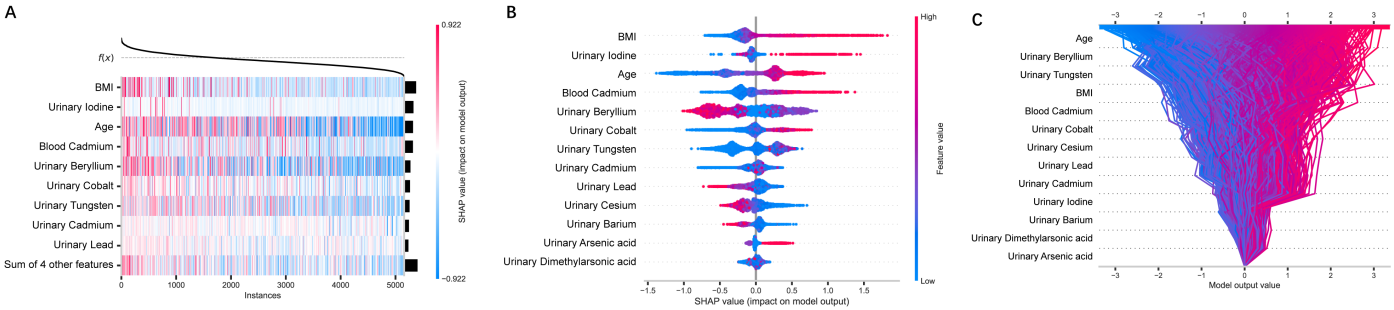

Figure 3 | SHAP visualizations for model interpretation

Figure 3A: SHAP heatmap. The y-axis displays different features arranged in descending order based on their maximum absolute SHAP values, indicating their relative contributions to the prediction of heart failure outcomes. The x-axis represents individual observations from the dataset. Each cell in the heatmap is color-coded to reflect the SHAP values, with red indicating positive contributions to heart failure risk and blue representing negative contributions. Figure 3B: SHAP beeswarm map. The features on the y-axis are organized in the same order as those in the heatmap. The x-axis quantifies the SHAP values, reflecting the impact of each feature on the model's predictions. Each point on the plot corresponds to a specific observation, with colors representing feature value levels; red indicates higher levels while blue denotes lower levels. Figure 3C: SHAP decision map. Illustrates individual predictions in relation to the cumulative effects of features, showing how each feature contributes to the final decision. Blue indicates negative predictions, while red indicates positive predictions.

set are presented in supplementary figure 2, and supplementary figure 3 displays the corresponding confusion matrices.

3.3. The Explainability of the Best Machine Learning Model

3.3.1. SHAP Visualization Plot

Figure 3A presents a SHAP heatmap that offers a comprehensive visualization of the contributions of various features to the predictions made by GBDT regarding heart failure risk. The model's output is shown above the heatmap, centered around the expected SHAP values for all observations. Additionally, the global importance of each input feature is depicted as a bar plot on the right side of the heatmap. Notably, BMI, urinary iodine, age, and blood cadmium emerge significant contributors to the model's predictions. Figure 3B presents the SHAP beeswarm plot for GBDT, illustrating the relationship between feature values and the risk of heart failure. Features such as urinary iodine, blood cadmium, urinary cobalt, body mass index (BMI), and age occupy the top positions and exhibit significant positive SHAP values, suggesting a strong association with an increased risk of heart failure. Urinary tungsten, urinary cadmium, and urinary arsenic acid are positioned further down the y-axis with lower SHAP value, indicating a minimal positive contribution to the risk of heart failure. Interestingly, lower levels of urinary beryllium, urinary lead, urinary cesium, and urinary barium are associated with higher SHAP values, suggesting a potential protective effect against heart failure. The SHAP decision plot for GBDT is illustrated in Figure 3C. Each line represents an individual participant, with the trajectory of each line converging from the bottom and extending toward the top indicating how the features influence the model's output for specific instances. Figure 4 depicts the SHAP interaction summary plot, where the horizontal axis represents interaction values that quantify the attribution of paired interaction effects between two features. Most variables demonstrate varying degrees of interaction effects. Features such as age, urinary beryllium, urinary tungsten, and BMI exhibit significant interaction effects with other variables, indicating the complex relationships that influence heart failure risk.

3.3.2. Permutation Importance Analysis

The permutation importance analysis was conducted to estimate the contribution of features to the prediction of heart failure risk within GBDT by measuring the decrease in the model's performance when the values of a feature were randomly shuffled (Figure 5). The results revealed that urinary beryllium and blood cadmium exhibited the highest importance scores of 0.147 and 0.084 among the heavy metal variables, indicating their significant influence on predictive accuracy. Age and BMI were identified as important determinants, with scores of 0.123 and 0.108, respectively.

3.3.3. ICE Plot and PDP Plot

The ICE plots (Figure 6), generated through partial conditional expectation, illustrated that heart failure risk increases with rising levels of age, BMI, and

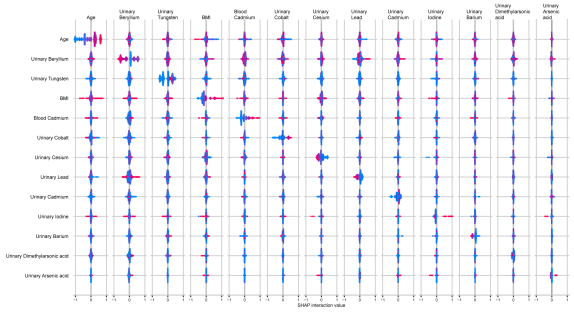

Figure 4 l SHAP interaction plot

Illustrate the combined effects of two features on model predictions.

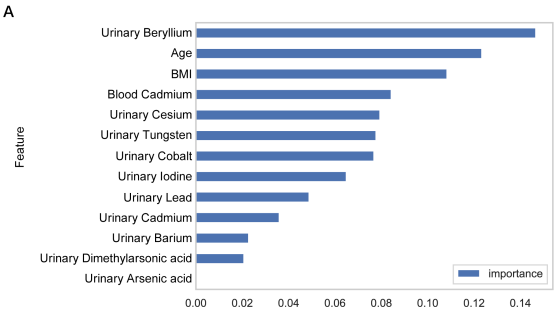

B

Feature	Importance
Urinary Beryllium	0.147
Age	0.123
BMI	0.108
Blood Cadmium	0.084
Urinary Cesium	0.079
Urinary Tungsten	0.078
Urinary Cobalt	0.077
Urinary Iodine	0.065
Urinary Lead	0.049
Urinary Cadmium	0.036
Urinary Barium	0.023
Urinary Dimethylarsonic acid	0.021
Urinary Arsenic acid	0.000

Figure 5 l Premutation importance analysis

The figure evaluates the contribution of individual features to the model's predictive performance through permutation importance analysis. Figure 5A: Bar plot of feature importance scores, ranking the features according to their significance. Figure 5B: Table displaying the feature importance scores.

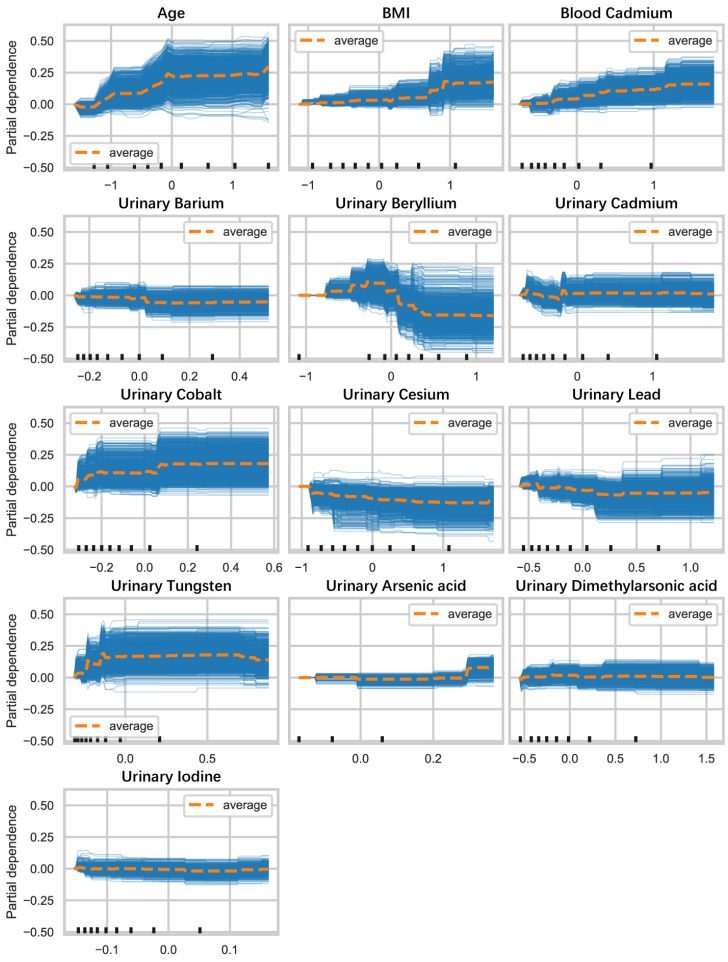

Figure 6 l Individual conditional Expectation (ICE) plots

This figure presents the ICE diagrams for each feature, enabling the examination of the effect of a single variable on predictions while eliminating the noise introduced by interactions with other features. Each thin blue line in the plot represents an individual observation, showcasing how the predicted response varies as the feature value changes, and each orange dashed line represents the average level.

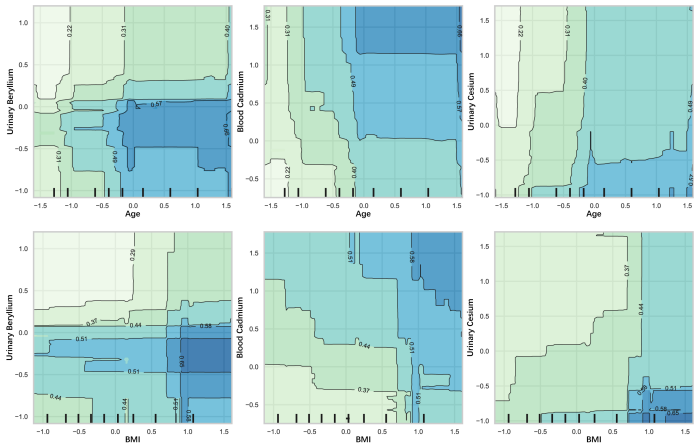

Figure 7 l Two-Dimensional Partial Dependence Plot (PDP)

This plot offers a comprehensive visualization of the interactive influence of age and BMI on the predicted outcomes associated with the top three metals ranked by importance. Lighter shades represent lower predicted outcomes, while darker shades indicate higher predictions. The equipotential lines illustrate levels of constant predicted outcomes across the combinations of the two features, signifying that any point along a given line produces the same average predicted response from the model.

blood cadmium, highlighting their potential as critical risk factors in assessments of heart failure. The relationship between urinary beryllium and heart failure risk was characterized by an inverted U-shaped curve, suggesting that risk is heightened within a specific range of exposure. Other assessed features displayed moderate effects, indicating their contribution to prediction but with less pronounced impacts. Additionally, the two-dimensional PDP plot clarified the joint predictive effects of the top three heavy metal variables in the permutation importance analysis, alongside age and gender, on heart failure risk

(Figure 7). The color gradient ranges from deep blue, indicating higher risk, to light green, reflecting lower risk. Notably, blood cadmium interacted synergistically with age and gender, suggesting potential combined effects on heart failure risk assessment.

4. Discussion

This study employed five machine learning models to explore the complex relationship between heavy metal exposure in blood and urine and the risk of heart failure. Following a thorough evaluation of various model performance metrics, the GBDT model was chosen as the optimal predictive model due to its superior accuracy and interpretability. To further explain the findings derived from GBDT, several machine learning interpretability techniques were applied, including SHAP (SHapley Additive exPlanations), permuted Feature Importance, individual conditional expectation (ICE), and partial dependence plots (PDP). These methods enabled a comprehensive assessment of the individual contributions of each feature to heart failure risk, as well as interactions between pairs of features, offering valuable insights into the prediction on heart failure. Notably, the interplay between different heavy metals and other demographic factors, such as age and BMI, suggests that risk assessments for heart failure must consider these complex interactions. Understanding these relationships not only furthers our knowledge of environmental determinants of cardiovascular disease but also emphasizes the need for continuous monitoring and potential regulatory measures regarding heavy metal exposure.

GBDT, the best prediction machine learning model in our study, is an ensemble learning technique that sequentially builds multiple decision trees, with each tree trained to correct the errors of its predecessor. The iterative approach allows GBDT to progressively minimize the residual errors through a method known as gradient descent[40, 41]. GBDT exhibits robustness against overfitting and has superior predictive accuracy compared to traditional models[41]. The capacity of GBDT to capture complex nonlinear relationships within the data is particularly pertinent in the context of researches where the relationships between features and targets are intricate, such as our study about the complex relationship between heavy metals and the risk of heart failure. In this study, we specifically focused on participants aged 50 years and older within the NHANES database. This demographic selection is particularly important given that older adults not only experience higher morbidity rates[42] but also significantly elevated mortality risks associated with heart failure[43]. Our analysis predominantly centered on heavy metals detected in blood and urine, underscoring our intent to investigate the impact of these environmental exposures on heart failure, intentionally setting aside other prevalent cardiovascular risk factors. And considering that our primary goal was to develop a robust predictive model capable of identifying at-risk individuals based on their exposure to heavy metals, we prioritized predictive accuracy over population-level inferences and chose not to apply sample weights in our analysis. Moreover, the NHANES database provides a large and diverse sample size conducive to model construction, alleviating concerns regarding the need for weighting and allowing us to derive meaningful insights from the unweighted data while maintaining a clear focus on predictive performance.

Our findings complement existing studies and, in certain instances, corroborate prior researches. Specifically, we found that blood cadmium is a positive predictor of heart failure, supporting previous findings. Major sources of cadmium exposure in the population include smoking and passive smoking[44, 45]. A case-cohort study reported that higher urinary cadmium levels are associated with an increased overall incidence of heart failure, with a hazard ratio (HR) of 1.1 per interquartile range difference (95% CI: 1.0-1.2)[17]. Furthermore, blood cadmium has been identified as an independent risk factor for heart failure, demonstrating an OR of 1.345 ($p < 0.001$)[46]. Similarly, an association study revealed a quantitative correlation between cadmium levels and heart failure risk, showing that a 50% increase in blood cadmium corresponds to a 48% increase in heart failure risk (OR: 1.48; 95% CI: 1.17-1.87), while a similar increase in urinary cadmium is associated with a 12% increase in risk (OR: 1.12; 95% CI: 1.03-1.20)[21]. The relationship between beryllium and lung cancer has been extensively researched[47], but its effects on cardiovascular health are less understood. Emerging studies suggest that beryllium exposure may increase the risk of cardiovascular disease[48], with significant associations observed in individuals with close contact to the metal, who demonstrate a heightened risk of ischemic heart disease mortality[49]. Cobalt, often found in human joint replacement implants, has also garnered attention due to its health implications[50]. Our research highlights

that cobalt exposure is linked to an increased risk of heart failure. A controlled trial indicated that patients undergoing multiple hip replacement surgeries exhibited significantly elevated myocardial cobalt levels, with autopsy reports revealing a prevalence of dilated heart chambers and decreased ejection fraction among these individuals[51]. In addition, we found that tungsten and arsenic also elevate the risk of heart failure. While both heavy metals are prevalent in the environment, research on their cardiovascular effects remains limited. A cross-sectional study indicated a positive correlation between urinary tungsten and cardiovascular disease risk[52, 53], and arsenic acid poisoning has been associated with significant alterations in heart rate, QRS duration, and symptoms of prolonged QT and QTc intervals due to arsenic acid poisoning[54]. In our study, we explored the combined effects of heavy metals, body mass index (BMI), and age on heart failure risk. Previous investigations have shown that heavy metals can significantly increase abdominal circumference and obesity rates, which may explain the observed synergistic effects of BMI and metals such as cadmium[55-57]. Additionally, there is a documented correlation between age and the duration of heavy metal exposure [58], and excessive accumulation of heavy metals in the human body may increase the risk of PhenoAge acceleration[59].

The value of our research lies in its multifaced approach, leveraging advanced computational techniques to enhance the understanding of environmental risk factors associated with heart failure. By integrating machine learning, we move beyond traditional statistical methods, enabling the identification of complex, nonlinear relationships. Furthermore, the significance of our findings contributes to the growing evidence linking heavy metals to adverse cardiovascular outcomes, highlighting potentially modifiable risk factors for clinical practice and public health strategies.

5. Limitation

While our study offers valuable insights into the relationship between heavy metal exposure and heart failure, several limitations warrant consideration. First, despite the GBDT model achieving an accuracy of 0.78, a high sensitivity of 0.93, and a strong AUC of 0.92, the model's relatively low precision and FDR indicate a need for refinement in its predictive capabilities. This suggests that the model may generate a considerable number of false positives, which can impact clinical decision-making. Second, while the use of machine learning algorithms has improved predictive accuracy compared to traditional methods, their inherent complexity may limit interpretability, which could impede acceptance in practical applications. Third, the cross-sectional design of the study restricts our ability to infer causality. While the observed associations are significant, they do not establish a direct cause-and-effect relationship between heavy metal exposure and heart failure outcomes.

6. Conclusion

In this study, GBDT demonstrated superior performance in modeling the relationship between heavy metal exposure and heart failure. Our analysis revealed that elevated concentrations of urinary iodine, blood cadmium, urinary cobalt, urinary tungsten, and urinary arsenic acid are significantly correlated with an increased risk of heart failure, while urinary beryllium appears to have a potentially detrimental effect. Additionally, we uncovered a synergistic relationship involving both age and BMI that amplifies the adverse effects of heavy metal exposure on the risk of heart failure. These findings highlight the critical need for further research to explore the underlying mechanisms and to inform targeted preventive measures and clinical strategies aimed at mitigating the risks associated with heavy metal exposure in vulnerable populations.

References

1. Järup L. Hazards of heavy metal contamination. Br Med Bull. 2003;68:167-82.
2. Lamas GA, Bhatnagar A, Jones MR, Mann KK, Nasir K, Tellez-Plaza M, et al. Contaminant Metals as Cardiovascular Risk Factors: A Scientific Statement From the American Heart Association. J Am Heart Assoc. 2023;12:e029852.
3. Lind L, Araujo JA, Barchowsky A, Belcher S, Berridge BR, Chiamvimonvat N, et al. Key Characteristics of Cardiovascular Toxicants. Environ Health Perspect. 2021;129:95001.
4. Singh P, O'Toole TE, Conklin DJ, Hill BG, Haberzettl P. Endothelial progenitor cells as critical mediators of environmental air pollution-induced cardiovascular toxicity. Am J Physiol Heart Circ Physiol. 2021;320:H1440-H55.
5. Pan Z, Gong T, Liang P. Heavy Metal Exposure and Cardiovascular Disease. Circ Res. 2024;134:1160-78.

6. Jiang Q, Xiao Y, Long P, Li W, Yu Y, Liu Y, et al. Associations of plasma metal concentrations with incident dyslipidemia: Prospective findings from the Dongfeng-Tongji cohort. Chemosphere. 2021;285:131497.
7. Marques M, Millás I, Jiménez A, García-Colis E, Rodriguez-Feo JA, Velasco S, et al. Alteration of the soluble guanylate cyclase system in the vascular wall of lead-induced hypertension in rats. J Am Soc Nephrol. 2001;12:2594-600.
8. Fu Z, Xi S. The effects of heavy metals on human metabolism. Toxicol Mech Methods. 2020;30:167-76.
9. Zhang Y, Huo X, Lu X, Zeng Z, Faas MM, Xu X. Exposure to multiple heavy metals associate with aberrant immune homeostasis and inflammatory activation in preschool children. Chemosphere. 2020;257:127257.
10. Zheng K, Zeng Z, Tian Q, Huang J, Zhong Q, Huo X. Epidemiological evidence for the effect of environmental heavy metal exposure on the immune system in children. Sci Total Environ. 2023;868:161691.
11. Riffo-Campos AL, Fuentes-Trillo A, Tang WY, Soriano Z, De Marco G, Rentero-Garrido P, et al. In silico epigenetics of metal exposure and subclinical atherosclerosis in middle aged men: pilot results from the Aragon Workers Health Study. Philos Trans R Soc Lond B Biol Sci. 2018;373.
12. Wang C, Pi X, Yin S, Liu M, Tian T, Jin L, et al. Maternal exposure to heavy metals and risk for severe congenital heart defects in offspring. Environ Res. 2022;212:113432.
13. Sun J, Mao B, Wu Z, Jiao X, Wang Y, Lu Y, et al. Relationship between maternal exposure to heavy metal titanium and offspring congenital heart defects in Lanzhou, China: A nested case-control study. Front Public Health. 2022;10:946439.
14. Fu Y, Liu Y, Liu Y, Wang Y, Zhu M, Lin W, et al. Relationship between cumulative exposure to metal mixtures and heart rate among Chinese preschoolers. Chemosphere. 2022;300:134548.
15. Wang X, Han X, Guo S, Ma Y, Zhang Y. Associations between patterns of blood heavy metal exposure and health outcomes: insights from NHANES 2011-2016. BMC Public Health. 2024;24:558.
16. Liu Q, Xu C, Jin J, Li W, Liang J, Zhou S, et al. Early-life exposure to lead changes cardiac development and compromises long-term cardiac function. Sci Total Environ. 2023;904:166667.
17. Sears CG, Eliot M, Raaschou-Nielsen O, Poulsen AH, Harrington JM, Howe CJ, et al. Urinary Cadmium and Incident Heart Failure: A Case-Cohort Analysis Among Never-Smokers in Denmark. Epidemiology. 2022;33:185-92.
18. Tomasoni D, Adamo M, Lombardi CM, Metra M. Highlights in heart failure. ESC Heart Fail. 2019;6:1105-27.
19. Savarese G, Becher PM, Lund LH, Seferovic P, Rosano GMC, Coats AJS. Global burden of heart failure: a comprehensive and updated review of epidemiology. Cardiovasc Res. 2023;118:3272-87.
20. Bozkurt B, Ahmad T, Alexander KM, Baker WL, Bosak K, Breathett K, et al. Heart Failure Epidemiology and Outcomes Statistics: A Report of the Heart Failure Society of America. J Card Fail. 2023;29:1412-51.
21. Peters JL, Perlstein TS, Perry MJ, McNeely E, Weuve J. Cadmium exposure in association with history of stroke and heart failure. Environ Res. 2010;110:199-206.
22. Tellez-Plaza M, Jones MR, Dominguez-Lucas A, Guallar E, Navas-Acien A. Cadmium exposure and clinical cardiovascular disease: a systematic review. Curr Atheroscler Rep. 2013;15:356.
23. Tellez-Plaza M, Guallar E, Howard BV, Umans JG, Francesconi KA, Goessler W, et al. Cadmium exposure and incident cardiovascular disease. Epidemiology. 2013;24:421-9.
24. Deering KE, Callan AC, Prince RL, Lim WH, Thompson PL, Lewis JR, et al. Low-level cadmium exposure and cardiovascular outcomes in elderly Australian women: A cohort study. Int J Hyg Environ Health. 2018;221:347-54.
25. Guo J, Su L, Zhao X, Xu Z, Chen G. Relationships between urinary antimony levels and both mortalities and prevalence of cancers and heart diseases in general US population, NHANES 1999-2010. Sci Total Environ. 2016;571:452-60.
26. Packer M. Cobalt Cardiomyopathy: A Critical Reappraisal in Light of a Recent Resurgence. Circ Heart Fail. 2016;9.
27. Li X, Zhao Y, Zhang D, Kuang L, Huang H, Chen W, et al. Development of an interpretable machine learning model associated with heavy metals' exposure to identify coronary heart disease among US adults via SHAP: Findings of the US NHANES from 2003 to 2018. Chemosphere. 2023;311:137039.
28. Handelman GS, Kok HK, Chandra RV, Razavi AH, Lee MJ, Asadi H. eDoctor: machine learning and the future of medicine. Journal of Internal Medicine. 2018;284:603-19.
29. Vallabhaneni R, Dontu S, Pareek PK. Method for interpreting predictions of black-box machine learning models, involves performing interpretation of explanations as feature importance plots or individual instance explanations by utilizing interactive visualizations. NITTE MEENAKSHI TECHNOLOGY INST (NITT-Non-standard) VALLABHANENI R (VALL-Individual) DONTU S (DONT-Individual) PAREEK P K (PARE-Individual).
30. Van den Broeck G, Lykov A, Schleich M, Suciu D. On the Tractability of SHAP Explanations. Journal of Artificial Intelligence Research. 2022;74:851-86.
31. Mou C, Ren J. Automated ICD-10 code assignment of nonstandard diagnoses via a two-stage framework. Artif Intell Med. 2020;108:101939.
32. Stekhoven DJ, Bühlmann P. MissForest--non-parametric missing value imputation for mixed-type data. Bioinformatics. 2012;28:112-8.

33. Chan JYL, Leow SMH, Bea KT, Cheng WK, Phoong SW, Hong ZW, et al. Mitigating the Multicollinearity Problem and Its Machine Learning Approach: A Review. Mathematics. 2022;10.
34. Gustavo E. A. P. A. Batista RCP, Maria Carolina Monard. A study of the behavior of several methods for balancing machine learning training data. SIGKDD Explor Newsl. 2004;6:20 – 9.
35. Lui TCC, Gregory DD, Anderson M, Lee W-S, Cowling SA. Applying machine learning methods to predict geology using soil sample geochemistry. Applied Computing and Geosciences. 2022;16:100094.
36. Saeed MH, Hama JI. Cardiac disease prediction using AI algorithms with SelectKBest. Medical & Biological Engineering & Computing. 2023;61:3397-408.
37. Schaffernicht E, Kaltenhaeuser R, Verma SS, Gross HM. On Estimating Mutual Information for Feature Selection. ARTIFICIAL NEURAL NETWORKS-ICANN 2010, PT I2010. p. 362-+.
38. Wainer J, Cawley G. Nested cross-validation when selecting classifiers is overzealous for most practical applications. EXPERT SYSTEMS WITH APPLICATIONS. 2021;182.
39. Vij A, Nanjundan P. Comparing Strategies for Post-Hoc Explanations in Machine Learning Models. MOBILE COMPUTING AND SUSTAINABLE INFORMATICS2022. p. 585-92.
40. Friedman JH. Stochastic gradient boosting. Computational Statistics & Data Analysis. 2002;38:367-78.
41. Zhang C, Liu C, Zhang X, Almpanidis G. An up-to-date comparison of state-of-the-art classification algorithms. Expert Systems with Applications. 2017;82:128-50.
42. Wang H, Chai K, Du M, Wang S, Cai J-P, Li Y, et al. Prevalence and Incidence of Heart Failure Among Urban Patients in China: A National Population-Based Analysis. Circ Heart Fail. 2021;14:e008406.
43. Elbadawi A, Dang A, Elgendy IY, Thakker R, Albaeni A, Omer MA, et al. Age-specific trends and outcomes of hospitalizations with acute heart failure in the United States. Int J Cardiol. 2021;330.
44. Fagerberg B, Barregard L. Review of cadmium exposure and smoking-independent effects on atherosclerotic cardiovascular disease in the general population. Journal of Internal Medicine. 2021;290:1153-79.
45. Kim J, Song H, Lee J, Kim YJ, Chung HS, Yu JM, et al. Smoking and passive smoking increases mortality through mediation effect of cadmium exposure in the United States. Sci Rep. 2023;13:3878.
46. Xing X, Xu M, Yang L, Shao C, Wang Y, Qi M, et al. Association of selenium and cadmium with heart failure and mortality based on the National Health and Nutrition Examination Survey. J Hum Nutr Diet. 2023;36:1496-506.
47. Hollins DM, McKinley MA, Williams C, Wiman A, Fillos D, Chapman PS, et al. Beryllium and lung cancer: a weight of evidence evaluation of the toxicological and epidemiological literature. Crit Rev Toxicol. 2009;39 Suppl 1.
48. Wagoner JK, Infante PF, Bayliss DL. Beryllium: an etiologic agent in the induction of lung cancer, nonneoplastic respiratory disease, and heart disease among industrially exposed workers. Environ Res. 1980;21:15-34.
49. Ward E, Okun A, Ruder A, Fingerhut M, Steenland K. A mortality study of workers at seven beryllium processing plants. Am J Ind Med. 1992;22:885-904.
50. Cheung AC, Banerjee S, Cherian JJ, Wong F, Butany J, Gilbert C, et al. Systemic cobalt toxicity from total hip arthroplasties: review of a rare condition Part 1 - history, mechanism, measurements, and pathophysiology. Bone Joint J. 2016;98-B.
51. Wyles CC, Wright TC, Bois MC, Amin MS, Fayyaz A, Jenkins SM, et al. Myocardial Cobalt Levels Are Elevated in the Setting of Total Hip Arthroplasty. J Bone Joint Surg Am. 2017;99:e118.
52. Nigra AE, Howard BV, Umans JG, Best L, Francesconi KA, Goessler W, et al. Urinary tungsten and incident cardiovascular disease in the Strong Heart Study: An interaction with urinary molybdenum. Environ Res. 2018;166:444-51.
53. Shiue I. Urinary environmental chemical concentrations and vitamin D are associated with vision, hearing, and balance disorders in the elderly. Environ Int. 2013;53:41-6.
54. Oyagbemi AA, Omobowale TO, Asenuga ER, Abiola JO, Adedapo AA, Yakubu MA. Kolaviron attenuated arsenic acid induced-cardiorenal dysfunction via regulation of ROS, C-reactive proteins (CRP), cardiac troponin I (CTnI) and BCL2. J Tradit Complement Med. 2018;8:396-409.
55. Yu Y-J, Li Z-C, Tian J-L, Hao C-J, Kuang H-X, Dong C-Y, et al. Why Do People Gain Belly Fat in Rural Areas? A Study of Urinary Metal(loid)s and Abdominal Obesity in China. Environ Sci Technol. 2023;57:7938-49.
56. Shen T, Zhong L, Ji G, Chen B, Liao M, Li L, et al. Associations between metal(loid) exposure with overweight and obesity and abdominal obesity in the general population: A cross-sectional study in China. Chemosphere. 2024;350:140963.
57. Wang X, Mukherjee B, Park SK. Associations of cumulative exposure to heavy metal mixtures with obesity and its comorbidities among U.S. adults in NHANES 2003-2014. Environ Int. 2018;121:683-94.
58. Wang M, Xu Y, Pan S, Zhang J, Zhong A, Song H, et al. Long-term heavy metal pollution and mortality in a Chinese population: an ecologic study. Biol Trace Elem Res. 2011;142:362-79.
59. Liu Y, Jin Z, Fu S. Threshold and combined effects of heavy metals on the risk of phenotypic age acceleration among U.S. adults. Biometals. 2024.

Supplementary Materials

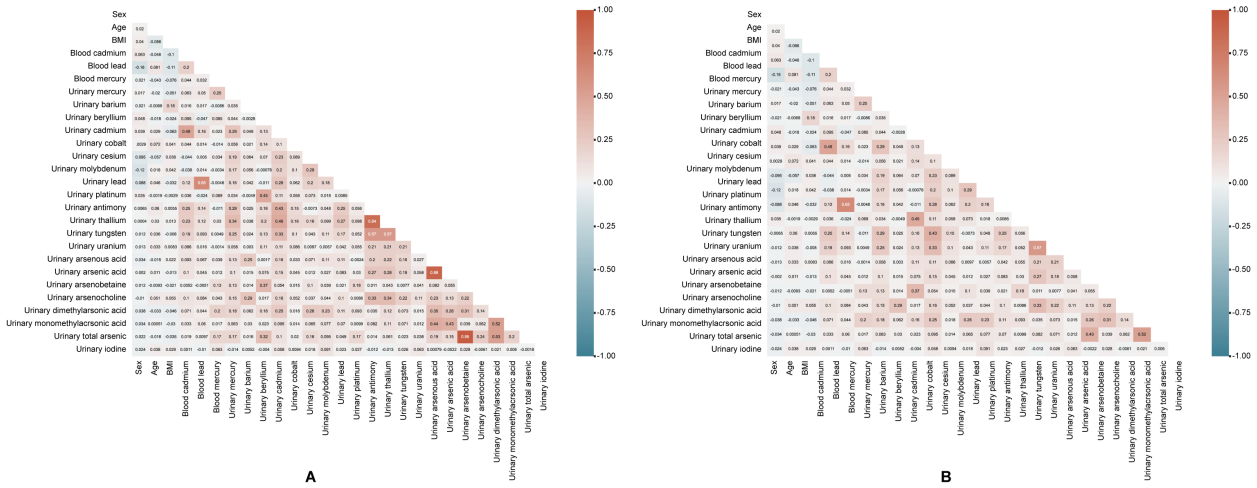

Supplementary Figure 1 | Correlation Heatmap of Features

This figure displays a correlation heatmap for each feature, with the numbers in each grid representing the Pearson correlation coefficients. Values close to +1 or -1 indicate strong positive or negative correlations, respectively, while values near 0 suggest little to no correlation. Panel A shows the heatmap prior to the removal of highly correlated variables, whereas Panel B presents the heatmap after these variables have been eliminated.

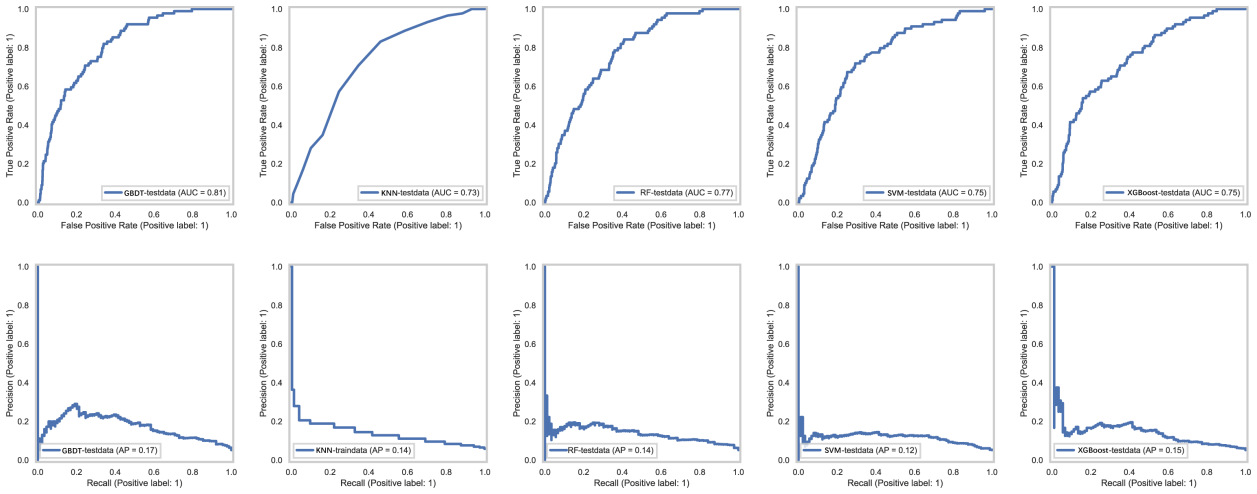

Supplementary Figure 2 | ROC and PR curves of the five models in the testing set

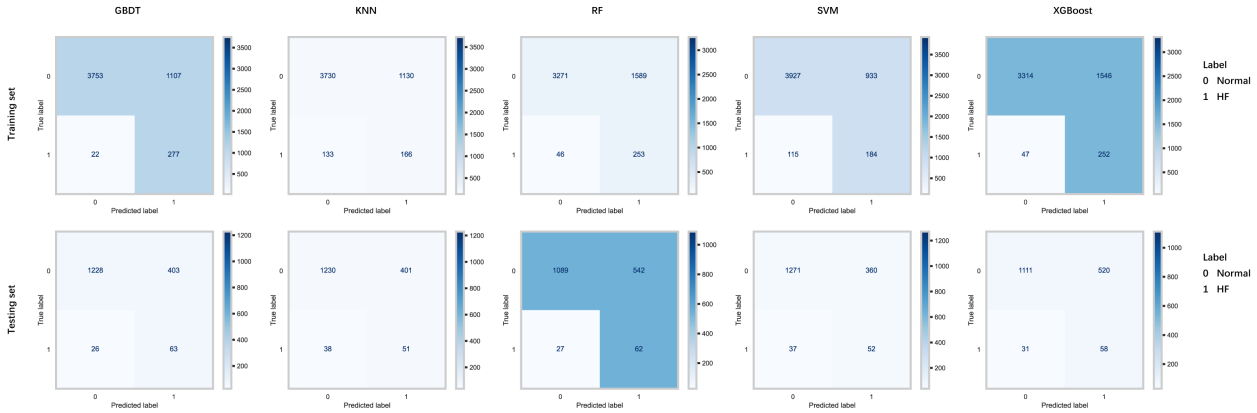

Supplementary Figure 3 | Confusion matrix of the five models

Each cell in the matrix indicates the number of instances classified into each category.

International Journal of Clinical Medicine & Pharmacology

https://doi.org/10.70731/6tk6cp54

Identification and Management Strategies for Low Cardiac Output Syndrome After Cardiac Surgery

Jingxiao Li [a], Chunlou Wei [a], Jianlin Wen [a], Ting Zhou [a,*]

[a] *The First Affiliated Hospital of Guangxi Medical University Cardiothoracic Surgery Intensive Care Unit, Nanning, Guangxi, China.*

KEYWORDS

Cardiac Surgery, Low Cardiac Output Syndrome, Vasoactive Drugs, Instrument Circulation Assistance

ABSTRACT

Low cardiac output syndrome is one of the common complications after cardiac surgery, and is also the main cause of postoperative death. In this paper, the risk factors, prediction models, diagnosis and treatment of low cardiac output syndrome were reviewed in recent years, so as to provide reference for early identification and appropriate management of low cardiac output syndrome.

1. Background

Low cardiac output syndrome (LCOS) is a clinical syndrome characterized by decreased cardiac output and inadequate peripheral organ perfusion. It is one of the most serious complications after cardiac surgery, with an incidence rate of up to 10% and a mortality rate that may exceed 20% [1-3]. Severe LCOS leads to prolonged use of ventilators, increased risk of acute kidney injury and pulmonary infection, prolonged stay in intensive care units (ICU), prolonged hospitalization, increased costs, and even patient death, posing great challenges to clinical doctors and imposing a heavy burden on society. Therefore, studying the potential risks of LCOS, understanding its occurrence and development patterns, and being able to identify and handle it in a timely manner are of great significance for improving the prognosis of patients after cardiac surgery.

2. Identification of LCOS

2.1. Potential Risk Factors for LCOS Occurrence

By analyzing literature, it was found that depending on the type of heart disease and surgical approach, the risk factors for LCOS vary and can be divided into three categories: (1) Heart valve surgery: Researchers have studied that the risk factors for LCOS are low body weight, cardiothoracic ratio > 0.7, preoperative renal insufficiency, pulmonary hypertension, preoperative left ventricular ejection fraction (LVEF) < 40%, cardiopulmonary bypass (CPB) time > 140 minutes, and postoperative bleeding volume [4-6]. (2) Coronary artery bypass grafting (CABG): studies had shown a history of myocardial infarction, preoperative arrhythmia, and heart function grade II to IV and LVEF < 45%, intraoperative CPB time > 100 minutes and blood loss > 800 ml are risk factors for postoperative LCOS; a study in Brazil identified risk factors for LCOS after CABG surgery: age > 60 years, emergency surgery, incomplete revascularization, and LVEF < 50% [6-9]. (3) Complex congenital

* Corresponding author. E-mail address: 921132@sr.gxmu.edu.cn

Received 20 January 2025; Received in revised form 18 February 2025; Accepted 26 February 2025; Available online 28 February 2025.

heart disease surgery: studies suggested that low age, small body weight, long aortic occlusion time and CPB time, increased postoperative CPB resistance and preoperative pulmonary hypertension are risk factors for postoperative LCOS; a Meta-analysis study pointed out that the independent significant risk factors of LCOS including age > 65 years, LVEF < 50%, CABG, emergency surgery or CPB and incomplete revascularization [6]. Diabetes mellitus and preoperative renal dysfunction are not independent predictors, but the combination of the two increases the risk of LCOS by 50% [10-12].

To sum up, older patients with preoperative LVEF < 50%, long operation time, more blood transfusion and unsatisfactory anatomic correction have a high incidence of postoperative LCOS, while children with complex congenital heart disease who are small months old and low weight have a much higher incidence of postoperative LCOS than adult cardiac surgery [6].

2.2. Related Research on Predicting the Occurrence of LCOS

There are many risk factors for LCOS, but its prediction model has not been uniformly recognized. At present, EuroSCORE II is widely used in the risk assessment model of cardiac surgery, which can predict the perioperative cardiovascular changes sensitively [13, 14]. By analyzing the data of 41729 CABG patients in Chinese Cardiac Surgery Registry (CCSR) database from 2013 to 2015, researchers established a new risk prediction model using 21 risk factors to predict, and verified it with the data of 15047 CABG patients in CCSR database in 2016. It was found that the new risk prediction model could more accurately predict the in-hospital mortality after CABG in patients in mainland China, which was helpful to identify high-risk patients before surgery [15, 16]. However, this model has not been widely used in clinic yet and needs further research.

2.3. Diagnosis and Controversy of LCOS

The expert consensus of LCOS in 2018 defined cardiac index < 2.0 L/min/m2 as low cardiac output [17]. The results of questionnaire survey catch by Shanghai Children's Medical Center showed that only 77% of the centers could monitor cardiac output and 41% could monitor microcirculation in China[18]. Therefore, for some centers with incomplete monitoring equipment, the diagnosis of LCOS is difficult to clarify and prone to missed diagnosis. At present, some cardiac centers have quantified the diagnosis of LCOS and found slight differences in its criteria through literature analysis. The diagnostic criteria of Beijing Anzhen Hospital include: (1) LVEF < 40%; (2) Cardiac index < 2.3 L/min/m2; (3) Persistent hypotension; (4) Oliguria (urine output < 1 ml/kg/h without diuretics); (5) Lactic acid > 3.0 mol/L; (6) Central venous oxygen saturation < 50%; (7) Vasoactive inotropic score > 15.5. When any one of (1) or (2), or any three of (3) - (7) appears after surgery, it is diagnosed as postoperative LCOS [19]. Another study refined the diagnostic criteria into 9 items, and patients who met two or more of items 1-8, or who developed item 9, were directly diagnosed with LCOS: (1) Cardiac index < 2.5 L/min/m2; (2) Postoperative echocardiography measured LVEF < 50%; (3) Systolic blood pressure < 90 mmHg, or mean arterial pressure < 60mmHg, or continuous decrease in systolic blood pressure exceeding 20% of preoperative baseline blood pressure for more than 2 hours; (4) Central venous pressure > 13 mmHg, or pulmonary capillary pressure > 15 mmHg, or central venous oxygen saturation < 50%; (5) Postoperative dopamine dosage > 10 ug/kg/min is required to maintain systolic blood pressure and cardiac output, and the duration of medication should exceed 30 minutes; (6) Lactic acid > 3.5 mmol/L or metabolic acidosis (pH < 7.4, lactic acid > 3.0 mmol/L, base excess < -2 mmol/L); (7) Urine output < 0.5ml/kg/h when diuretics are not used; (8) Insufficient peripheral perfusion, coldness and cyanosis at the extremities; (9) The patient needs intra-aortic ballon pumps (IABP) due to hemodynamic disorders [6]. The essence of LCOS is a decrease in cardiac output leading to inadequate tissue perfusion and an imbalance between cellular oxygen supply and consumption. The different stages of pathological and physiological changes in LCOS patients, as well as the differences in intervention methods, intervention intensity, and intervention effects received by patients, can lead to heterogeneity in clinical manifestations and related monitoring indicators. Therefore, people can fully understand that different studies will propose different diagnostic criteria for LCOS, and they can also understand why the incidence of LCOS varies greatly among different studies.

2.4. Monitoring Methods for the Development and Changes of LCOS

At present, mature monitoring methods of LCOS include: (1) Ultrasound technology: In recent years,

echocardiography developed rapidly in the field of cardiac surgery, including ultrasound-guided interventional closure surgery in congenital heart disease surgery and evaluation of valve function in valve surgery. echocardiography has become the second eye of surgeons. After cardiac surgery, echocardiography can reveal the type of LCOS and evaluate ejection fraction, cardiac volume, systolic and diastolic function, valve pathology, pulmonary circulation, ventricular filling pressure, pericardial effusion, and fluid reactivity [20]. As a portable and non-invasive examination method, echocardiography can provide targeted real-time assessment of the patient's condition in a short period of time, guide the rapid treatment of LCOS causes, provide intuitive and rapid evaluation of treatment outcomes [21]. However, echocardiography has a high degree of technical dependence on the operator, subjective examination results, and cannot provide continuous hemodynamic measurements. (2) The pulmonary artery floating catheter (PAC), also known as the Swan-Ganz balloon floating catheter, can provide reliable hemodynamic parameters that reflect changes in the patient's cardiac output per unit of time. In addition, it can also provide pulmonary artery pressure, right heart and pulmonary artery capillary filling pressure, peripheral blood vessel and pulmonary artery resistance [22, 23]. However, placing PAC in the right heart is an invasive surgery that may lead to cardiovascular complications such as pneumothorax, pulmonary artery rupture, arrhythmia, pericardial tamponade, infection, catheter entanglement, thromboembolism, etc. Currently, it is not widely used in clinic. (3) Pulse index continuous cardiac output (PICCO) is a novel minimally invasive hemodynamic monitoring technique that measures a series of clinical monitoring indicators, such as CO, stroke volume (SV), stroke volume variation (SVV), global end diastolic volume (GEDV), intrathoracic blood volume (ITBV), and indicators related to cardiac preload or afterload, through a central vein and arterial catheter using thermal dilution method. Therefore, some clinical doctors use it as a substitute for PAC [24]. The safety of PICCO operation is higher than PAC. However, the measurement of data requires calibration with low-temperature saline, which can easily cause arrhythmia after cardiac surgery and is limited in use. (4) The FloTrac/Vigileo system: With only one arterial catheter, cardiac output can be continuously and timely calculated by collecting arterial waveforms and combining them with the patient's basic information (age, gender, height, body mass, etc.) to analyze and calculate cardiac output, SV, SVV easily, but the accuracy is low in patients with severe arrhythmia or severe aortic valve insufficiency. Currently, large-scale clinical applications have not been carried out.

3. Management Strategy of LCOS

3.1. Basic Principles of LCOS Management

The treatment for the etiology of LCOS includes several aspects: (1) Actively correcting reversible factors that lead to low cardiac output, especially for LCOS caused by surgical factors, it must be resolved as soon as possible. (2) Optimize capacity status to maintain optimal preload levels. (3) The application of vasoactive drugs stabilizes heart rate and rhythm, and ensures atrioventricular synchronization in pacemaker dependent patients. (4) Mechanical circulation assisted therapy is used when the drug treatment effect is invalid [17].

3.2. Vasoactive Drugs

Goal-directed fluid therapy (GDFT) refers to the therapeutic concept of using monitoring technology for hemodynamic management, individualized fluid replacement based on the patient's cardiac function, load status, and fluid needs. Therefore, hemodynamic management not only includes individualized volume management, but also means individualized treatment with vasoactive drugs.

Vasoactive drugs mainly regulate the cardiovascular system by acting on adrenergic and non-adrenergic receptors, including positive inotropic drugs, vasopressors, and vasodilators. According to the different stages of hemodynamic changes in LCOS, the direct effects of drugs on myocardium and vascular tension can be divided into four categories: (1) Cardiac vasodilators: dobutamine, milrinone; (2) Simple vasodilator: Sodium nitroprusside; (3) Cardioconstrictors: Norepinephrine, epinephrine, dopamine; (4) Simple vasoconstrictors: epinephrine, vasopressin. In addition, levosimendan is a novel calcium sensitizing positive inotropic drug and an ATP sensitive potassium channel opener that enhances myocardial contractility, dilates peripheral and coronary vessels, improves the hemodynamic effects of heart failure and clinical symptoms of patients without increasing myocardial oxygen consumption. It can effectively prevent or treat LCOS after cardiac surgery. Researches had shown that levosimendan can improve postoperative cardiac output and tissue perfusion, reduce the

occurrence of LCOS, then improve survival rate [25, 26]. European experts suggested that levosimendan can effectively stabilize the hemodynamics of patients undergoing cardiac surgery, thereby reducing the need for positive inotropic drugs and mechanical circulatory support [27]. The optimal time for preoperative treatment of levosimendan is the day before surgery, with a recommended dose of 0.1 μg/kg/min and continuous infusion for 24 hours. The latest meta-analysis showed that levosimendan can reduce the mortality rate of preoperative LVEF patients, but does not affect the overall mortality rate. The adverse reactions of levosimendan include hypotension and ventricular arrhythmia, which should be selected according to the patient's condition [28].

The application of vasoactive drugs should be based on clinical pathological and physiological status as well as hemodynamic conditions, and appropriate drugs and doses should be selected to reduce potential adverse reactions. According to a survey questionnaire from Shanghai Children's Medical Center, dopamine is the main medication used for preventive medication in each center [18]. The selection of therapeutic drugs is basically the same for each center: (1) Milrinone is used for LCOS with increased systemic circulation resistance; (2) Dopamine and adrenaline are used to reduce systemic circulation resistance in LCOS; (3) LCOS with increased pulmonary circulation resistance is treated with milrinone, catecholamines, and pulmonary vasodilators [18]. A systematic literature review studied positive inotropic drugs after CPB and showed that dobutamine and phosphodiesterase inhibitors are effective drugs for treating LCOS [29]. Another meta-analysis collected data from 2385 individuals and three ongoing studies, showing uncertainty in the impact of vasoactive drugs on LCOS all-cause mortality. Therefore, the effectiveness of drug therapy is limited, and mechanical circulation assisted therapy is an indispensable means of treating LCOS.

3.3. Instrument Circulation Assistance

Optional extracorporeal life support includes IABP, extracorporeal membrane oxygenation (ECMO), ventricular assist devices (VADs), Impella pumps, and etc. The most widely used currently are ECMO and IABP [31].

3.3.1. ECMO

In the 1970s, ECMO was applied clinically as a respiratory and cardiac function support technology, but its application was limited in the early stages due to the high incidence of complications. With the continuous development of technology, complications are gradually decreasing, and the application of ECMO is becoming more and more common. Its applications in the field of cardiac surgery include the treatment of postoperative cardiogenic shock, severe donor organ failure after heart transplantation, the installation of VAD or transitional treatment for heart transplantation in the end-stage of heart failure, and the prevention and treatment of right heart failure after LVAD [32]. According to literature reports, the incidence of ECMO use in patients after cardiac surgery ranges from 0.4 to 3.7% [33]. Maxwell and colleagues evaluated over 9000 ECMO patients from the National Inpatient Sample Database in the United States from 1998 to 2009, and found 4493 patients, approximately 50% of patients had postoperative cardiogenic shock [34]. The basic working principle of ECMO is to drain the patient's venous blood outside the body, oxygenate it, and then return it to the patient's artery or vein, replacing or partially replacing the patient's heart and lung function. It can maintain the patient's basic vital signs for a period of time to strive for the opportunity for recovery and functional recovery of heart and lung lesions, or provide transitional time for the next step of transplantation. At present, most cardiac surgeries in China use the venous-arterial (V-A) mode for ECMO assisted circulation [35]. Existing studies had shown that ECMO increases systemic perfusion through countercurrent blood, reduces LV preload, increases LV afterload, reduces stroke volume, increases myocardial oxygen demand, and reduces PAWP. A meta-analysis [36] showed that the hemodynamic support provided by V-A ECMO has a reasonable survival benefit with medium and long-term results in the treatment of intractable cardiogenic shock after cardiac surgery in adults. A research showed that ECMO is an important support method for the treatment of reversible cardiopulmonary failure after cardiac surgery, the timing of ECMO, the application of protective pulmonary ventilation, and the effective control and prevention of bleeding are the key factors for the success of ECMO treatment [37]. In addition, patients who established ECMO within 24 hours after operation had a higher survival rate than patients who established ECMO after 24 hours after operation, and the incidence of complications such as acute renal failure and ischemic hepatitis was lower [38, 39]. In conclusion, the success rate of ECMO treatment is high. Ariyaratnam et al. classified the causes of cardiac dys-

function after cardiac surgery into three categories: (1) Reversible, caused by myocardial stunning, which can be restored by short-term support of ECMO. (2) Potentially reversible, mainly caused by localized small focal acute myocardial infarction and acute pulmonary edema, which may require long-term ECMO support. (3) Irreversible, caused by severe heart failure, extensive myocardial infarction, and chronic pulmonary hypertension, ECMO cannot play a fundamental role in the treatment, and heart transplantation should be considered [40]. This explains the reason why ECMO, as the most powerful device support at present, still has high mortality [41]. ECMO is expensive and can lead to serious complications, so its benefits and risks need to be weighed.

3.3.2. IABP

Since the application of IABP in clinic in the 1960s, more than one million patients have received therapy. Since 1973, when IABP was first used in cardiac surgery to assist CPB during operation, IABP has been more and more widely used in cardiac surgery [42]. IABP inflates the balloon in diastole and deflates the balloon in systole, which plays an auxiliary role in the heart. Compared with ECMO, it only has circulation support function, but has no respiratory or circulatory replacement effect. However, because of its simplicity, effectiveness and relatively low price, IABP is widely used and plays an irreplaceable role in the management of LCOS after cardiac surgery. In addition, the timing of intervention is still an important factor affecting the outcome of circulatory assistance. A randomized controlled study pointed out that 1 hour before operation, prophylactic implantation of IABP can reduce the mortality and incidence of LCOS in patients with high-risk CABG [43]. ECMO and IABP cannot be replaced by each other. At present, it is considered that the effect of their combined application is good, but the timing is still controversial. Studies have shown that ECMO combined with IABP in the treatment of high-risk coronary heart disease can significantly improve the hemodynamic indexes of patients, reduce the in-hospital mortality [44]. For patients with LCOS, there is no clear consensus on whether IABP or ECMO should be implanted first, which needs further research.

4. Summary and Prospects

In conclusion, the occurrence of LCOS after cardiac surgery is inevitable, and effective treatment can reduce the mortality. Preoperative comprehensive consideration should be given to various factors of patients, screening high-risk patients with LCOS and carrying out goal-directed therapy based on adequate monitoring, which is conducive to the early identification and appropriate treatment of LCOS.

Reference

1. Duncan AE, Kartashov A, Robinson SB, et al. Risk factors, resource use, and cost of postoperative low cardiac output syndrome. J Thorac Cardiovasc Surg. 2020 .
2. Algarni KD, Maganti M, Yau TM. Predictors of low cardiac output syndrome after isolated coronary artery bypass surgery: trends over 20 years. Ann Thorac Surg. 2011. 92(5): 1678-84.
3. Maganti MD, Rao V, Borger MA, Ivanov J, David TE. Predictors of low cardiac output syndrome after isolated aortic valve surgery. Circulation. 2005. 112(9 Suppl): I448-52.
4. Li Zhao, Liu Peng, Zhang Yu, limongdie, Wu Yue, Zhang Guobao. Risk factors of low cardiac output syndrome in patients with giant left ventricular valvular disease after operation [in Chinese]. Journal of Zhengzhou University (Medical Edition). 2021.56 (01): 89-93.
5. Xiao Hongyan, Yang Guangtian. Clinical study on low cardiac output syndrome after heart valve replacement surgery [in Chinese]. Journal of Emergency and Critical Care Medicine in Internal Medicine. 2012. 18(05): 271-273+276.
6. Tang Maohua. Analysis of factors related to low cardiac output after extracorporeal circulation surgery [in Chinese]. Zunyi Medical University, 2021. DOI:10.27680/d.cnki.gzyyc. 2021.000353.
7. Li Shuzhen, Zhu Xianming, Liu Zhiping, Zhang Yulong, Zhao Long, Wang Jian. Analysis and prevention of risk factors for low cardiac output syndrome after coronary artery bypass grafting [in Chinese]. Journal of Inner Mongolia Medical College 2009. 31(05): 461-465.
8. Liu Haiyuan, Zhang Chengxin, Liu Zhi, Li Xin, Ge Shenglin. Analysis of risk factors for low cardiac output syndrome in patients undergoing coronary artery bypass grafting under extracorporeal circulation Lingnan [in Chinese]. Journal of Cardiovascular Disease 2020. 26(02): 170-175.
9. Sá MP, Nogueira JR, Ferraz PE, et al. Risk factors for low cardiac output syndrome after coronary artery bypass grafting surgery. Rev Bras Cir Cardiovasc. 2012. 27(2): 217-23.
10. Low Cardiac Output Syndrome after Cardiac .
11. Pan W, Hindler K, Lee VV, Vaughn WK, Collard CD. Obesity in diabetic patients undergoing coronary artery bypass graft surgery is associated with increased postoperative morbidity. Anesthesiology. 2006. 104(3): 441-7.

12.Tolpin DA, Collard CD, Lee VV, Elayda MA, Pan W. Obesity is associated with increased morbidity after coronary artery bypass graft surgery in patients with renal insufficiency. J Thorac Cardiovasc Surg. 2009. 138(4): 873-9.

13.Nashef SA, Roques F, Sharples LD, et al. EuroSCORE II. Eur J Cardiothorac Surg. 2012. 41(4): 734-44; discussion 744-5.

14.Ding W, Ji Q, Shi Y, Ma R. Predictors of low cardiac output syndrome after isolated coronary artery bypass grafting. Int Heart J. 2015. 56(2): 144-9.

15.Hu Z, Chen S, Du J, et al. An In-hospital Mortality Risk Model for Patients Undergoing Coronary Artery Bypass Grafting in China. Ann Thorac Surg. 2020. 109(4): 1234-1242.

16.Chinese Cardiovascular Health and Disease Report 2020 [in Chinese].

17.Du Yu, Zhang Haitao. Interpretation of Chinese expert consensus on low cardiac output syndrome [in Chinese]. Chinese Circulation Magazine 2018. 33(S2): 84-88.

18.Gong Xiaolei, Zhu Limin, Liu Yujie, Zhang Mingjie, Xu Zhuoming. A multicenter survey on perioperative monitoring and application of vasoactive drugs in children with congenital heart disease [in Chinese]. Chinese Journal of Extracorporeal Circulation 2019. 17(03): 132-136+152.

19.Mao Jun, Xu Yaoqiang, Chen Yan. Analysis of related risk factors for low cardiac output syndrome after complete anomalous pulmonary vein drainage [in Chinese]. Chinese Journal of Critical Care Medicine (Electronic Edition), 2020, 13 (04): 253-257.

20.Jozwiak M, Monnet X, Teboul JL. Monitoring: from cardiac output monitoring to echocardiography. Curr Opin Crit Care. 2015. 21(5): 395-401.

21.Spencer KT, Kimura BJ, Korcarz CE, Pellikka PA, Rahko PS, Siegel RJ. Focused cardiac ultrasound: recommendations from the American Society of Echocardiography. J Am Soc Echocardiogr. 2013. 26(6): 567-81.

22.American Society of Anesthesiologists Task Force on Pulmonary Artery Catheterization. Practice guidelines for pulmonary artery catheterization: an updated report by the American Society of Anesthesiologists Task Force on Pulmonary Artery Catheterization. Anesthesiology. 2003. 99(4): 988-1014.

23.Amabili P, Benbouchta S, Roediger L, et al. Low Cardiac Output Syndrome After Adult Cardiac Surgery: Predictive Value of Peak Systolic Global Longitudinal Strain. Anesth Analg. 2018. 126(5): 1476-1483.

24.Zhao Z, Jiang L, Xi X, et al. Prognostic value of extravascular lung water assessed with lung ultrasound score by chest sonography in patients with acute respiratory distress syndrome[J]. BMC Pulm Med, 2015,15:98. DOI: 10.1186/s12890-015-0091-2.

25.Na Heya, Faxian En, Zhou Yuyang. The impact of levosimendan on the prognosis of patients with left ventricular ejection fraction<40% after cardiac surgery [in Chinese]. Chinese Journal of Practical Diagnosis and Treatment, 2021, 35 (05): 513-515.

26.Zou Honglin, Jia Zheng, Xing Zhengjiang. Clinical application of levosimendan in the treatment of low cardiac output syndrome after cardiopulmonary bypass [in Chinese]. Journal of Kunming Medical University, 2019, 40 (09): 62-67.

27.Toller W, Heringlake M, Guarracino F, et al. Preoperative and perioperative use of levosimendan in cardiac surgery: European expert opinion. Int J Cardiol, 2015,184:323-336. DOI: 10.1016/j.ijcard.2015.02.022.

28.Sanfilippo F, Knight JB, Scolletta S, et al. Levosimendan for patients with severely reduced left ventricular systolic function and/or low cardiac output syndrome undergoing cardiac surgery: a systematic review and meta-analysis. Crit Care, 2017,21(1):252. DOI: 10.1186/s13054-017-1849-0.

29.Gillies M, Bellomo R, Doolan L, et al. Bench-to-bedside review: Inotropic drug therapy after adult cardiac surgery -- a systematic literature review[J]. Crit Care, 2005,9(3):266-279. DOI: 10.1186/cc3024.

30.Uhlig K, Efremov L, Tongers J, et al. Inotropic agents and vasodilator strategies for the treatment of cardiogenic shock or low cardiac output syndrome[J]. Cochrane Database Syst Rev, 2020,11:CD009669. DOI: 10.1002/14651858.CD009669.pub4.

31.Werdan K, Gielen S, Ebelt H, et al. Mechanical circulatory support in cardiogenic shock[J]. Eur Heart J, 2014,35(3):156-167. DOI: 10.1093/eurheartj/eht248.

32.Chen Kai, Tang Hanwei, Hou Jianfeng. Application of extracorporeal membrane oxygenation in cardiac surgery [in Chinese]. Chinese Journal of Circulation, 2019, 34 (12): 1244-1248.

33.Lorusso R, Raffa GM, Alenizy K, et al. Structured review of post-cardiotomy extracorporeal membrane oxygenation: part 1-Adult patients[J]. J Heart Lung Transplant, 2019,38(11):1125-1143. DOI: 10.1016/j.healun.2019.08.014.

34.Maxwell BG, Powers AJ, Sheikh AY, et al. Resource use trends in extracorporeal membrane oxygenation in adults: an analysis of the Nationwide Inpatient Sample 1998-2009[J]. J Thorac Cardiovasc Surg, 2014,148(2):416-421.e1. DOI: 10.1016/j.jtcvs.2013.09.033.

35.Rastan AJ, Dege A, Mohr M, et al. Early and late outcomes of 517 consecutive adult patients treated with extracorporeal membrane oxygenation for refractory postcardiotomy cardiogenic shock[J]. J Thorac Cardiovasc Surg, 2010,139(2):302-311, 311.e1. DOI: 10.1016/j.jtcvs.2009.10.043.

36.Khorsandi M, Dougherty S, Bouamra O, et al. Extracorporeal membrane oxygenation for refractory cardiogenic shock after adult cardiac surgery: a systematic review and meta-analysis[J]. J Cardiothorac Surg, 2017,12(1):55. DOI: 10.1186/s13019-017-0618-0.

37.Lu Andong, Guo Jian, Miao Lixia. Exploration of clinical application of extracorporeal membrane oxygenation support after cardiac surgery [in Chinese]. Chinese

Journal of Extracorporeal Circulation, 2017,15 (02): 100-104.

38. Yao Jingxin, Lv Lin, Gao Guodong. The impact of the timing of establishing outer membrane oxygenation in adults after cardiac surgery on prognosis [in Chinese]. Chinese Journal of Molecular Cardiology, 2018, 18 (02): 2426-2429.
39. ELSO E. Extracorporeal Life Support (ECLS) registry report international summary, 2018[J].
40. Ariyaratnam P, McLean LA, Cale AR, et al. Extra-corporeal membrane oxygenation for the post-cardiotomy patient[J]. Heart Fail Rev, 2014,19(6):717-725. DOI: 10.1007/s10741-014-9428-9.
41. Cheng R, Hachamovitch R, Kittleson M, et al. Complications of extracorporeal membrane oxygenation for treatment of cardiogenic shock and cardiac arrest: a meta-analysis of 1,866 adult patients[J]. Ann Thorac Surg, 2014,97(2):610-616. DOI: 10.1016/j.athoracsur.2013.09.008.
42. Ferguson JJ 3rd, Cohen M, Freedman RJ Jr, et al. The current practice of intra-aortic balloon counterpulsation: results from the Benchmark Registry[J]. J Am Coll Cardiol, 2001,38(5):1456-1462. DOI: 10.1016/s0735-1097(01)01553-4.
43. Theologou T, Bashir M, Rengarajan A, et al. Preoperative intra aortic balloon pumps in patients undergoing coronary artery bypass grafting[J]. Cochrane Database Syst Rev, 2011,(1):CD004472. DOI: 10.1002/14651858.CD004472.pub3.
44. Liu Fengfeng, Zheng Jianjie. Analysis of the effect of ECMO combined with IABP in the treatment of high-risk coronary heart disease and the influencing factors of patient prognosis [in Chinese]. Clinical Medical Research and Practice, 2022,7 (01): 19-22.

International Journal of Clinical Medicine & Pharmacology

https://doi.org/10.70731/625k6788

Integrated Traditional Chinese and Western Medicine in the Treatment of Heart Failure with Reduced Ejection Fraction Combined with Variant Angina：A Case Report

Siqi Li [a], Xiaowan Han [b], Lanjun Kou [b], Diying Zhang [a], Guozhong Pan [b,*]

[a] *Dongzhimen Hospital, Beijing University of Chinese Medicine, Beijing, China*
[b] *Second Department of Cardiology, Dongzhimen Hospital, Beijing University of Chinese Medicine, Beijing, China*

KEYWORDS

Heart Failure With Reduced Ejection Fraction, Variant Angina, Integration of Traditional Chinese and Western Medicine

ABSTRACT

This article reported a case of heart failure with reduced ejection fraction combined with Variant angina. The patient developed variant angina pectoris after taking the conventional Western medicines for heart failure with reduced ejection fraction. On the basis of adjusting the relevant medications, Zhishi Xiebai Guizhi Decoction and Guo Weiqin's Yiqi Xiefei Decoction were added, after which the cardiac function was improved, the left ventricular ejection fraction was increased, and the symptoms of chest tightness and pain did not recur.

1. Introduction

Heart failure (HF) encompasses a series of clinical syndromes such as dyspnea, fatigue, and fluid retention. Its main feature is systemic and/or pulmonary circulation congestion accompanied by inadequate perfusion of tissues and organs. Different cardiac structural or functional abnormalities can induce these symptoms by reducing the efficiency of the heart's pumping function and its metabolic demands.(1) This disease is a global epidemic. In 2017, the results of a study involving 50 million people aged 25 and above in six provinces in China showed that the incidence rate of HF was 1.10% for both genders, with a total of 12.1 million patients.(2) Heart failure with reduced ejection fraction (HFrEF), as one of the types, refers to that the left ventricular ejection fraction (LVEF) is ≤40%, which is most commonly caused by left ventricular dysfunction and clinically manifested as decreased cardiac output, myocardial hypertrophy, increased end-diastolic ventricular pressure and so on. A survey in the UK showed that the prevalence of HF with HFrEF among hospitalized patients with HF was 41%, and the mortality rate was as high as 47%, imposing a heavy burden on society and families.(3)

Variant angina (VA), also known as vasospastic angina or Prinzmetal's angina, is a special type of unstable angina. It mainly results from coronary artery spasm. During an attack, it can cause transient myocardial ischemia and trigger symptoms such as chest pain and chest tightness. The degree of pain is severe and the duration is variable. It often occurs suddenly during rest or daily activities.(4) Clinically, the incidence of VA also remains high. It has been reported that the prevalence of this disease ranges

* Corresponding author. E-mail address: panguozhong108@sina.com

Received 19 January 2025; Received in revised form 19 February 2025; Accepted 26 February 2025; Available online 28 February 2025.

from 33.4% to 57.6% in Western countries and from 40% to 79% in Asian countries.[5]

The traditional drug treatment for HF is the "new quadruple" therapy, namely renin-angiotensin system inhibitors, beta-blockers (BB) , mineralocorticoid receptor antagonists, and sodium-glucose cotransporter 2 inhibitors. Recently, the Heart Failure Association of the European Society of Cardiology released a clinical consensus on the management of heart failure exacerbation, pointing out that vericiguat has the potential to reduce the risk of cardiovascular death or hospitalization after exacerbation in patients with HFrEF. It is recommended that symptomatic patients with a LVEF < 45% should add vericiguat on the basis of the "HFrEF quadruple treatment" after a heart failure exacerbation event.[6] It can be seen that the current clinical drug treatment for HFrEF has gradually shifted from the "new quadruple" therapy to the "new five-combination" therapy. However, the clinical use of these drugs may all lead to hypotension, resulting in inadequate perfusion of tissues and organs. For VA caused by transient coronary artery stenosis due to coronary artery vasoconstriction and resulting in insufficient blood perfusion, the decrease in blood pressure leads to myocardial ischemia and will further aggravate this spasm. Meanwhile, BB inhibit the vasodilatory effect of beta-receptors on coronary arteries, which makes the excitation of alpha-receptors more significant, so that it is difficult to relieve coronary artery spasm.

Therefore, for patients with HFrEF combined with VA, when contradictions arise in Western medicine treatment, turning to traditional Chinese medicine (TCM) decoctions is a good strategy. Based on this, this article reviews a valid medical record of a patient with HFrEF combined with VA who was treated with a clinical integrated traditional Chinese and Western medicine regimen. The details are as follows.

2. Case Introduction

2.1. Chief Complaint

Mr. Wang, male, 53 years old, was admitted to the hospital due to “intermittent chest tightness and shortness of breath for 10 days”.

2.2. Present Medical History

On August 20, 2024, the patient experienced chest tightness, shortness of breath, weakness and fainted after drinking alcohol. He was conscious and visited the emergency department of a certain hospital in Beijing. The troponin level was found to be 30 ng/ml (normal range: 0 - 17.5). After receiving drug treatment, the symptoms were relieved and the patient refused hospitalization. Since then, the patient had experienced chest tightness and shortness of breath during daily activities, which could relieve spontaneously after about 30 minutes without taking any medication for control. On August 30, the patient had another episode of chest tightness and shortness of breath, with a blood pressure of 170/125 mmHg. He then came to our hospital for hospitalization.

2.3. Past Medical History

The patient had a 15-year history of hypertension, with the highest blood pressure reaching 180/120 mmHg. He regularly took Yufeng Ningxin Capsules orally but did not monitor his blood pressure regularly. He denied a history of coronary heart disease, hyperlipidemia, diabetes mellitus, etc. He had undergone resection of bladder cancer 21 years ago.

2.4. Personal and Family History

He had a 30-year smoking history and had not quit, with an average of 20 - 30 cigarettes per day. He had a 10-year drinking history and had not quit, with an average of 3 liang per day. His mother had a history of hypertension.

2.5. Traditional Chinese Medicine Four Diagnostic Methods

The patient looked listless, was short of breath and disinclined to speak. H His facial complexion and lip color were dark purple. He had frequent urination with light yellow color, and his stools were loose. He had difficulty falling asleep. His tongue was pale, white and tender, with a thick white greasy coating and cracks in the middle. The sublingual collateral vessels were dark-red without significant distension. The pulse was wiry and slippery.

2.6. Physical Examination

Body temperature was 36 °C, heart rate was 92 beats per minute, respiration rate was 18 breaths per minute, and blood pressure was 156/94 mmHg. The breath sounds of both lungs were clear, and no obvious dry or wet rales were heard. The heart rhythm was regular, and no pathological murmurs were heard in each valve. The skin on the feet was desquamating, and there was mild edema in both lower limbs. No other obvious abnormalities were found during the rest of the physical examination.

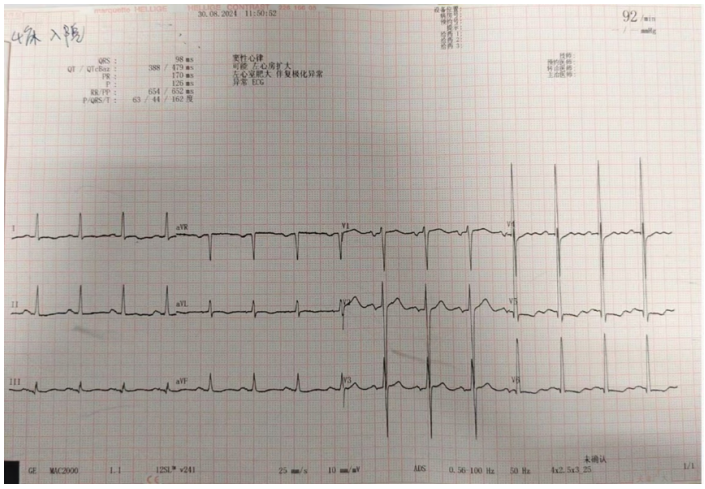

Figure 1 l Electrocardiogram on admission

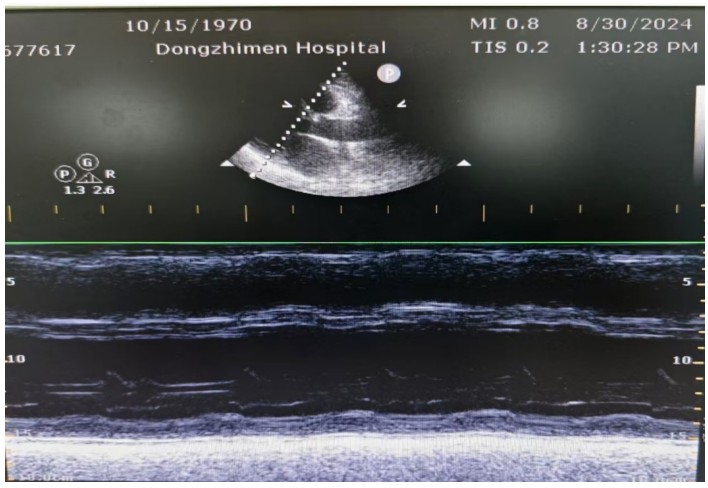

Figure 2 l Echocardiogram on admission

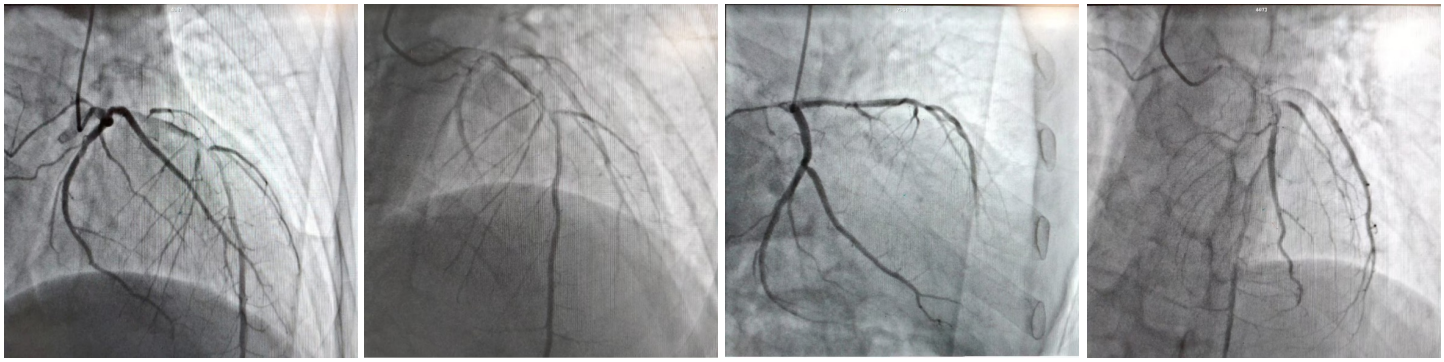

Figure 3 l Coronary Angiography on Admission

2.7. Laboratory Tests

Blood Routine: white blood cell count was 7.56×10^9/L, percentage of neutrophils was 84.2%, red blood cell count was 4.84×10^{12}/L, hemoglobin was 149 g/L, platelet count was 184×10^9/L, and C-reactive protein was 5.74 mg/L.

Blood Biochemistry: serum creatinine was 112 μmol/L, urea was 6.4 mmol/L, uric acid was 581 μmol/L, blood potassium was 3.52 mmol/L, blood sodium was 134 mmol/L, blood calcium was 2.32 mmol/L. Blood Lipids: Total cholesterol was 4.49 mmol/L, triglyceride was 1.57 mmol/L, low-density lipoprotein cholesterol was 3.14 mmol/L, and high-density lipoprotein cholesterol was 1.12 mmol/L.

Myocardial Injury Markers: creatine kinase isoenzyme was 1.7 U/L, troponin I (cTnI) was 0.0221 ng/mL; B-type natriuretic peptide (BNP) was 3214 pg/mL.

2.8. Examinations

The electrocardiogram (ECG) showed sinus rhythm, with a heart rate of 92 beats per minute and regular rhythm. The T waves in leads I, avL, V5, and V6 were inverted (Figure 1).

The echocardiogram showed that the left atrial end-diastolic diameter was 59 mm, the interventricular septum thickness was 10 mm, the left ventricular posterior wall thickness was 10 mm, and the LVEF was 32%. The average E/e' was 24.5, suggesting enlargement of the left heart and right atrium, generally decreased ventricular wall motion, mild to moderate mitral insufficiency, moderate tricuspid insufficiency, mild pulmonary hypertension, and decreased left ventricular function (Figure 2).

Coronary angiography revealed a 50% stenosis in the middle segment of the left anterior descending artery and a 70% stenosis at the opening of the left circumflex artery OM1 (Figure 3).

2.9. Diagnosis

The admission diagnoses were as follows:

Western Medicine Diagnosis:

(1) Coronary atherosclerotic heart disease;

(2) Heart failure with reduced ejection fraction, cardiac function grade III (NYHA classification);

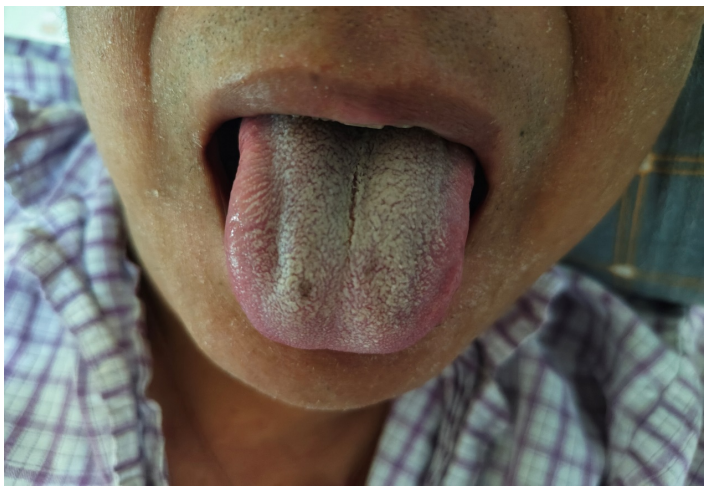

Figure 4 l Tongue manifestation during the onset of variant angina

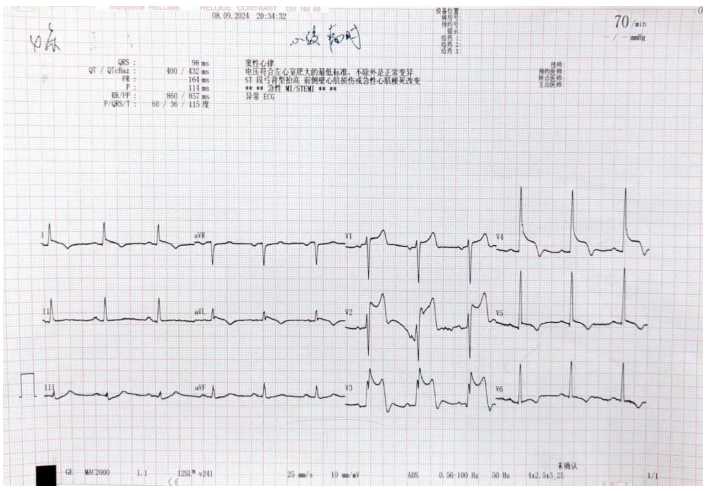

Figure 5 l Electrocardiogram during the onset of variant angina.

(3) Hypertension grade 3 (very high risk);
(4) After bladder surgery;
(5) Tinea pedis.

TCM Diagnosis: Chest pain and heartache, syndrome of qi deficiency, phlegm and blood stasis blocking the collaterals.

2.10.Treatment Plan

In terms of Western medicine, for coronary atherosclerotic heart disease, considering the results of coronary angiography, conservative drug treatment was adopted. The patient was given isosorbide mononitrate at a dose of 20 mg twice a day, enteric-coated aspirin tablets at 100 mg once a day, clopidogrel bisulfate at 75 mg once a day, and atorvastatin calcium at 20 mg once a night. Since the patient's LVEF was 32% and the diagnosis of HFrEF was clear, the "new five-combination" regimen was gradually implemented. The specific drugs included sacubitril/valsartan sodium tablets at 100 mg once a day, metoprolol tartrate at 25 mg twice a day, dapagliflozin at 10 mg once a day, spironolactone at 20 mg once a day, furosemide at 20 mg once a day, and vericiguat tablets at 2.5 mg once a day. Given that the patient's basal heart rate still fluctuated around 90 beats per minute after using metoprolol tartrate, extended-release metoprolol succinate tablets at 47.5 mg once a day were added.

In terms of TCM, appropriate TCM techniques such as acupoint application, auricular point pellet pressing, and wax application therapy were used in combination.

2.11.Disease Progression

On September 8th, the patient experienced severe chest tightness and shortness of breath without obvious precipitating factors while at rest. There was also intense stabbing pain under the xiphoid process, which was aggravated after physical activity, accompanied by radiating pain in the shoulder and back, palpitations, sweating, vomiting (the vomitus was gastric contents), cold limbs, a dark red tongue, a thick white greasy coating with a slightly yellowish root (Figure 4), and a wiry and tight pulse. The blood pressure was 90/60 mmHg. The N-terminal pro-B-type natriuretic peptide (NT-proBNP) was 2273 pg/ml. The blood potassium level was 4.46 mmol/L, the blood sodium level was 136.1 mmol/L, the creatinine level was 226 μmol/L, the alanine aminotransferase level was 19.9 U/L, and the aspartate aminotransferase level was 14.8 U/L. The electrocardiogram showed sinus rhythm, with a heart rate of 70 beats per minute and regular rhythm. The ST segments in leads V_{1-5} were significantly elevated, and the inversion of the T waves in leads I, avL, V_5, and V_6 was deepened (Figure 5).

We suspected that the patient had developed VA and acute kidney injury. Promptly, 0.5 mg of nitroglycerin was administered sublingually. Meanwhile, metoprolol tartrate, metoprolol succinate, sacubitril/valsartan sodium, and spironolactone were discontinued. In parallel, TCM decoctions were introduced into the treatment regimen. Firstly, a modified version of Zhishi Xiebai Guizhi Decoction (ZSXBGZ) was prescribed to invigorate blood circulation, promote qi flow, dredge yang and alleviate chest obstruction. The specific medications and their dosages were as

follows: stir-fried Fructus Aurantii Immaturus (15 g), Allium macrostemon (20 g), Ramulus Cinnamomi (10 g), Magnolia officinalis processed with ginger (20 g), Fructus Trichosanthis (15 g), Rhizoma Coptidis tablets (9 g), Rhizoma Zingiberis (10 g), Poria (15 g), Radix et Rhizoma Rhei (processed with wine and added at the end) (6 g), Radix Salviae Miltiorrhizae (30 g), Lignum Santali Albi (9 g), Fructus Amomi (10 g), Pheretima (10 g), Rhizoma Curcumae (processed with vinegar) (20 g). Subsequently, the modified Guo Weiqin's Yiqi Xiefei Decoction (YQXF) was given to tonify qi and warm yang, activate blood circulation to remove blood stasis, and drain the lung to promote diuresis. The detailed drug prescriptions and dosages were: Radix Codonopsis tablets (15 g), raw Radix Astragali (20 g), Cortex Mori (processed with honey) (12 g), Semen Lepidii (6 g), Herba Lycopi (6 g), Poria (15 g), Polyporus (15 g), Bambusa textilis McClure (6 g), raw Semen Coicis (30 g), Pericarpium Citri Reticulatae (12 g), Pinellia ternata processed with ginger (12 g), Fructus Jujubae (15 g), Radix Glycyrrhizae Praeparata (6 g).

After one week of treatment, the reexamination results were as follows: Blood pressure was 135/89 mmHg, NT-proBNP was 598.2 pg/ml, with blood potassium at 4.14 mmol/L, blood sodium at 136.9 mmol/L, creatinine at 214 μmol/L, alanine aminotransferase at 18.8 U/L, and aspartate aminotransferase at 14.6 U/L. The electrocardiogram showed sinus rhythm, a heart rate of 67 beats/minute and regular rhythm, with ST segments in leads $V_{1\text{-}5}$ having fallen back and the depression of T waves in leads I, avL, V_5, and V_6 alleviated, returning to the admission level (Figure 6). The echocardiogram indicated that the left ventricular end-diastolic diameter was 56 mm, the interventricular septum thickness was 8 mm, the left ventricular posterior wall thickness was 10 mm, and the LVEF was 41%, suggesting left heart enlargement, reduced motion amplitudes of the septum and anterior wall, mild mitral and tricuspid regurgitation, and decreased left ventricular function (Figure 7). The tongue was light purple with a less white and greasy coating than before (Figure 8). After discharge, the patient continued on YQXF. Two weeks later, during follow-up, the patient reported no recurrence of chest tightness, pain, fatigue or shortness of breath. Cardiac MRI results from another hospital showed an LVEF of 40%, demonstrating the obvious effectiveness of the TCM treatment.

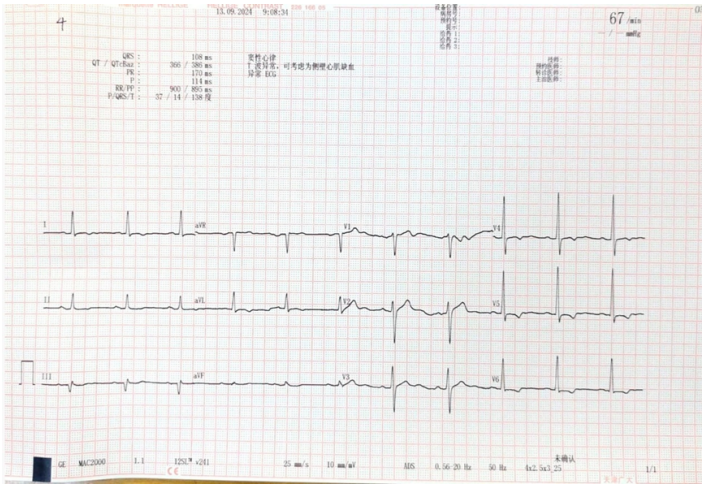

Figure 6 | Electrocardiogram after treatment with traditional Chinese medicine

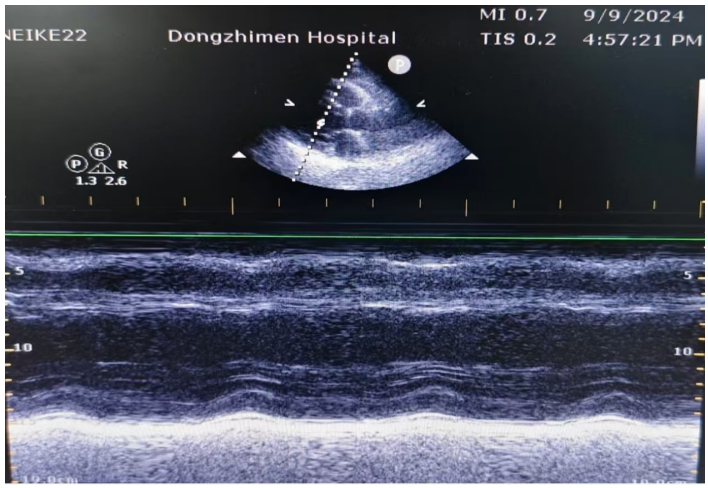

Figure 7 | Echocardiogram after treatment with traditional Chinese medicine

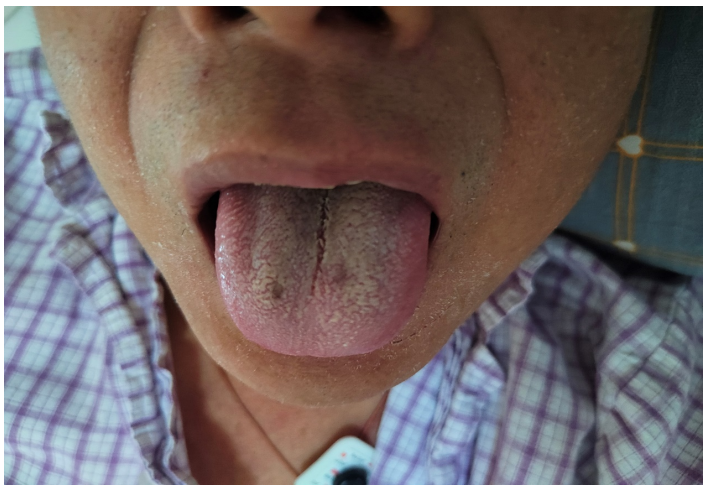

Figure 8 | Tongue manifestation after treatment with traditional Chinese medicine

3. Discussion

3.1. The Contradictions in Western Medicine Treatment

On September 8th, the patient suddenly developed VA complicated by acute kidney injury. Considering the disease characteristics and the patient's treatment regimen, it was speculated that the patient had not developed tolerance to the "new five-combination" drugs, resulting in hypotension and insufficient body perfusion. The HARP-III trial in the UK pointed out that compared with irbesartan, sacubitril/valsartan sodium can reduce the mean systolic and diastolic blood pressures by 5.4 mmHg and 2.1 mmHg respectively through dual inhibition of neprilysin and the renin-angiotensin system.[7] When combined with BB, the hypotensive effect is even more pronounced. Excessively low blood pressure fails to maintain the body's blood circulation, leading to myocardial ischemia and inducing VA. There is evidence suggesting that BB without alpha-1-adrenergic antagonist activity may be harmful to VA by exacerbating coronary epicardial vasospasm. This is due to the antagonistic effect on beta-2-adrenergic receptors, which leads to unopposed activation of alpha-1-adrenergic receptors, thereby enhancing the vasoconstrictive response to sympathetic stimulation. Therefore, it is advisable to avoid their use in VA.[8]

The crux of VA treatment lies in alleviating coronary artery spasm. Calcium channel blockers (CCB) are the commonly prescribed medications, which function by impeding the entry of calcium ions into vascular smooth muscle cells. This leads to the relaxation of vascular smooth muscle, subsequently resulting in the dilation of coronary arteries, the relief of spasms, and the augmentation of coronary blood flow.[9] In the context of patients with HFrEF, the application of CCB demands prudence. Certain CCB variants can exert detrimental effects on cardiac function, particularly those possessing negative inotropic properties. For instance, non-dihydropyridine CCBs, while effectuating coronary artery dilation, concomitantly suppress myocardial contractility, curtail cardiac output, and exacerbate heart failure symptoms.[10] Although dihydropyridine CCBs exhibit a relatively milder inhibitory impact on myocardial contractility, they may precipitate reflex tachycardia, augment myocardial oxygen consumption, and potentially engender adverse consequences for patients with HFrEF as well.[11]

One of the cornerstone drugs for the treatment of HFrEF is BB. They can improve patients' survival rates and quality of life by slowing down the heart rate, reducing myocardial oxygen consumption and improving myocardial remodeling.[10] For patients with both HFrEF and VA, if BB are overused to control the heart rate and improve heart failure, the frequency and severity of angina attacks may increase. However, reducing the use of beta-blockers to avoid inducing coronary artery spasms will affect the treatment effect of HFrEF and miss the opportunity to improve cardiac remodeling and prognosis.

For patients with HFrEF, strengthening myocardial contractility is an important aspect of improving cardiac function. In some cases, positive inotropic drugs, such as digitalis drugs (digoxin), will be used. Digoxin can inhibit the Na^+- K^+- ATPase on the myocardial cell membrane, increase the intracellular sodium ion concentration, and then promote the influx of calcium ions, enhance myocardial contractility and increase cardiac output.[12] In the treatment of VA, the focus is on improving myocardial blood supply. Excessively strengthening myocardial contractility may increase myocardial oxygen consumption. Digoxin may increase systemic vascular resistance due to its direct arteriolar vasoconstrictive effect, which will reduce coronary blood flow and exacerbate myocardial damage.[13]

Given the contradictions in Western medicine treatment for HFrEF combined with VA, TCM has caught our attention due to its unique advantages of holistic regulation and multi-target effects. Based on syndrome differentiation and treatment, TCM starts from aspects like invigorating qi, activating blood circulation, and warming and dredging meridians. It can improve myocardial blood supply, relieve coronary artery spasm, regulate cardiac function, enhance the body's healthy qi, and reduce the adverse reactions of Western medicine, thus opening up a new way for treating such complex cardiovascular diseases.

3.2. Traditional Chinese Medicine's Understanding of the Disease

TCM's understanding of HF originated from the "Huangdi Neijing", which states that "Those with heart distension will have an irritable mood, shortness of breath and be unable to sleep peacefully." It described the clinical features of heart failure and defined such symptoms as "heart distension". Meanwhile, it was pointed out that emotions, external pathogenic factors and so on could all affect cardiac func-

tion. Zhang Zhongjing creatively put forward the term "heart water" on the basis of his predecessors' work. The main characteristics of patients with this condition were "a sense of heaviness in the body, shortness of breath and inability to lie down". The main causes of the disease were deficiency of heart qi and deficiency of heart yang, which led to the overflow of water and dampness, as well as blood stasis. And he left behind classic prescriptions such as Shenfu Decoction, Zhigancao Decoction and Zhenwu Decoction for later generations. The "Mai Jing" written by Wang Shuhe first mentioned the disease name of "heart failure" in traditional Chinese medicine literature and discussed the characteristics of the pulse manifestations and treatment methods of HF. It said that "When the heart fails, the pulse will be hidden; when the liver qi is weak, the pulse will be deep. Therefore, the pulse is hidden and deep." Later generations, based on the experience of predecessors, summarized the main pathogenesis of HF as deficiency of heart qi, weakness of heart yang, deficiency of lung and spleen qi, retention of phlegm-fluid inside the body, and internal obstruction of blood stasis. And they also put forward treatment methods such as tonifying qi and nourishing the heart, warming yang and promoting diuresis, activating blood circulation to remove blood stasis, and resolving phlegm and expelling dampness.

In the theory of TCM, VA falls into the categories of "chest impediment", "true heart pain", and "syncope-induced heart pain". Records about VA can be traced back to the "Huangdi Neijing". For example, in the "Jue Bing" chapter of the "Ling Shu", it is mentioned that "For true heart pain, the hands and feet turn bluish up to the joints, the heart pain is severe, and those suffering from it may die in the evening if it occurs in the morning, or die in the morning if it occurs in the evening." The severity and critical prognosis of true heart pain described here are similar to the severe chest pain and the feeling of impending death during a VA attack, initially revealing the critical situation of sudden severe pain in the heart and the disorder of qi and blood. Later physicians continuously deepened their understanding on this basis. The "Zhu Bing Yuan Hou Lun" in the Sui and Tang Dynasties mentioned that "For the symptoms of chest impediment, there is a feeling of fullness in the chest as if stuffed, with a sense of blockage and discomfort, a tickling sensation, a dry and rough feeling in the throat, and spitting out dry froth." It vividly depicted the symptoms of chest stuffiness and qi stagnation, which are similar to the feeling of chest tightness before a VA attack, laying a foundation for further exploration of this disease. The main pathogenesis of VA is internal obstruction by blood stasis, which is mostly caused by the invasion of cold pathogens and emotional disorders. The common treatment methods include expelling cold and unblocking yang, soothing the liver and regulating qi, resolving phlegm and draining turbidity, and activating blood circulation to remove blood stasis.

3.3. Treatment Strategies in Traditional Chinese Medicine

3.3.1. Syndrome Analysis in Traditional Chinese Medicine

3.3.1.1. At the Time of Admission

The following is an analysis based on the symptoms of TCM when the patient was admitted to the hospital.

Lethargy is one of the typical manifestations of qi deficiency. Qi is the driving force for the vital activities of the human body. When there is qi deficiency, the functional activities of the body will be weakened and it will be unable to maintain a normal mental state. Shortness of breath and reluctance to talk reflect that the patient lacks qi and is thus powerless. Speech can only be carried out normally with the impetus of qi. When there is qi deficiency, there will be insufficient strength for speaking. These two symptoms indicate that the healthy qi in the human body is insufficient and the functions of qi in promoting, warming and so on are weakened. The normal color of the tongue should be light red. A pale tongue indicates that qi and blood fail to nourish the tongue. And the tenderness of the tongue body is due to qi deficiency, as the tongue body cannot obtain sufficient nourishment from qi.

The dark purple complexion and lip color serve as significant external indicators of blood stasis. In cases of blood stasis, qi and blood are unable to flow freely to reach the face and lips. As a result, the stagnated blood manifests as a dark purple hue. The sublingual collaterals' dark red appearance implies the presence of blood stasis within the body. Even though there isn't prominent dilation, the dark red shade already signals that the blood circulation is impeded and shows a propensity for stagnation.

A thick, white and greasy tongue coating is a typical tongue manifestation of phlegm-dampness retention within the body. The pathogenic factors of phlegm-dampness block the spleen, stomach or other

zang-fu organs and meridians, causing the dysfunction of the spleen and stomach in transportation and transformation, and impairing the metabolism of water and dampness. As a result, the turbid qi ascends and spreads onto the tongue. The presence of cracks in the middle of the tongue coating is due to the blockage of phlegm-dampness, which prevents qi, blood, and body fluids from nourishing the tongue. When phlegm-dampness impairs the spleen, the normal function of the spleen in transportation and transformation is disrupted, and the essence of food and water cannot be properly digested and absorbed, leading to loose stools. Phlegm-dampness also blocks qi movement, giving rise to a wiry and slippery pulse.

In the theory of TCM, the kidney and the bladder are externally and internally related, and the kidney yang plays a role in steaming and transforming. When the kidney yang is insufficient, the qi transformation function of the bladder becomes abnormal and it fails to control urine properly, resulting in frequent urination. The light yellow color of the urine indicates that there is no obvious heat sign in the body. Conditions such as qi and blood deficiency and internal blockage by phlegm-dampness can all affect the mind and spirit, leading to sleep disorders.

To sum up, the syndrome of the patient at the time of admission was deficiency of heart yang qi, blood stasis, and internal blockage by phlegm-dampness.

3.3.1.2. During the Progression of the Disease

When alterations occur in the patient's condition, the presence of severe chest distress, pectoral pain, and frigid extremities indicates that yang deficiency engenders cold, and cold congelation induces qi stagnation. Yang deficiency serves as the fundamental basis of this syndrome. In the human body, yang qi plays crucial roles in warming and propelling physiological processes. When yang qi becomes deficient and debilitated, the warming capacity wanes, giving rise to cold manifestations such as cold limbs. Insufficient heart yang fails to effectively impel the circulation of qi and blood, leading to the endogenous generation of cold pathogen which then congeals in the thoracic region. The thorax, being the abode of the heart and lungs, experiences impeded qi and blood flow when cold congeals and induces qi stagnation, thereby resulting in chest distress. The intense pain stems from the fact that the cold-congealing pathogen obstructs the cardiac vessels, rendering the qi and blood within them occluded. According to the principles of traditional Chinese medicine, "obstruction begets pain", and the pain caused by yang deficiency and cold congelation is typically rather acute. A thick, white, and greasy tongue coating with a faintly yellowish radix intimates that phlegm turbidity exhibits signs of transforming into heat due to stagnation. Prolonged accumulation of phlegm turbidity within the body obstructs qi movement, and when qi becomes stagnant, it is prone to transforming into heat. Nevertheless, from an overall perspective, yang deficiency and phlegm turbidity remain preponderant, and the slightly yellowish radix represents merely a localized manifestation of heat transformation.

The dusky red tongue and wiry-taut pulse mirror yang deficiency and blood stasis. The tongue, regarded as the outgrowth of the heart, reflects the stagnation of heart blood as a dusky red coloration on its surface, which is the consequence of the combined influence of feeble propulsion due to yang deficiency and blockade by phlegm turbidity. The wiry-taut pulse comprehensively reflects the pathological state of yang deficiency and cold congelation, internal occlusion by phlegm turbidity, and impeded flow of qi and blood.

In summary, during the progression of the patient's illness, the root lies in the deficiency of heart yang qi, while the manifestations encompass blood stasis and internal blockage by phlegm-dampness, accompanied by a propensity for heat transformation, characterizing a condition of root debility and branch excess.

3.3.2. Thoughts on the Selection of Prescriptions

The "Synopsis of the Golden Chamber" says, "When taking the pulse, one should observe the excessive and insufficient aspects. When the yang pulse is weak and the yin pulse is wiry, it indicates chest impediment accompanied by pain.... The ZSXBGZ should be used as the principal one." It is pointed out that during the acute stage of the onset of chest impediment and heart pain, the ZSXBGZ has a rather good curative effect. Allium macrostemon, Ramulus Cinnamomi and Rhizoma Zingiberis can warm and unblock heart yang, dispel cold and relieve pain. Among them, Allium macrostemon can unblock yang and dissipate masses; Ramulus Cinnamomi can assist yang in transforming qi and warm and unblock the meridians; Rhizoma Zingiberis can warm the middle jiao to dispel cold and restore yang to unblock the vessels. The combination of these three can effectively relieve the symptoms of chest pain and cold limbs caused by cold congealing. Lignum Santali Albi

and Fructus Amomi can promote qi movement and relieve pain, enhance the power of qi movement, make qi movement smooth and relieve chest tightness. Stir-fried Fructus Aurantii Immaturus and Magnolia officinalis processed with ginger can regulate qi and promote qi movement, improving the condition of weak qi and blood circulation caused by qi deficiency. Radix Salviae Miltiorrhizae, Pheretima and Rhizoma Curcumae can activate blood circulation to remove blood stasis. Meanwhile, Pheretima has a good effect on dredging the meridians and activating collaterals for the blockage of heart vessels. Fructus Trichosanthis can clear heat, remove phlegm, relieve chest stuffiness and dissipate masses. Poria can promote diuresis and drain dampness as well as strengthen the spleen. Rhizoma Coptidis tablets can clear heat and dry dampness. The combination of these three can further eliminate phlegm-dampness. Radix et Rhizoma Rhei can purge the bowels to remove heat, expel blood stasis and dredge the meridians.

After the symptoms are relieved, modified YQXF is administered.

Radix Codonopsis tablets and raw Radix Astragali can tonify qi and ascend yang. By replenishing healthy qi, they can enhance the functional activities of the body, improve the state of qi deficiency, and boost the patient's vitality. Both of them have the effects of tonifying qi and warming yang, supplementing yang qi, improving the state of yang deficiency, enabling yang qi to warm the limbs and relieve the coldness of the limbs. Meanwhile, sufficient yang qi is also beneficial to the recovery of heart function and can alleviate angina pectoris. In addition, raw Radix Astragali can promote diuresis and reduce swelling, and it also has a certain improvement effect on the possible slight stagnation of water and dampness. Pericarpium Citri Reticulatae, Pinellia ternata processed with ginger, and Bambusa textilis McClure can dry dampness and resolve phlegm, regulate qi and harmonize the middle jiao. By regulating the qi movement of the spleen and stomach, they can promote the transportation and transformation of phlegm-dampness.

Fructus Jujubae and Radix Glycyrrhizae Praeparata can tonify the spleen and harmonize the stomach, which helps to strengthen the function of the spleen and stomach and fundamentally reduce the generation of phlegm-dampness. They also have the function of nourishing blood and tranquilizing the mind. By tonifying qi and blood and nourishing the mind, they can assist patients in improving sleep quality. Herba Lycopi can activate blood circulation to regulate menstruation, remove blood stasis and dissipate carbuncles, improve blood circulation, eliminate potential blood stasis in the body, prevent the further aggravation of blood stasis, and maintain the smooth flow of qi and blood. Cortex Mori and Semen Lepidii can purge the lung to relieve asthma, promote diuresis and reduce swelling, relieve pulmonary blood stasis and edema, improve respiratory function, and reduce the afterload of the heart. Polyporus, Poria and raw Semen Coicis enhance the power of promoting diuresis and excreting dampness, promote the metabolism of body fluids, reduce the preload of the heart, and thus relieve angina pectoris. This formula comprehensively regulates from multiple aspects such as replenishing qi and warming yang, promoting blood circulation and removing blood stasis, purging the lung and promoting diuresis, resolving phlegm and regulating qi, etc. It has an effect on improving the overall pathological state of patients, including various factors such as qi deficiency, yang deficiency, blood stasis and phlegm turbidity. It can comprehensively adjust the body function and relieve symptoms during the attack of angina pectoris, and is also very important in the subsequent consolidation treatment.

3.4. Summary and Prospects

The integrated treatment of traditional Chinese and Western medicine in this case has achieved remarkable results, accumulating valuable experience for the diagnosis and treatment of similar diseases. Precise syndrome differentiation and treatment is the key. Based on the individual symptoms, tongue manifestations and pulse conditions of the patient, it is accurately differentiated as the syndrome of qi deficiency and blood stasis. Only by prescribing and using medicine on this basis can we directly target the disease location and achieve individualized treatment. The synergistic effect of Chinese and Western medicines is significant. Western medicines control blood pressure, dilate coronary arteries, promote diuresis and resist remodeling, rapidly relieving symptoms and stabilizing the condition; while Chinese medicines tonify qi and activate blood circulation, unblock yang and resolve phlegm, regulating the qi and blood of the zang-fu organs as a whole, reducing the occurrence of angina pectoris and improving heart function. The two complement each other and enhance the curative effect.

The research prospects of the integrated treatment of heart failure with reduced ejection fraction com-

bined with variant angina pectoris are broad. At the basic research level, modern scientific and technological means should be used to deeply explore the mechanism of action of Chinese herbal compound prescriptions, clarify their molecular targets in regulating myocardial cell energy metabolism, inhibiting myocardial fibrosis, improving vascular endothelial function and other aspects, providing theoretical support for precise medication. At the same time, large-sample, multi-center, random-controlled trials urgently need to be carried out to systematically compare the long-term efficacy and safety of the integrated treatment of Chinese and Western medicine with those of single Western medicine and single Chinese medicine treatments, optimize the combined medication regimens, standardize the treatment procedures and raise the level of clinical evidence.

4. Conclusions

The main diagnoses for the patient in this case were HFrEF combined with VA. Although there are quite a number of contradictions in the choice of medications for these two diseases, remarkable curative effects were achieved with the help of traditional Chinese medicine decoctions. After treatment, the patient's blood pressure rose, the cardiac and renal functions were improved, and there were improvements in both symptoms, physical signs and imaging manifestations. The quality of life was greatly enhanced. The author shares this successful case, hoping to provide one more option for the clinical treatment of such diseases.

Statement of Ethics and Consent of Participation

This case has been approved by the Medical Ethics Committee of Dongzhimen Hospital, Beijing University of Chinese Medicine (2024DZMEC-491-01). Meanwhile, we have obtained the written informed consent from the patient for the publication of this case report.

Funding

This article was supported by the Youth Project of the National Natural Science Foundation of China (Grant No. 82204856) and the Clinical Special Project of the Wu Jieping Medical Foundation (Grant No. 320.6750.2022-25-3).

CRediT Authorship Contribution Statement

Siqi Li: Conceptualization, Funding acquisition, Project administration, Writing – original draft. Xiaowan Han: Investigation, Writing – review & editing. Diying Zhang: Writing – review & editing. Lanjun Kou: Supervision, Writing – review & editing. Guozhong Pan: Conceptualization, Supervision, Writing – review & editing.

Declaration of Competing Interest

The authors declare that they have no known competing financial interests or personal relationships that could have appeared to influence the work reported in this paper.

Reference

1. McDonagh TA, Metra M, Adamo M, et al. 2021 ESC Guidelines for the diagnosis and treatment of acute and chronic heart failure. Eur Heart J. 2021; 42: 3599-726.
2. Wang H, Chai K, Du M, et al. Prevalence and Incidence of Heart Failure Among Urban Patients in China: A National Population-Based Analysis. Circ Heart Fail. 2021; 14: e008406.
3. Fletcher R, Cannata AC, Rockenschaub P, et al. Modern epidemiology of heart failure with reduced and preserved ejection fraction in population-wide linked electronic health records: a study of 208815 heart failure patients in England. European Heart Journal. 2024; 45.
4. Picard F, Sayah N, Spagnoli V, et al. Vasospastic angina: A literature review of current evidence. Arch Cardiovasc Dis. 2019; 112: 44-55.
5. Bil J, MoŻeŃska O, Segiet-ŚwiĘcicka A, et al. Revisiting the use of the provocative acetylcholine test in patients with chest pain and nonobstructive coronary arteries: A five-year follow-up of the AChPOL registry, with special focus on patients with MINOCA. Transl Res. 2021; 231: 64-75.
6. Metra M, Tomasoni D, Adamo M, et al. Worsening of chronic heart failure: definition, epidemiology, management and prevention. A clinical consensus statement by the Heart Failure Association of the European Society of Cardiology. Eur J Heart Fail. 2023; 25: 776-91.
7. Singh JSS, Burrell LM, Cherif M, et al. Sacubitril/valsartan: beyond natriuretic peptides. Heart. 2017; 103: 1569-77.
8. Ajani AE, Yan BP. The mystery of coronary artery spasm. Heart Lung Circ. 2007; 16: 10-5.
9. Gradman AH. The evolving role of calcium channel blockers in the treatment of angina pectoris: focus on felodipine. Can J Cardiol. 1995; 11 Suppl B: 14b-21b.
10. Heidenreich PA, Bozkurt B, Aguilar D, et al. 2022 AHA/ACC/HFSA Guideline for the Management of Heart Failure: A Report of the American College of Cardiology/

American Heart Association Joint Committee on Clinical Practice Guidelines. Circulation. 2022; 145: e895-e1032.

11. McKelvie RS, Moe GW, Ezekowitz JA, et al. The 2012 Canadian Cardiovascular Society heart failure management guidelines update: focus on acute and chronic heart failure. Can J Cardiol. 2013; 29: 168-81.
12. Gustafsson F, Damman K, Nalbantgil S, et al. Inotropic therapy in patients with advanced heart failure. A clinical consensus statement from the Heart Failure Association of the European Society of Cardiology. Eur J Heart Fail. 2023; 25: 457-68.
13. Vatner SF, Higgins CB, Franklin D, et al. Effects of a digitalis glycoside on coronary and systemic dynamics in conscious dogs. Circ Res. 1971; 28: 470-9.

International Journal of Clinical Medicine & Pharmacology

https://doi.org/10.70731/kbgvvt42

NADPH Oxidase 4 in Prostate Cancer: Expression and Potential Role in Ferroptosis

Kunlin He [a,†], Jingxiao Li [a,†], Gusheng Li [a], Guanqiang Yan [a], Xiang Gao [a], Huafu Zhou [a,*], Jun Liu [a,*]

[a] *Department of Thoracic Surgery, The First Affiliated Hospital of Guangxi Medical University, Nanning, 530021, Guangxi Zhuang Autonomous Region, P. R. China*

KEYWORDS

Prostate Cancer,
NOX4,
Ferroptosis,
Gene Expression,
Metabolic Pathways

ABSTRACT

Prostate cancer (PCa), the most common male malignant tumor worldwide, is associated with high morbidity and mortality, particularly when it progresses to metastatic disease. Ferroptosis, an iron-dependent form of cell death, has been implicated in various cancers. This study investigated the role of NADPH oxidase 4 (NOX4) in PCa and its potential connection to ferroptosis. By analyzing mRNA expression data from TCGA and GEO, NOX4 was found to be significantly upregulated in PCa tissues compared to non-cancerous tissues (SMD = 0.75, 95% CI: 0.41–1.10) and exhibited a moderate diagnostic accuracy (AUC = 0.79, 95% CI: 0.75–0.82). A total of 464 differentially co-expressed genes (DCEGs) were identified, including the hub genes BUB1, CCNB1, and CCNB2. Furthermore, NOX4 expression showed significant correlations with ferroptosis-related genes such as ALOX15, UBC, FTH1, and SLC2A6. Functional enrichment analyses (GO and KEGG) revealed that NOX4-associated DCEGs were enriched in metabolic pathways, cell cycle regulation, mitotic nuclear division, chromatin binding, and centromeric regions. These results suggest that NOX4 may contribute to ferroptosis regulation in PCa through its involvement in metabolic and cell cycle pathways, highlighting its potential as a therapeutic target.

1. Introduction

Prostate cancer (PCa) is the most common male malignant tumor in worldwide. According to *Cancer Statistics, 2025*, PCa accounted for 30% of all estimated new cases in men, which means over 313,780 new PCa cases in this year [1]. PCa in early stages is less harmful to patients and the 15-year survival rate could reach 94% [2]. Current guidelines recommend surgery as the preferred treatment for PCa in early stages [3]. However, once the metastasis of tumor occurred, the 5-year survival rate of patients suffered PCa will reduce to 28% or less [4]. In recent years,

† These authors contributed equally to this work.
* Corresponding author. E-mail address: zhouhuafu_gxmu@163.com (Huafu Zhou), lj_gxmuyfy_c_t_s@163.com (Jun Liu)

Received 19 January 2025; Received in revised form 18 February 2025; Accepted 24 February 2025; Available online 28 February 2025.

androgen-targeted therapy (ADT) was widely used in metastatic PCa, but in the long-term follow-up process, some studies found that the low level of drug response and drug-induced apoptosis escape were still the main defects of ADT [5,6]. Therefore, finding new targets for molecular targeted therapy and proving the potential molecular mechanisms and signal pathways, then applying the new targets for diagnostic and treatment of PCa is vital.

Ferroptosis is an iron-dependent apoptosis pathway, which was considered to be related to neurodegeneration [7]. As a newly found apoptotic pathway, the groups of Galmiche and Louandre first reported the interaction mechanisms between ferroptosis and the anti-tumor drug sorafenib in hepatocellular carcinoma [8,9]. To date, ferroptosis had been pointed out related to the development of many cancers such as gastric cancer, head and neck cancer and liver cancer [10-12]. Moreover, some studies have indicated the relationship between ferroptosis and the development of PCa. Both Zhou and Tousignant reported that downregulation of GPX4 promotes ferroptosis in PCa cells, thereby inhibiting their proliferation and invasion [13,14]. When inducing PCa cells ferroptosis by drugs, Ghoochani et al. observed that some genes were differentially expressed in PCa cells with ferroptosis, which indicated the process of ferroptosis in PCa cells was probably related to differential expression of genes [15]. Nevertheless, existed researches had never clarified the relationship between the expression of transcription profile and ferroptosis in PCa cells and the research on the mechanisms of ferroptosis was still at a low stage.

NADPH oxidase 4 (NOX4), located in 11q14.3, acts not only in cellular energy metabolism but also as an electron donor to catalyze the electron transfer of molecular oxygen on the biofilm to produce reactive oxygen species (ROS) [16]. The growing evidence shows that NOX4 could be considered as an oncogene of PCa. Sampson et al. reported downregulated NOX4 was able to inhibit the activation of fibroblasts in prostate and block the process of tumorigenicity [17]. Wu et al. also indicated that low expressed NOX4 regulated by miRNA-137 influences glycolysis, cell proliferation and apoptosis in PCa, and NOX4 might be a potential target for PCa treatment [18]. Singh et al. observed that arsenic-induced overexpression of NOX4 promotes mitochondrial peroxidation in prostate epithelial cells, and then induces PCa [19]. However, it was a pity that despite numerous studies on NOX4 in PCa, none had addressed the expression levels of NOX4 in PCa. In addition, the specific roles and potential mechanisms of ferroptosis regulated by NOX4 in PCa were still uncertain.

Thus, the present study aimed to explore the expression levels of NOX4 and potential mechanisms of NOX4-regulated ferroptosis in PCa. By detecting the mRNA expression levels of NOX4 and ferroptosis-related proteins in clinical samples and integrating with data from public databases, we aimed to reveal the relationship between the differentially expressed NOX4 and ferroptosis. Moreover, we herein estimated the correlation between NOX4 and tumor infiltrating immune cells in different tumor microenvironments based on Tumor Immune Estimation Resource (TIMER). Gene ontology (GO), Kyoto Encyclopedia of Genes and Genomes (KEGG) and Protein-protein interaction (PPI) networks analysis were applied to reveal signal pathways of NOX4 in ferroptosis process.

2. Method

2.1. The Clinical Significance of NOX4 in Pan-Cancer

2.1.1. The mRNA Expression Levels of NOX4 in Pan-Cancer

Tumor immune estimation resource, version 2 (TIMER 2.0) is a database including RNA-seq and and tumor immune invasion data. In the present study, to explore the mRNA expression levels of NOX4 in pan-cancer, the authors entered NOX4 into TIMER 2.0. NOX4 expression data were observed for a total of 33 cancer types in TCGA, and box plot and independent sample t test were herein used to obtain the expression differences.

2.1.2. Prognostic Value of Differentially Expressed NOX4

Based on data from TCGA database, we extracted disease-free survival time of 12,357 patients from 33 cancer types. Univariate survival analysis was applied, and harzard ratios were performed to estimate the disease-free interval. By plotting the summary forest plot, the effect of differentially expressed NOX4 on the prognosis of patients with DFI could be observed directly.

2.2. The mRNA Expression Levels of NOX4 in PCa

2.2.1. MRNA Data Sources and Processing

Microarray and RNA-seq data for PCa were downloaded and screened from TCGA and Gene Expres-

Table 1 | The included databases with NOX4 expression.

ID	Country	Platform	Year	Number of samples	
				PCa	Non-PCa
GSE26910	Italy	GPL570	2011	6	6
GSE32448	USA	GPL570	2011	40	40
GSE32982	Finland	GPL570	2011	6	3
GSE38043	USA	GPL570	2012	3	3
GSE46602	Denmark	GPL570	2013	34	14
GSE69223	Germany	GPL570	2015	15	15
GSE104749	China	GPL570	2017	4	4
GSE27616	USA	GPL4133	2011	9	4
GSE12378	UK	GPL5175	2008	36	3
GSE72220	USA	GPL5175	2015	57	90
GSE94767	UK	GPL5175	2017	185	33
GSE28204	China	GPL6480	2011	4	4
GSE35988	USA	GPL6480	2012	76	12
GSE32571	Germany	GPL6947	2011	59	39
GSE134073	Germany	GPL11154	2020	56	8
GSE60329	Italy	GPL14550	2014	108	28
GSE73397	China	GPL20952	2015	3	3
GSE88808	USA	GPL22571	2016	49	49
GSE134051	Germany	GPL26898	2020	216	39
TCGA+GTEx	NA	NA	NA	499	152

NOX4: NADPH oxidase 4; PCa: prostate cancer; TCGA: The Cancer Genome Atlas; GTEx: The Genotype-Tissue Expression.

sion Omnibus (GEO). A total of 22 datasets were collected using "prostate cancer" as the search keyword (Table 1). In order to make the results more objective, data from GEO and TCGA was subjected to log2(x+1) conversion. Subsequently, the authors removed batch effects based on platforms, resulting in the selection of 11 studies.

2.2.2. Diagnostic Value of NOX4 in PCa

We performed a diagnostic test to assess the clinical significance of NOX4 in PCa. Based on expression levels of NOX4 in 11 studies, Stata 14.0 was used to estimate standard mean difference (SMD). If $P < 0.05$ or $I^2 > 50\%$, the study was considered to be heterogeneous,and a random-effect model would be applied. Otherwise a fixed-effects model was adopted. Receiver operating characteristic (ROC) curves of above studies were drawn by using IBM SPSS Statistics v23.0. Additionally, to evaluate the diagnostic potential of NOX4 comprehensively, a summary receiver operating characteristic (sROC) was plotted through using Stata 14.0. The area under the curve (AUC) of sROC represents the diagnostic value of NOX4.

2.3. Obtention of NOX4 Differentially Co-Expressed Genes in PCa

2.3.1. Identification of NOX4 Co-Expressed Genes in PCa

Co-expressed genes (CEGs) were considered genes that had close relationship with NOX4 and were probably regulated by NOX4 in PCa. Gene expression from 11 studies was extracted. Through evaluating Pearson's coefficient, we assessed the correlation between genes and NOX4. When $|r| > 0.3$ and $P < 0.05$, the gene would be considered one CEG. CEGs appeared more than five times in all 11 studies would be selected for subsequent research.

2.3.2. Identification of Differential Genes in PCa

After identifying CEGs of NOX4, we ran limma package to screen the differentially expressed genes (DEGs) of NOX4 in all GEO datasets, and we

Table 2 | The means and standard deviations of NOX4 expression values for PCa and non-PCa based on 11 studies.

Study	Sample type	PCa			Non-PCa		
		N	M	SD	N	M	SD
GPL570	Tissue	110	2.853	1.052	85	2.654	1.085
GPL4133	Tissue	9	2.354	0.870	4	0.199	1.182
GPL5175	Tissue	278	4.077	0.639	126	4.098	0.496
GPL6480	Tissue	80	2.123	1.350	16	0.647	1.067
GPL6947	Tissue	59	7.228	0.590	39	6.493	0.272
GPL11154	Tissue	56	7.953	1.525	8	6.153	0.870
GPL14550	Tissue	108	-0.073	1.342	28	-0.048	0.489
GPL20952	Tissue	3	9.627	0.239	3	9.575	0.070
GPL22571	Tissue	49	6.591	0.726	49	5.772	0.546
GPL26898	Tissue	216	6.430	0.616	39	5.952	0.340
TCGA+GTEx	Tissue	499	0.580	0.476	152	0.278	0.389

NOX4: NADPH oxidase 4; PCa: prostate cancer; N: number; M: mean; SD: standard deviation; TCGA: The Cancer Genome Atlas; GTEx: The Genotype-Tissue Expression.

screened DEGs in TCGA data with limma voom package. If the corrected $P < 0.05$ and $\log2FC > 1$, the gene would be considered potential DEG. DEGs appeared more than five times in all 11 studies would be selected as NOX4 DEGs. Lastly, genes met in both two selection criteria would be identified as NOX4 DCEGs in PCa.

2.4. Obtention of Ferroptosis-Related Genes Regulated by NOX4 in PCa

FerrDB is a database focused on the research of genes that affect ferroptosis. Before performing the correlation analysis, we downloaded drivers, suppressors and markers of ferroptosis from ferrDB, and screened 219 genes using “Human only” as the screening criteria. Next, we intersected the above genes with NOX4 DCEGs, and ALOX15, UBC, FTH1 and SLC2A6 were identified as genes regulated by NOX4 in PCa. Correlation analysis was adopted to further explore the relationship between the expression levels of these genes.

2.5. Functional Enrichment Analysis of NOX4 DCEGs

In order to further explore the molecular mechanisms and potential functions of differentially expressed NOX4 regulated ferroptosis in PCa, we entered NOX4 DCEGs into Database for Annotation, Visualization, and Integrated Discovery (DAVID) v6.8. We herein chose GO and KEGG enrichment analysis to identify the molecular mechanisms and potential functions of differentially expressed NOX4 regulated ferroptosis in PCa. GO terms and KEGG signaling pathways with $P < 0.05$ were identified. Moreover, PPI networks was constructed through Search Tool for the Retrieval of Interacting Genes (STRING) and Cytoscape v3.6.1. Hub genes of NOX4 DCEGs were identified based on the degree of nodes.

2.6. Immune-Related Analysis

We herein assessed the abundance of immune infiltrates in PCa tumor and paired paracancerous tissue through the correlation modules of TIMER 2.0. Besides, significantly correlated immune genes of NOX4 were also been assessed in Gene Expression Profiling Interactive Analysis (GEPIA). TISIDB integrates multiple heterogeneous datasets, which are able to predict interaction between tumor and immune system. In the present study, we observed the immune infiltration of NOX4 in a variety of tumors through TISIDB and showed the correlation between NOX4 and immune cells on scatter plots.

3. Results

3.1. The Clinical Significance of NOX4 in Pan-Cancer

The mRNA expression levels of NOX4 were analyzed in various cancer types based on TCGA. The results indicated that NOX4 was differentially expressed in many malignant tumors (Figure 1A).

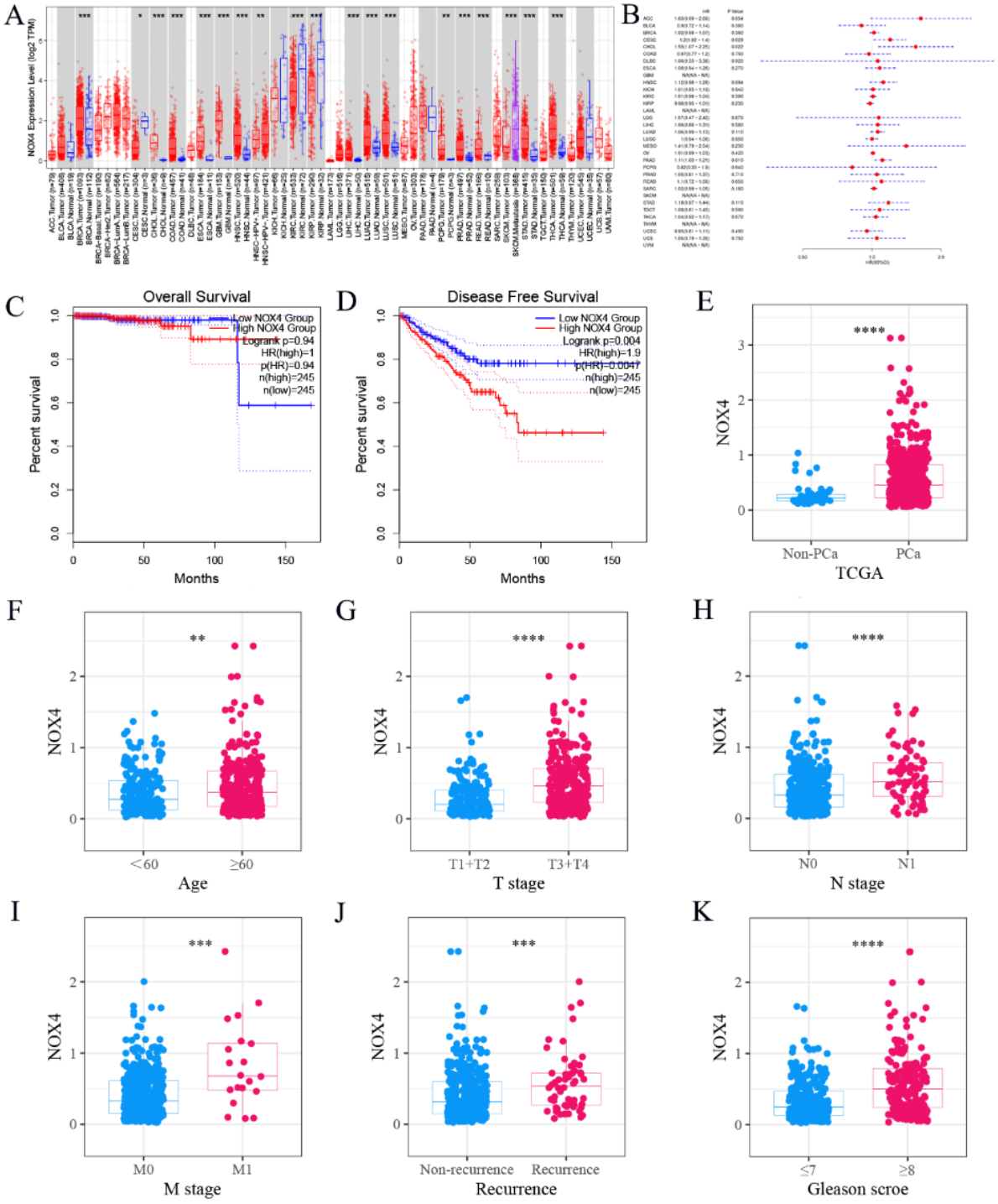

Figure1 I (A) The mRNA expression levels of NOX4 in pan-cancer. (B) Disease-free intervals of patients with differentially expressed NOX4. (C,D) The OS and DFS between high and low expressed NOX4. (E-K) Expression of NOX4 in tissues of patients with different clinical parameters.

OS: overall survival. DFS: disease-free survival

Among these, NOX4 was upregulated in breast cancer, cholangiocarcinoma, colon adenocarcinoma, esophageal carcinoma, glioblastoma multiforme, head and neck squamous cell carcinoma, hepatocellular carcinoma, lung cancer, pheochromocytoma, paraganglioma, PCa, rectum adenocarcinoma, Stomach adenocarcinoma and thyroid carcinoma. Conversely, NOX4 was downregulated in cervical cancer, kidney cancer. Additionally, disease-free interval of patients with differentially expressed NOX4 was shown on Figure 1B.

3.2. The mRNA Expression Levels and Diagnostic Value of NOX4 in PCa

In order to explore the mRNA expression of NOX4 in PCa, we extracted NOX4 expression data from 22 datasets from 11 platforms, including the TCGA and GEO database. The scatter plots comparing NOX4 expression between PCa and non-PCa tissues were shown in Figure 2. We used a random-effects model to calculate the standardized mean difference (SMD) for the included datasets, yielding significant heterogeneity (I^2 = 88.3%, P < 0.001) and an SMD of 0.75 (95% CI: 0.41-1.10), which indicated that NOX4 was overexpressed in PCa (Figure 3A). However, no significant heterogeneity was detected (Figure 3B). Funnel plots revealed no publication bias (Figure 3C-E). Moreover, sROC showed that the AUC of NOX4 value was 0.79 (95%CI: 0.75-0.82), suggesting moderate sensitivity and specificity for PCa diagnosis (Figure 4). The overall survival (OS) and disease-free survival (DFS) were displayed on Figure 1C to D. To further investigate the clinical significance of differentially expressed NOX4 in PCa patients with different clinical parameters, independent sample t test was applied to estimate the NOX4 expression levels, and scope of the test included ages, TNM stages, recurrences and gleason scores of patients (Figure 1E-K).

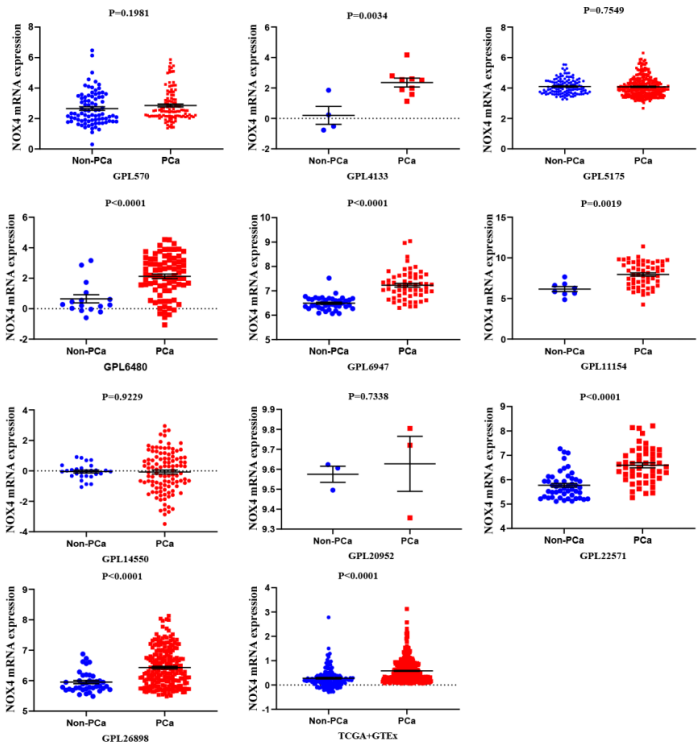

Figure2 | The expression levels of NOX4 in 22 datasets from 11 platforms.

PCa: prostate cancer. TCGA: The Cancer Genome Atlas. GTEx: The Genotype-Tissue Expression project.

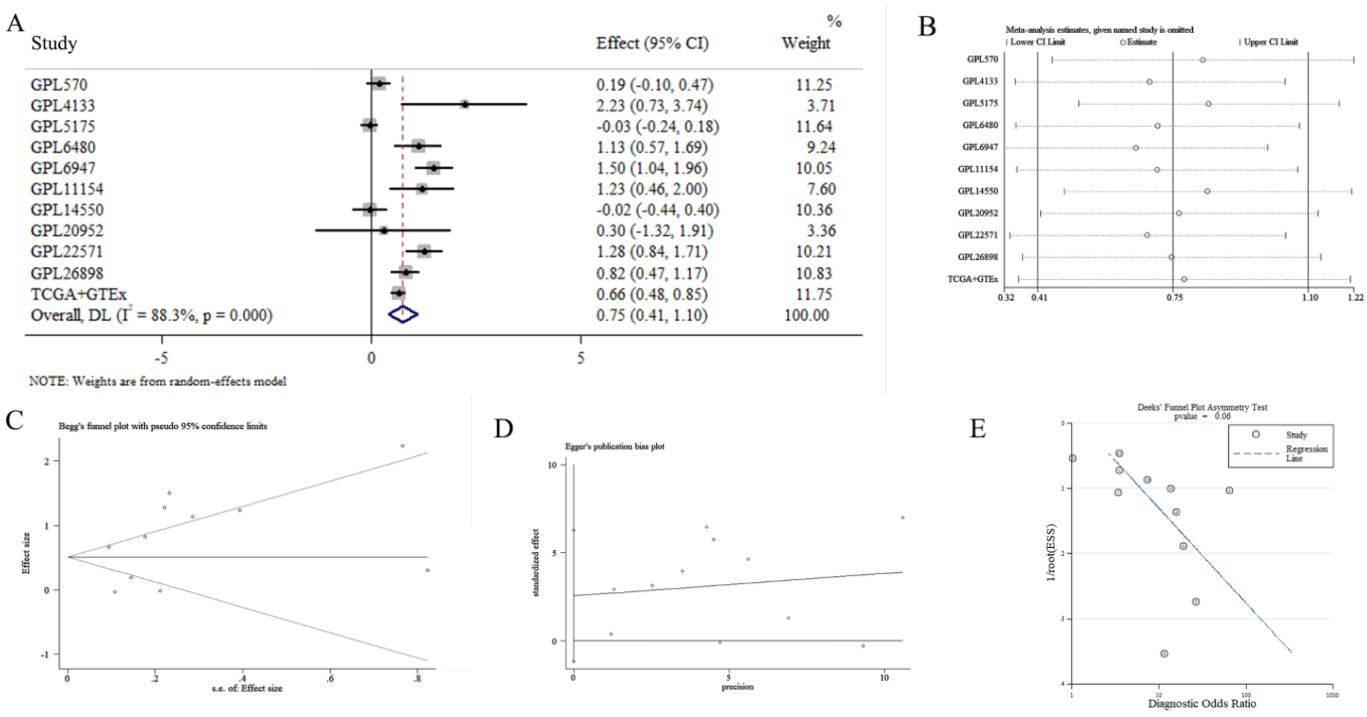

Figure3 | The mRNA expression levels of NOX4 in PCa. (A) Forest plot showing a combined SMD of 0.75 (0.41 to 1.10), indicating that the expression of NOX4 in PCa is higher than that in non-PCa. (B) Sensitivity analysis showing the combined SMD is sTable (C, D, E) Begg' s, Egger's and Deek' s tests showing no publication bias (p > 0.05).

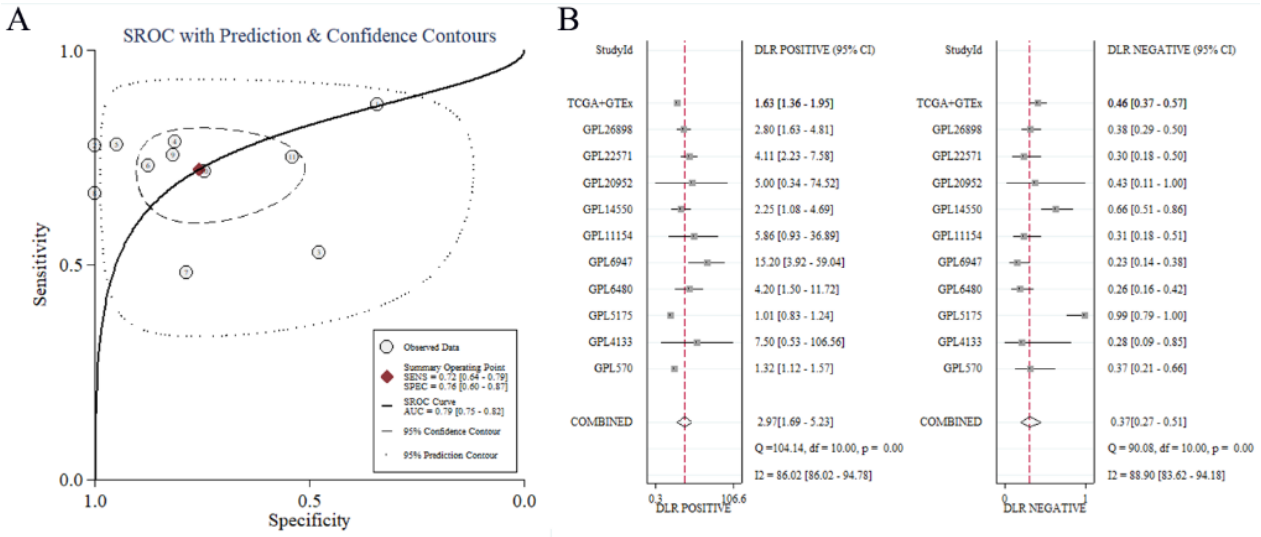

Figure4 | Discrimination potential of CELSR3 in PCa. (A) SROC curve assessing the discrimination potential of NOX4 in PCa. (B) Sensitivity and specificity analysis showed that NOX4 had a moderate predict potential in PCa.

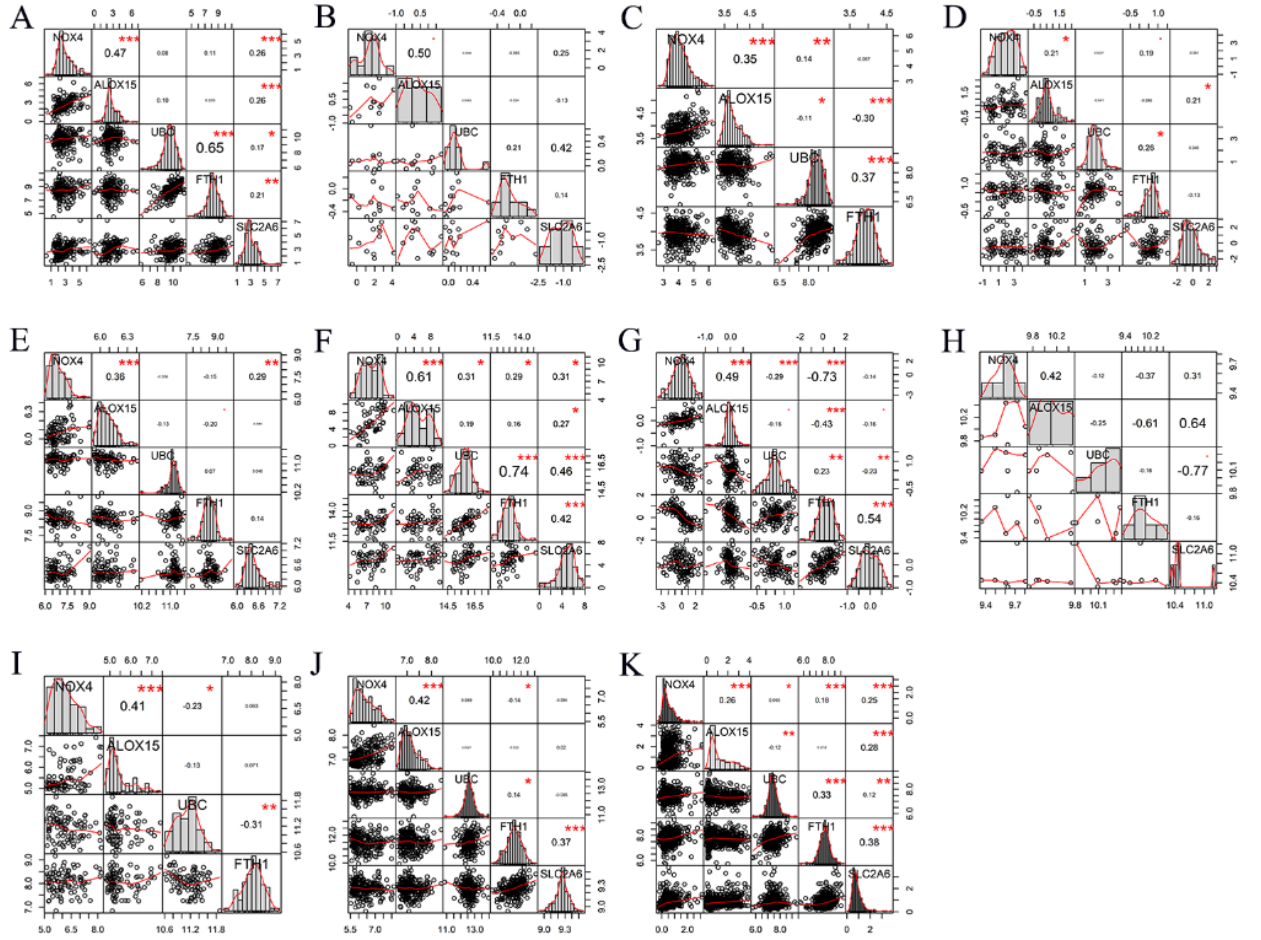

Figure5 | Correlation analysis showed that the expression of NOX4 had a considerable correlation with ferroptosis-related genes.

The pure number in bold represents Pearson correlation coefficient, and one or more "*" represent significant difference. (A-D) GPL570, GPL4133, GPL5175, GPL6480. (E-H) GPL6947, GPL11154, GPL14550, GPL20952. (I-K) GPL22571, GPL26898, TCGA+GTEx.

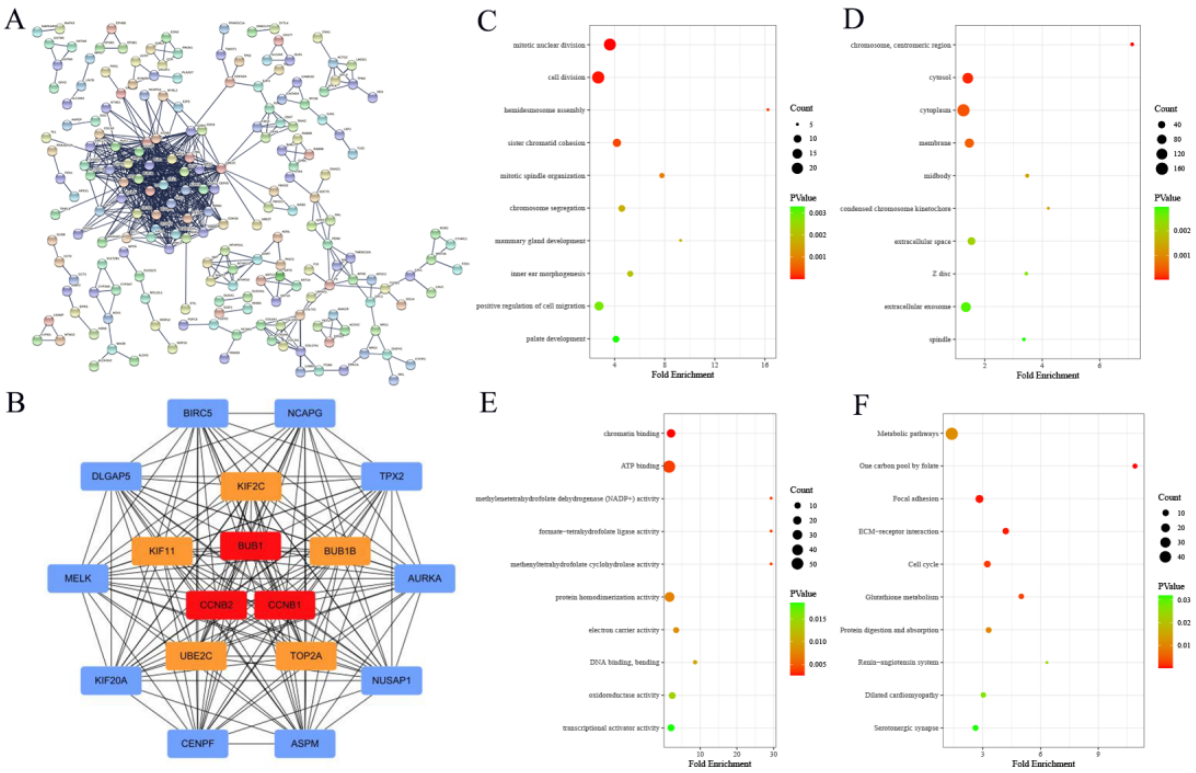

Figure6 I Enrichment analysis

(A) PPI network analysis of NOX4 DCEGs. (B) BUB1, CCNB1, CCNB2 were identified as hub genes of NOX4. (C) Enrichment terms of NOX4 DCEGs in biological process. (D) Enrichment terms of NOX4 DCEGs in cellular component. (E) Enrichment terms of NOX4 DCEGs in molecular function. (F) Enrichment terms of NOX4 DCEGs in Kyoto Encyclopedia of Genes and Genomes.

3.3. Correlation Between NOX4 and Ferroptosis-Related Genes

We herein extracted mRNA expression data from 11 studies, and Pearson's coefficient analysis revealed that 945 CEGs were closely related to NOX4, including 685 positive related genes and 260 negative related genes. Differential expression analysis exhibited that 2663 DEGs were identified in PCa. A total of 464 genes were finally identified as NOX4 DCEGs in PCa. These 464 genes were used to intersect with genes from ferrDB, yielding 4 ferroptosis-related genes: ALOX15, UBC, FTH1 and SLC2A6, which were used for subsequent analysis. The correlation analysis was applied to assess the correlation between NOX4 and above 4 ferroptosis-related genes. The results showed that NOX4 had a considerable correlation with ferroptosis-related genes, indicating that NOX4 was probably related to ferroptosis (Figure 5).

3.4. Functional Enrichment Analysis of NOX4 DCEGs

To explore the molecular mechanisms and signal pathways, we used PPI network analysis to reveal the potential relationship among NOX4 DCEGs. The PPI result was shown in Figure 6A. Next, we calculated the connection degrees of nodes and identified BUB1, CCNB1, and CCNB2 as hub genes of NOX4 (Figure 6B). Based on GO analysis, NOX4 DCEGs were significantly enriched in mitotic nuclear division, chromosome, centromeric region and chromatin binding (Figure 6C-E). According to KEGG analysis, the metabolic pathways were the most significantly enriched pathways among NOX4 DCEGs (Figure 6F).

3.5. Immune-Related Analysis

To investigate the relationship between NOX4 and immune infiltrating cells, we explored the correlations between NOX4 and immune marker sets of a variety of immune cells in PCa from TIMER 2.0 and GEPIA databases. The immune cells analyzed included different functional T cells, B cells, monocytes, TAMs, M1 and M2 macrophages, neutrophils, NK cells and DCs. We also adjusted the results for purity and found that NOX4 expression was significantly correlated with most of immune marker sets (Table 3). Additionally, we herein entered NOX4 into TISIDB and found that the expression levels of NOX4 were signif-

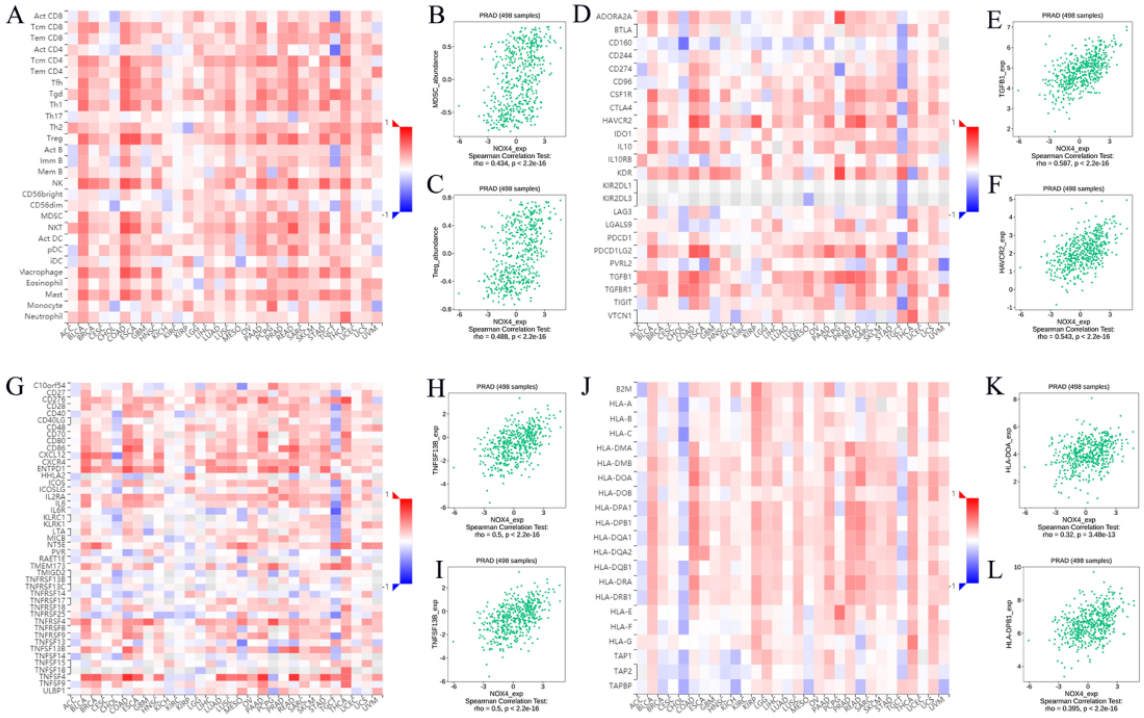

Figure7 l (A,B,C) Associations of the NOX4 expression levels with lymphocytes, immunomodulators and chemokines in PCa. (D,E,F) Correlation analysis between the NOX4 expression levels and immunosuppressant. (G,H,J) The analysis results showed that NOX4 was related to immunoactivators. (J,K,L) Associations of the NOX4 expression levels with MHC molecules.

icantly correlated with lymphocytes, immunosuppressant, immunoactivators and MHC molecules in various cancer types. In this study, we displayed heat maps and scatter plots on Figure 7.

4. Discussion

NOX4 had been reported that correlated with ferroptosis of tumor cells in glioma and renal cell carcinoma [20,21]. The relationship between overexpressed NOX4 and the process of tumor cells development in PCa had also been covered [18]. However, there had no research indicated that the correlation between NOX4 and ferroptosis in PCa. The present study through analyzing the expression levels of NOX4 of PCa and paired paracancerous tissue samples from clinical collection and public databases, considered that upregulated NOX4 inhibit the development of PCa by regulating ferroptosis. Moreover, we performed an enrichment analysis to NOX4 DCEGs and considered metabolism pathway was probably a potential signal pathway for NOX4 to regulate ferroptosis. Immune infiltration analysis showed the expression levels of NOX4 was significantly related to various immune cells.

In previous studies, some scholars had mentioned the NOX4 expression levels in PCa. Low expression NOX4 was observed by Kim et al. in PCa cells treated with chalcone, and downregulated NOX4 inhibited the growth of tumor cells via ire1α-rid-miRNA-23b axis [22]. Harrison et al. also considered that NOX4 was overexpressed in PCa and had a positive correlation with metastasis [23]. Interestingly, Wu' s group collected and analyzed the expression data of NOX4 from 65 clinical PCa samples. The results showed that downregulated NOX4 could increase the rate of apoptosis, which suggested that expressed NOX4 was a risk factor of PCa [18]. Through analyzing 20 paired epithelial tumor samples, Meitzler et al. reported that the overexpression frequency of NOX4 in PCa was only 36.8% [24]. To date, the expression levels of NOX4 in PCa had not been determined and the shortcomings of the existed research were also obvious, such as small sample sizes ($n < 65$) and most of them were single center studies. The present study collected and analyzed samples from clinical collection and public databases and reported the expression of NOX4 was upregulated in PCa for the first time based on a large sample size ($n = 2014$). Nevertheless, though we have obtained a larger sample

Table 3 | Correlation analysis between NOX4 markers of immune cells in PCa based on TIMER and GEPIA.-1

Gene marker	None		Purity		Tumour		Normal	
	Cor	P	Cor	P	Cor	P	Cor	P
CD19	0.141	**	0.108	*	0.14	**	0.39	**
CD20(KRT20)	0.192	***	0.167	***	0.057	0.21	0.093	0.51
CD38	-0.302	***	-0.352	***	-0.21	***	-0.21	0.13
CD8A	0.184	***	0.18	***	0.15	***	0.2	0.15
CD8B	0.126	**	0.131	**	0.26	***	0.2	0.16
BCL6	0.084	0.0635	0.05	0.308	0.017	0.71	0.18	0.19
ICOS	0.311	***	0.288	***	0.18	***	0.27	0.057
CXCR5	0.24	***	0.208	***	0.18	***	0.077	0.59
T-bet (TBX21)	0.284	***	0.278	***	0.23	***	0.29	*
STAT4	0.29	***	0.278	***	0.27	***	0.26	*
IL12RB2	0.233	***	0.247	***	0.17	***	0.073	0.61
WSX1(IL27RA)	0.254	***	0.243	***	0.24	***	0.25	0.078
STAT1	0.209	***	0.208	***	0.11	*	0.27	0.052
IFN-γ (IFNG)	0.215	***	0.167	***	0.14	**	0.24	0.089
TNF-α (TNF)	0.179	***	0.174	***	0.063	0.16	0.1	0.46
GATA3	0.095	*	0.047	0.344	-0.019	0.67	-0.22	0.12
CCR3	0.287	***	0.293	***	0.15	**	0.17	0.22
STAT6	-0.014	0.754	-0.023	0.638	-0.055	0.22	-0.019	0.89
STAT5A	0.221	***	0.213	***	0.2	***	0.11	0.44
TGFBR2	0.314	***	0.303	***	0.25	***	0.16	0.25
IRF4	0.315	***	0.308	***	0.092	*	0.37	**
PU.1(SPI1)	0.501	***	0.509	***	0.45	***	0.38	**
STAT3	0.176	***	0.165	***	0.057	0.21	0.27	0.053
IL-17A	0.027	0.543	0.005	0.927	-0.0022	0.96	0.06	0.67
CCR10	0.224	***	1.236	***	0.054	0.23	0.2	0.16
AHR	0.337	***	0.348	***	0.12	***	0.15	0.29
FOXP3	0.312	***	0.3	***	0.3	***	0.27	0.052
CD25(IL2RA)	0.499	***	0.485	***	0.4	***	0.48	***
CCR8	0.364	***	0.348	***	0.29	***	0.45	***
PD-1 (PDCD1)	0.236	***	0.243	***	0.26	***	0.42	**
CTLA4	0.357	***	0.352	***	0.48	***	0.37	**
LAG3	0.121	**	0.088	0.0736	0.11	*	-0.097	0.49
TIM-3 (HAVCR2)	0.57	***	0.572	***	0.53	***	0.34	*
CD68	0.524	***	0.514	***	0.38	***	0.37	**
CD11b (ITGAM)	0.448	***	0.454	***	0.34	***	0.35	**
INOS (NOS2)	0.044	0.324	0.001	0.981	-0.058	0.2	0.031	0.83
IRF5	0.526	***	0.525	***	0.36	***	-0.18	0.2
COX2(PTGS2)	0.061	0.178	0.043	0.385	-0.012	0.79	-0.13	0.38
ARG1	0.143	**	0.148	**	0.066	0.15	0.44	**
MRC1	0.428	***	0.44	***	0.29	***	0.29	*
MS4A4A	0.521	***	0.524	***	0.46	***	0.34	*
CCL2	0.264	***	0.247	***	0.054	0.23	0.23	0.096
CD80	0.444	***	0.417	***	0.42	***	0.24	0.091
CD86	0.553	***	0.571	***	0.43	***	0.35	*
CCR5	0.353	***	0.36	***	0.27	***	0.34	*
CD14	0.411	***	0.409	***	0.33	***	0.21	0.13
CD16(FCGR3B)	0.088	0.0489	0.082	0.0968	0.11	*	0.22	0.12
CD115 (CSF1R)	0.488	***	0.505	***	0.39	***	0.29	*
CD66b (CEACAM8)	0.001	0.978	-0.008	0.867	0.035	0.44	-0.04	0.78
CD15(FUT4)	0.043	0.338	0.023	0.639	0.037	0.41	-0.067	0.64
CD11b (ITGAM)	0.448	***	0.454	***	0.34	***	0.35	**
XCL1	0.144	**	0.128	**	0.16	***	0.17	0.23
CD7	0.187	***	0.194	***	0.19	***	0.35	*
KIR3DL1	0.112	*	0.104	0.0343	0.15	***	-0.071	0.91
CD1C(BDCA-1)	0.279	***	0.278	***	0.25	***	0.39	**
CD141(THBD)	0.239	***	0.228	***	0.14	**	0.026	0.86
CD11c (ITGAX)	0.513	***	0.501	***	0.39	***	0.35	*

size, long-term follow-up investigation and deeper research were essential if reliable conclusions were to be drawn.

In the process of discussing the prognosis of PCa patients, clinical parameters play a significant role. Based on TCGA database, we extracted the clinical parameters of PCa patients, including age, TNM stages, recurrence and gleason scores, and analyzed NOX4 expression levels in patients with different clinical parameters. The results were indicative of differentially expressed NOX4 existed in patients with diverse clinical parameters. NOX4 was expressed higher in patients with older ages, higher TNM stages, recurrence and higher gleason scores. To our knowledge, it was the first time to report NOX4 mRNA was differentially expressed in tissues of patients with diverse clinical parameters.

As a member of NADPH oxidases family, NOX4 mainly generates the ROS in astrocytes [25]. In the process of searching for literature, the authors found that NOX4 had been reported to be correlated with ferroptosis. Park et al. indicated the lipid peroxidation mediated by NOX4 in Alzheimer's disease was harmful to mitochondrion and promoted the accumulation of iron in astrocytes, resulting in the occurrence of ferroptosis [26]. Through knocking out NOX4 gene, Chen et al. observed that left ventricular remodeling occurred in rats and the incidence of ferroptosis in cardiomyocytes was reduced [27]. Yang et al. considered NOX4 was a hub gene of ROS-producing enzyme in renal cell carcinoma and the overexpressed NOX4 was a necessary condition of ferroptosis [21]. To date, the relationship between NOX4 and PCa cells ferroptosis had never been clarified. Based on the above results and the current researching gap, we decided to explore the correlation between the expression levels of NOX4 and ferroptosis-related proteins. We herein screened 4 ferroptosis-related genes and performed a correlation analysis with NOX4. The obtained results suggested that NOX4 had a moderate correlation with ferroptosis-related proteins in 20 studies from 11 platforms, which indicated NOX4 was probably related with ferroptosis in PCa.

To further explore the potential molecular mechanisms and signal pathways of ferroptosis regulated by NOX4 in PCa, herein we entered NOX4 DCEGs into STRING and constructed a PPI network. According to the PPI network analysis, we screened 3 hub genes, including BUB1, CCNB1 and CCNB2. Among the 3 selected hub genes, CCNB1 had been reported to be correlated with ferroptosis. In the process of treating T-cell lymphoma with artesunate (ART), Ishikawa et al. found ART induced tumor cell peroxidation by activating CCNB1, thereby causing cell cycle arrest and iron accumulation and inhibiting the proliferation of tumor cells [28]. Though the mentioned research did not directly indicate the relationship between NOX4 and CCNB1, according to the pathway of tumor cell cycle arrested by CCNB1, we could infer that NOX4 caused lipid peroxidation, which was one of the factors leading to ferroptosis of tumor cells. However, this was the only study of NOX4 hub genes in ferroptosis, and the potential mechanisms of the above 3 genes and NOX4 in ferroptosis remained to be further explored in vivo and in vitro experiments.

As stated above, NOX4 and its hub genes were reported correlated with ferroptosis in other cancer types, we also found the expression of NOX4 was related to ferroptosis-related proteins. So how does differentially expressed NOX4 induce ferroptosis in PCa? We tried to applied enrichment analysis to DCEGs of NOX4, and the KEGG results showed that NOX4 DCEGs were significantly enriched in metabolism pathway. We searched the literature immediately based on this results. But unfortunately, there was no report about NOX4 regulating ferroptosis in PCa through metabolism pathway. Nevertheless, we found some serviceable information. In a cell experiment managed by Yi et al. , LnCap cells exhibited different levels of lipid metabolism and incidence of ferroptosis with different phospholipid content, they considered the changes in phospholipid metabolism may be an important pathway of ferroptosis in PCa [29]. Another article indicated that the activation of PI3K-AKT-mTOR pathway was able to influence the lipid metabolism in PCa cells, thereby inhibiting the occurrence of ferroptosis [30]. Tousignant et al. reported that the increase of lipid content in PCa cells could lead to the increase of membrane fluidity and lipid peroxidation, resulting in ferroptosis [14]. Considering these findings, the authors believed that DCEGs of NOX4 regulated the process of PCa ferroptosis by participating in metabolism pathway.

However, this study had some limitations. First, significant heterogeneity was observed in the present research. Due to the lack of sample size and clinical information, we could not find out the source of heterogeneity yet. Therefore, a random-effect model was applied. A larger clinical cohort should be used to validate our results in the future. Second, all PCa samples were extracted from tissues. The value of NOX4 in PCa ferroptosis should be verified in body fluids of

PCa patients. Lastly, the function of NOX4 in PCa needs to be further explored in vivo and in vitro.

5. Conclusion

In summary, based on results from clinical samples and mRNA microarray and sequencing data from public databases, we herein concluded that NOX4 was downregulated in PCa and indicated the expression levels of NOX4 were correlated with ferroptosis-related proteins. Differentially expressed NOX4 might regulate the development of ferroptosis by participating in metabolism pathway, which needs to be verified in vivo and in vitro.

Reference

1. Siegel RL, Kratzer TB, Giaquinto AN, et al. Cancer statistics, 2025. CA Cancer J Clin. 2025 Jan-Feb;75(1):10-45.
2. Klotz L, Vesprini D, Sethukavalan P, et al. Long-term follow-up of a large active surveillance cohort of patients with prostate cancer[J]. Journal of Clinical Oncology: Official Journal of the American Society of Clinical Oncology, 2015, 33(3): 272-277.
3. Ahdoot M, Lebastchi A H, Turkbey B, et al. Contemporary treatments in prostate cancer focal therapy[J]. Current Opinion in Oncology, 2019, 31(3): 200-206.
4. Kelly S P, Anderson W F, Rosenberg P S, et al. Past, Current, and Future Incidence Rates and Burden of Metastatic Prostate Cancer in the United States[J]. European Urology Focus, 2018, 4(1): 121-127.
5. Harada K, Shiota M, Minato A, et al. Treatment Strategies for Metastatic Castration-Sensitive Prostate Cancer: From “All-Comers” to “Personalized” Approach[J]. OncoTargets and Therapy, 2021, 14: 2967-2974.
6. Crawford E D, Heidenreich A, Lawrentschuk N, et al. Androgen-targeted therapy in men with prostate cancer: evolving practice and future considerations[J]. Prostate Cancer and Prostatic Diseases, 2019, 22(1): 24-38.
7. Dixon S J, Lemberg K M, Lamprecht M R, et al. Ferroptosis: an iron-dependent form of nonapoptotic cell death[J]. Cell, 2012, 149(5): 1060-1072.
8. Louandre C, Ezzoukhry Z, Godin C, et al. Iron-dependent cell death of hepatocellular carcinoma cells exposed to sorafenib. Int J Cancer. 2013 Oct 1;133(7):1732-42.
9. Galmiche A, Chauffert B, Barbare J C. New biological perspectives for the improvement of the efficacy of sorafenib in hepatocellular carcinoma[J]. Cancer Letters, 2014, 346(2): 159-162.
10. Zhang H, Deng T, Liu R, et al. CAF secreted miR-522 suppresses ferroptosis and promotes acquired chemoresistance in gastric cancer. Mol Cancer. 2020 Feb 27;19(1):43.
11. Shin D, Kim EH, Lee J, et al. Nrf2 inhibition reverses resistance to GPX4 inhibitor-induced ferroptosis in head and neck cancer. Free Radic Biol Med. 2018 Dec;129:454-462.
12. Mao L, Zhao T, Song Y, et al. The emerging role of ferroptosis in non-cancer liver diseases: hype or increasing hope? Cell Death Dis. 2020 Jul 9;11(7):518.
13. Zhou X, Zou L, Chen W, et al. Flubendazole, FDA-approved anthelmintic, elicits valid antitumor effects by targeting P53 and promoting ferroptosis in castration-resistant prostate cancer[J]. Pharmacological Research, 2021, 164: 105305.
14. Tousignant K D, Rockstroh A, Poad B L J, et al. Therapy-induced lipid uptake and remodeling underpin ferroptosis hypersensitivity in prostate cancer[J]. Cancer & Metabolism, 2020, 8: 11.
15. Ghoochani A, Hsu E C, Aslan M, et al. Ferroptosis Inducers Are a Novel Therapeutic Approach for Advanced Prostate Cancer[J]. Cancer Research, 2021, 81(6): 1583-1594.
16. Lu JP, Monardo L, Bryskin I, et al. Androgens induce oxidative stress and radiation resistance in prostate cancer cells though NADPH oxidase. Prostate Cancer Prostatic Dis. 2010 Mar;13(1):39-46.
17. Sampson N, Brunner E, Weber A, et al. Inhibition of Nox4-dependent ROS signaling attenuates prostate fibroblast activation and abrogates stromal-mediated protumorigenic interactions. Int J Cancer. 2018 Jul 15;143(2):383-395.
18. Wu QQ, Zheng B, Weng GB, et al. Downregulated NOX4 underlies a novel inhibitory role of microRNA-137 in prostate cancer. J Cell Biochem. 2019 Jun;120(6):10215-10227.
19. Singh B, Kulawiec M, Owens KM, et al. Sustained Early Disruption of Mitochondrial Function Contributes to Arsenic-Induced Prostate Tumorigenesis. Biochemistry (Mosc). 2016 Oct;81(10):1089-1100.
20. Wang Z, Ding Y, Wang X, et al. Pseudolaric acid B triggers ferroptosis in glioma cells via activation of Nox4 and inhibition of xCT[J]. Cancer Letters, 2018, 428: 21-33.
21. Yang WH, Ding CC, Sun T, et al. The Hippo Pathway Effector TAZ Regulates Ferroptosis in Renal Cell Carcinoma. Cell Rep. 2019 Sep 3;28(10):2501-2508.e4.
22. Kim H K, Lee H Y, Riaz T A, et al. Chalcone suppresses tumor growth through NOX4-IRE1α sulfonation-RIDD-miR-23b axis[J]. Redox Biology, 2021, 40: 101853.
23. Harrison I P, Vinh A, Johnson I R D, et al. NOX2 oxidase expressed in endosomes promotes cell proliferation and prostate tumour development[J]. Oncotarget, 2018, 9(83): 35378-35393.
24. Meitzler J L, Makhlouf H R, Antony S, et al. Decoding NADPH oxidase 4 expression in human tumors[J]. Redox Biology, 2017, 13: 182-195.
25. Nayernia Z, Jaquet V, Krause KH. New insights on NOX enzymes in the central nervous system. Antioxid Redox Signal. 2014 Jun 10;20(17):2815-37.

26.Park M W, Cha H W, Kim J, et al. NOX4 promotes ferroptosis of astrocytes by oxidative stress-induced lipid peroxidation via the impairment of mitochondrial metabolism in Alzheimer's diseases[J]. Redox Biology, 2021, 41: 101947.
27.Chen X, Xu S, Zhao C, et al. Role of TLR4/NADPH oxidase 4 pathway in promoting cell death through autophagy and ferroptosis during heart failure[J]. Biochemical and Biophysical Research Communications, 2019, 516(1): 37-43.
28.Ishikawa C, Senba M, Mori N. Evaluation of artesunate for the treatment of adult T-cell leukemia/lymphoma[J]. European Journal of Pharmacology, 2020, 872: 172953.
29.Yi X, Li Y, Hu X, et al. Changes in phospholipid metabolism in exosomes of hormone-sensitive and hormone-resistant prostate cancer cells[J]. Journal of Cancer, 2021, 12(10): 2893-2902.
30.Yi J, Zhu J, Wu J, et al. Oncogenic activation of PI3K-AKT-mTOR signaling suppresses ferroptosis via SREBP-mediated lipogenesis[J]. Proceedings of the National Academy of Sciences of the United States of America, 2020, 117(49): 31189-31197.

Supplementary material 2 Datasets collection flowchart

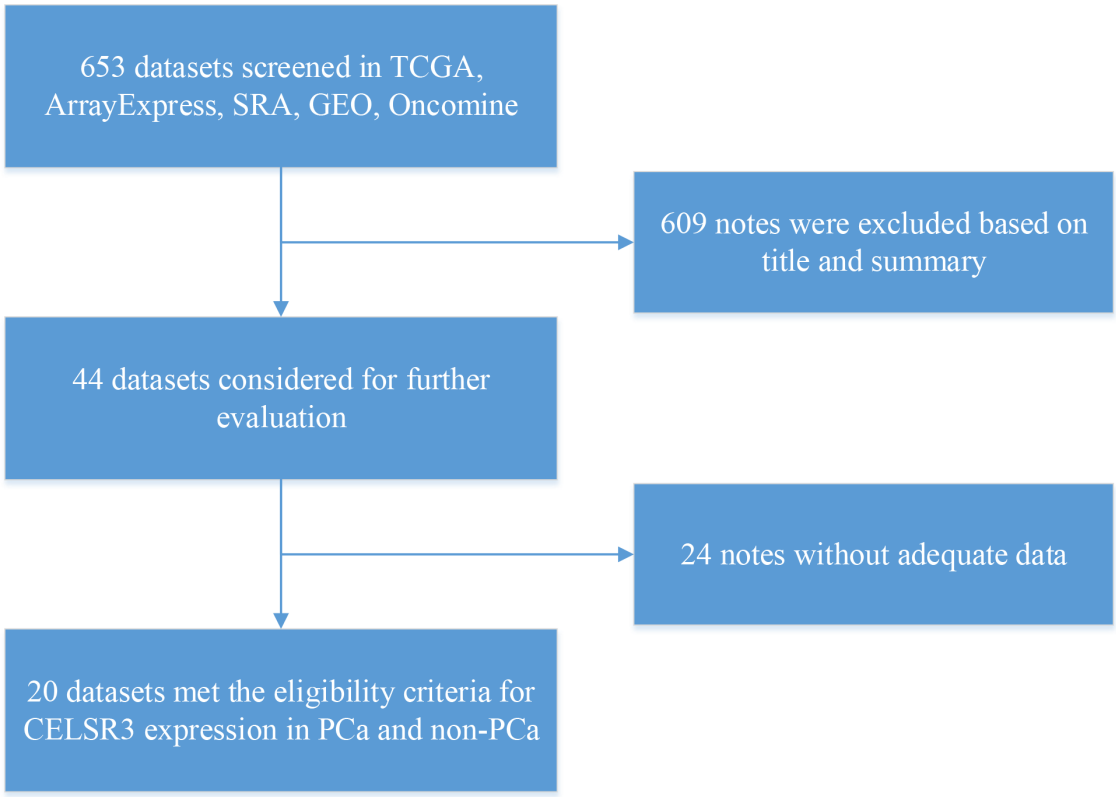

Supplementary material 1 Research design flowchart

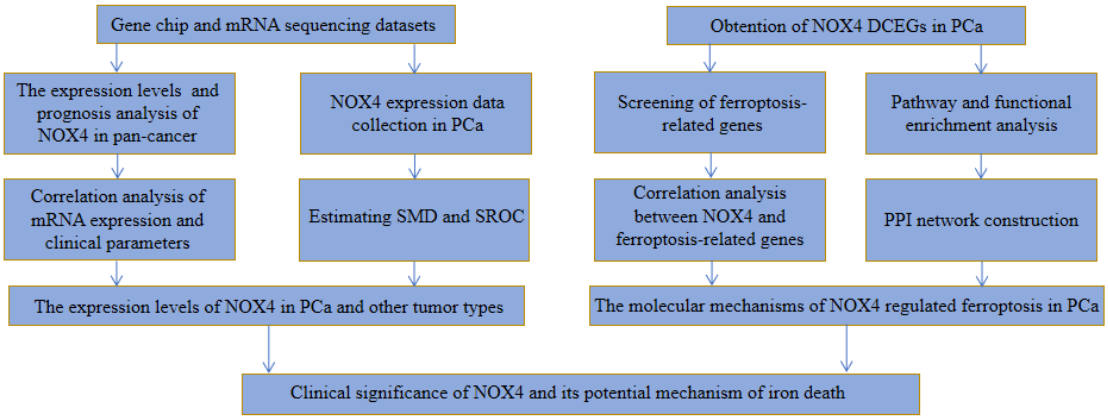

Call for Papers

International Journal of Clinical Medicine and Pharmacology (IJCMP) is a peer-reviewed, open-access journal dedicated to advancing interdisciplinary research and fostering innovation in clinical medicine, pharmacology, and healthcare sciences. The journal serves as an international platform for high-quality research, critical analyses, and discussions addressing challenges and opportunities in global healthcare.

Scope of the Journal

IJCMP publishes original contributions that span a wide range of topics, including but not limited to:

- **Clinical Medicine**: Advances in diagnostics, therapeutics, and patient care across specialties such as oncology, cardiology, pediatrics, and mental health.
- **Pharmacology**: Drug development, pharmacokinetics, pharmacodynamics, and safety monitoring.
- **Public Health**: Epidemiology, health policy, health equity, and strategies for improving access to healthcare.
- **Biomedical Sciences**: Innovations in imaging, genetics, artificial intelligence, and emerging medical technologies.
- **Ethics and Society**: Ethical considerations, cultural factors, and social determinants of health impacting clinical practices.

Types of Submissions

- **Full-Length Research Articles (4,000–8,000 words):** Presenting original research presenting novel findings or methodologies.
- **Review Articles (4,000–8,000 words):** Critical overviews and syntheses of literature in clinical medicine and pharmacology.
- **Case Studies (4,000–6,000 words):** Analysis of unique or illustrative clinical cases highlighting innovative approaches.
- **Viewpoints (1,500–2,000 words):** Short articles presenting commentary or proposing new ideas.
- **Special Issue Proposals:** Special issues may contain 6–10 articles addressing timely and impactful themes.

**Note: Translations of articles originally published in another language will not be considered.*

Open Access and Peer Review

IJCMP is committed to the principles of open access, ensuring all published research is freely available to readers worldwide. Articles undergo a rigorous double-anonymous peer review process to maintain academic integrity, objectivity, and fairness.

Submission Guidelines

Manuscripts must adhere to the Author Guidelines and be prepared in Microsoft Word or PDF format. Detailed formatting instructions are available on the journal's website. Submissions should be made via the online portal at: https://press.jandoo.ac/journals/ijcmp. For inquiries, please contact the IJCMP editorial team at **E-mail (**editorialoffice.jgtss@press.jandoo.ac).

Submission Deadline

Submissions are accepted on a rolling basis, ensuring timely review and publication.

IJCMP strives to support authors in the seamless submission and publication of high-quality research. Adherence to these guidelines ensures efficient processing and maximizes the impact of your work.

International Journal of Clinical Medicine and Pharmacology (IJCMP) is a peer-reviewed, open-access academic journal dedicated to advancing global medical knowledge and fostering innovation in clinical medicine, pharmacology, and healthcare sciences. IJCMP provides an inclusive platform for researchers, clinicians, healthcare professionals, and policymakers to share high-quality research, critical reviews, and practical solutions addressing the challenges of modern medicine and healthcare delivery.

Address:
1-53-13, Nishigahara
Kita City, Tokyo
114-0024
Japan

Tel: +81 (0)80-8515-9423
E-mail: editorialoffice.jgtss@press.jandoo.ac
Offical website: https://press.jandoo.ac/journals/jgtss

INTERNATIONAL JOURNAL OF CLINICAL MEDICINE & PHARMACOLOGY
VOLUME 1, NUMBER 2
(FEBRUARY 2025)

EAN-13 Barcode for 9772759875600

ISSN: 2759-8756